NSSDC
71-05

THE NATIONAL
SPACE SCIENCE DATA CENTER

# Handbook of Correlative Data

FEBRUARY 1971

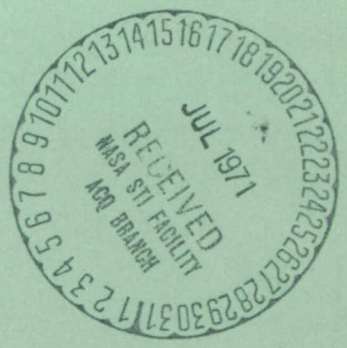


NATIONAL SPACE SCIENCE DATA CENTER
NATIONAL AERONAUTICS AND SPACE ADMINISTRATION • GODDARD SPACE FLIGHT CENTER, GREENBELT, MD.

NSSDC 71-05

The National Space Science Data Center

# HANDBOOK OF CORRELATIVE DATA

Joseph H. King, Editor

February 1971

# FOREWORD

In previous years, the National Space Science Data Center (NSSDC) has generated a Catalog of Correlative Data. This catalog listed and, to some extent, described the correlative data holdings of NSSDC. However, it was felt desirable to have a document of a more general nature, which would point to correlative data available at any data center or in any readily accessible publication. This Handbook of Correlative Data was generated to fulfill this need.

This Handbook can be used to acquaint the reader with many solar and geophysical phenomena, to point the reader to more detailed discussions of the phenomena, and to direct him to the data. It is anticipated that many readers will require this Handbook for only the last one or two of these purposes.

A second edition of this Handbook will be generated when warranted. Accordingly, I would appreciate receiving comments from the users of this Handbook. Any recommendations for improving its usefulness will be most helpful in the generation of a second edition.

I want to thank the NSSDC personnel who served as authors of the individual sections; their names appear on the pages introducing each of the nine major parts. I would like to acknowledge the assistance of other NSSDC personnel, particularly Miss Mary Anne Beeler, who were involved in the various stages of the generation of this Handbook. I would also like to thank scientists outside the NSSDC, S. J. Bauer, J. E. Jackson, G. D. Mead, and A. J. Zmuda, who reviewed certain sections of this Handbook.

January 15, 1971

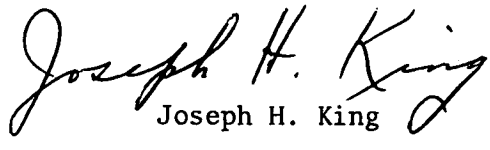

Joseph H. King

# CONTENTS

## LIST OF FIGURES

LIST OF TABLES

# INTRODUCTION

The National Space Science Data Center (NSSDC) is issuing this Handbook of Correlative Data to inform scientists of the availability of data potentially useful as correlative data in space science studies. Although the major activities of NSSDC are concerned with the acquisition, storage, retrieval, and dissemination of space science data, the significance of correlative data in many studies is recognized, and assistance in this area is therefore given to investigators.

For the purposes of this document, correlative data are those data that are routinely gathered and that can be used to correlate with space science data.

This Handbook of Correlative Data contains six major discipline oriented parts covering galactic cosmic rays, solar electromagnetic radiation, energetic solar protons, geomagnetism, the ionosphere, and the neutral atmosphere. In addition, a miscellaneous data part covers magnetospherically trapped particles, solar wind, airglow, aurora, calendar records, activity charts, and Jovian radio emission. Each section includes:

- a brief description of the phenomenon
- reference to more extensive discussions of the phenomenon
- reference to discussion of measurement techniques
- a brief discussion of available data
- the time periods for which data exist
- the medium on which data are stored
- sources of more extensive data availability listings, if appropriate
- sources from which the actual data can be obtained (both places and publications)

In the cases of geomagnetism, neutral atmosphere, and magnetospherically trapped particles, models based on syntheses of large amounts of data are discussed.

Following the miscellaneous data part is a miscellaneous information part in which various coordinate systems useful in space science, the International Ursigram and World Days Service, and rocket data availability are discussed. These fall outside the definition of correlative data, but were judged to be of sufficient usefulness to warrant their inclusion.

All parts except for Part IX are intended to stand alone, and each has a separate list of references.

The final part of the Handbook lists and discusses the major sources of correlative data. Also listed are all other documents referred to in the text as containing some correlative data. Sufficient detail is given on all sources to enable the reader to obtain the document and the data. If the sources cannot supply the needed data, NSSDC will endeavor to assist users in locating the data. It should be pointed out here that no attempt has been made to survey or reference the data catalogs of individual observatories. Station lists are included in the WDC-A Catalogue of Data on Solar-Terrestrial Physics. The World Data Center A for Upper Atmosphere Geophysics can provide the mailing addresses of the individual observatories as required.

It is the policy of NSSDC to obtain and provide correlative data for the use of other NASA personnel or contractors. NSSDC visitors are welcome to utilize any part of the NSSDC correlative data holdings. All inquiries concerning correlative data or requests for copies of this Handbook or for the NSSDC Data Catalog of Satellite Experiments, which describes the available spacecraft space science data, should be sent to:

National Space Science Data Center
Code 601.4
Goddard Space Flight Center
Greenbelt, Maryland 20771

Phone (301) 982-6695

# PART I

# COSMIC-RAY DATA

Prepared By

Julius J. Brecht

CONTENTS

# INTRODUCTION

The measurement of cosmic-ray intensity by ground-based monitors lends itself to the observation of unpredictable and rare events and to the study of the systematic behavior of the cosmic-ray flux. Because of the long duration of these cosmic-ray experiments, data of high statistical quality are secured. These experiments are confined to locations relatively deep in the atmosphere and therefore measure principally secondary cosmic rays. Primary effects can be extrapolated from measurements of secondary effects and from the atmospheric cascade theory. A discussion of cascade theory and cosmic-ray phenomena is given in Rossi (1952), Hess and Mead (1965), and Nishimura (1967).

Discussed in Part I are the various types of detectors used to measure secondary particles and the pertinent information concerning the data coverage and procurement.

The map in figure 1 shows the location of cosmic-ray monitoring stations throughout the world. The WDC-A Catalogue of Data on Solar-Terrestrial Physics lists these stations in alphabetical order by station name. This list includes a statement of the projects going on at each station, the form of the collected data, and the time interval of coverage. The vertical cutoff rigidities, measured in Bv and calculated using the quiescent magnetic field model of Finch and Leaton for epoch 1955.0, are also given in this list for each observing station.

Data taken with some of the detection devices described below are reported as bihourly counting rates. Pressure data are also included. A given station may submit an additional data sheet for cosmic-ray data corrected for pressure effects. In the case of neutron monitor stations, this is the general practice. Pressure, temperature, and pressure distribution throughout the atmosphere above the station are all of importance for ionization chamber and cubical meson telescope detectors.

A number of methods exist to correct for these effects. Hence, the experimenter normally supplies meteorological data, allowing the user to make his own corrections. In many cases, the World Data Center A (WDC-A) for Upper Atmosphere Geophysics or the National Space Science Data Center (NSSDC) will aid the requester in obtaining more detailed information about instrument calibration and specified analysis procedures that can be used to extract the desired information from the data.

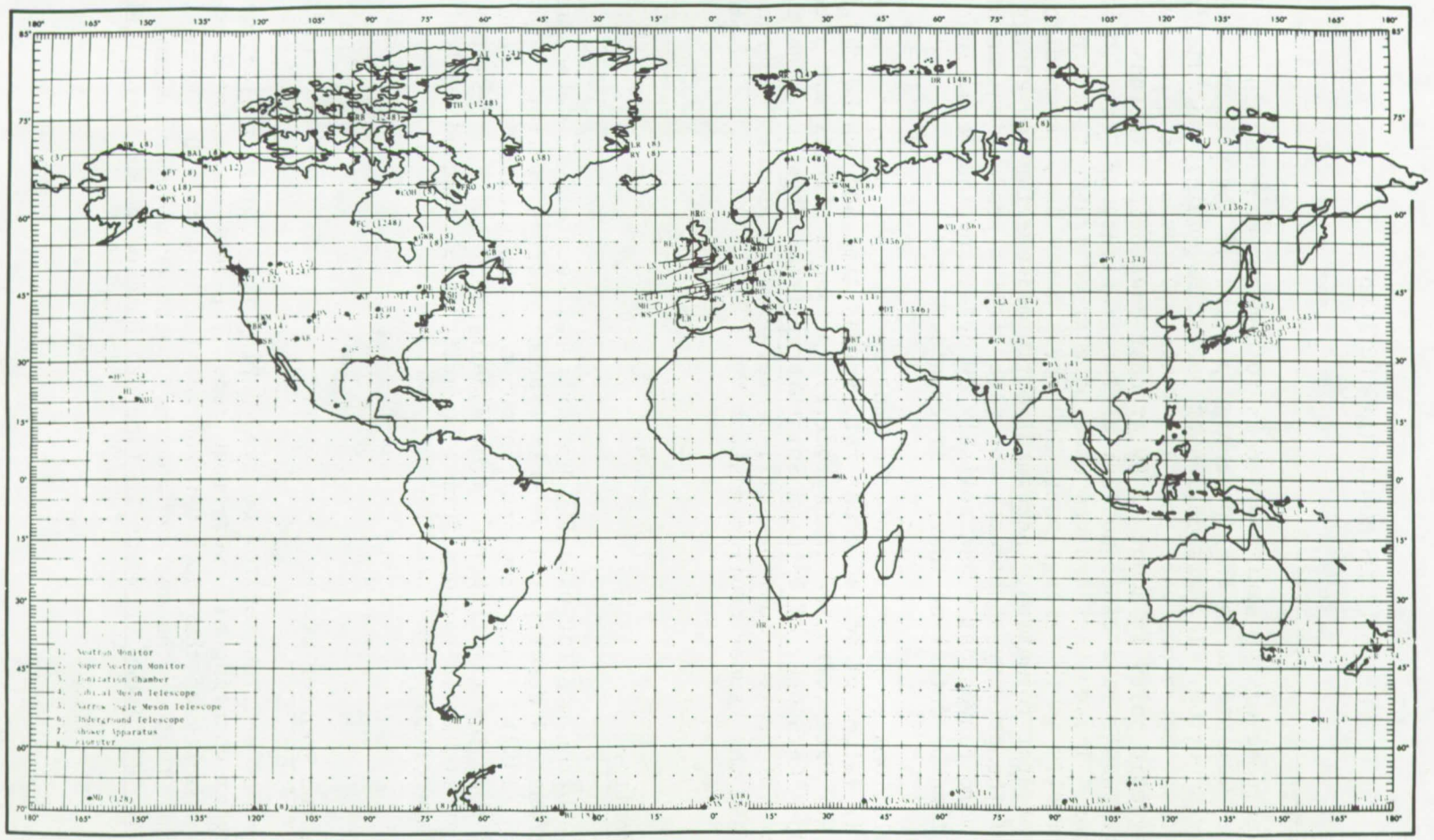


Figure 1. Cosmic-Ray Monitoring Stations

## NEUTRON MONITORING DEVICES

The purpose of the neutron pile is to detect, deep within the atmosphere, variations in the low-energy portion of the primary cosmic-ray spectrum. The rigidities of particles, mainly secondaries, reaching these detectors vary from less than 0.01 Bv at stations near the geomagnetic poles to about 15 Bv at near-equatorial stations. Low-energy cosmic rays cause nuclear disintegrations, or "stars," in the monitor. These stars are composed of charged fragments and neutrons typically in the energy range 100 Mev $\leq E \leq$ 1 Bev. By monitoring the rate of star formation, one can directly measure the low-energy portion of the primary spectrum. The rate of star production can be obtained more conveniently and reliably by detecting the resulting neutrons than by detecting charged fragments.

Tabulations of intensity of the neutron flux are presented as hourly or bihourly values of scaled count rate versus time and can be obtained from WDC-A. Data corrected for barometric pressure effects are noted in the WDC-A Catalogue of Data on Solar-Terrestrial Physics. The two basic types of neutron monitors will be referred to as the "neutron monitor" and the "super neutron monitor."

### Neutron Monitor

The neutron monitor uses $BF_3$ proportional counters to detect incident neutrons. A description of this type of neutron monitor is given by Simpson (1957). Data from neutron monitors are available through WDC-A and span the time interval from January 1957 to the present. The data are available in various forms: magnetic tape, punched cards, hard copy, or microfilm.

### Super Neutron Monitor

The super neutron monitor evolved during the IQSY when instruments with a higher counting rate were required. The total calculated counting rate capacity of the super neutron monitor is about 20 times greater than that of the neutron monitor. Data from super neutron monitors are available on magnetic tape and punched cards through WDC-A.

They span the time interval from January 1962 to the present. A sample of typical super neutron monitor data distributed by WDC-A in hard-copy form would contain daily or hourly average counts per hour for a given month and year at a given station. A description of this type of monitor is given by Carmichael (1968).

Super neutron monitor cosmic-ray data from four stations (Churchill, Deep River, Climax, and Dallas) are available (from November 1964 to the present) in the Solar-Geophysical Data bulletin for the month 2 months prior to publication. The data are in tabular form and include daily (UT) average counting rates (counts/hour). The data from these four stations can be used to estimate the rigidity dependence of fluctuations occurring in the primary cosmic-ray spectrum. More detailed descriptions of the super neutron monitor and of this program are contained in the Solar-Geophysical Data "Descriptive Text" (February 1970).

## MESON MONITORING DEVICES

Mesons of various types are generated by collisions between incident primary cosmic rays and atmospheric particles. Meson data are presented as hourly or bihourly values of scalar count rate versus time. These data must be corrected for barometric and temperature effects. There are several instruments used to measure this component of the cosmic-ray beam.

### Ionization Chamber

The ionization chamber measures the total ionization produced by secondary cosmic rays capable of passing through approximately 10 cm of lead. It measures primarily the μ-meson component of the secondary radiation. Hence, the response of the ionization chamber detector is similar to that of the counter telescopes, which are discussed later, but it is more sensitive to heavily ionizing events, e.g., bursts and showers. The ionization chamber is also more sensitive to nucleons and air showers than the counter telescope. Ionization chamber data are available on punched cards (1957 to 1959) or in hard-copy form (1960 to the present) through WDC-A at Boulder. The typical ionization chamber detector data distributed by WDC-A in hard-copy form contain bihourly mean values, probably uncorrected for barometric pressure, as a function of day, month, and year for a given station. This type of detector is described in reference 3.

## Cubical Meson Telescope

The early models of the cubical meson telescope consisted of three trays of Geiger tubes in coincidence. A detailed description of this telescope is given by Elliot (1957). Carmichael (1968) describes a newer version (MT-64) which uses scintillation plastic. The detector responds to all incident particles that can penetrate the lead absorber and arrive within the solid angle of the detector; i.e., the detector responds to the hard component of secondary radiation. (This component is composed mainly of μ-mesons near sea level.)

Cubical meson telescope data are available on punched cards (1957 to 1959) or hard copy (1960 to present) through WDC-A at Boulder. A sample of the typical cubical meson telescope data distributed by WDC-A in hard-copy form would contain bihourly count rates as a function of day, month, and year for a given station.

## Narrow-Angle Telescope

The narrow-angle telescope is similar to the cubical meson telescope, except that the narrow-angle telescope has a much narrower response pattern about the vertical. A description of this detector is given in reference 3.

Narrow-angle telescope data are available through WDC-A for the time interval 1957 to 1964 (1957 to 1959 on punched cards and 1960 to 1964 on hard copy). The typical narrow-angle telescope data distributed by WDC-A in hard-copy form contain bihourly rates as a function of day, month, and year for a given station.

## Underground Telescope

The underground telescope is similar to the cubical meson telescope but is placed underground. This detector responds to even higher energies than the cubical meson telescope at sea level due to the added absorber between the production layer and the detector. A description of this apparatus is given by Vasilov et al. (1966), and further information concerning underground telescopes can be found in papers by Peacock et al. (1968) and Barton and Stockel (1968).

Underground telescope data are available on punched cards (1957 to 1959) or hard copy (1960 to 1968) through WDC-A. The typical underground telescope data distributed by WDC-A in hard-copy form contain bihourly rates as a function of day, month, and year for a given station.

## SHOWER APPARATUS

A shower apparatus consists of an array of detectors, covering several square meters, used to measure the component of cosmic rays having energies about $10^{12}$ ev. The data obtained are highly complex and difficult to analyze without a good knowledge of the experimental setup and the corrections to be made. An extensive bibliography and a discussion of air showers and shower apparatus appear in Fujimoto and Hayakawa (1967). A limited amount of data is available through WDC-A at Boulder for the period 1957 to 1967.

## REFERENCES


1. Barton, J. C., and C. T. Stockel, "Some Problems in the Interpretation of Underground Cosmic-Ray Data," Can. J. Phys., 46, S318-S323, 1968.

2. Carmichael, H., "Cosmic Rays (Instruments)," Ann. IQSY, 1, 178-197, 1968.

3. Cosmic Ray Intensity during the International Geophysical Year, 4, National Committee for the International Geophysical Coordination, Science Council of Japan, Mar. 1961.

4. Elliot, H., "Standard Meson Intensity Recorder," Ann. IGY, 4, 374-393, 1957.

5. Fujimoto, Y., and S. Hayakawa, "Cosmic Rays and High-Energy Physics," Handbuch Der Physik, 46/2, 115-180, Springen-Verlag, New York, 1967.

6. Hess, Wilmot N., and Gilbert D. Mead, Introduction to Space Science, Gordon and Breach Science Publishing Co., New York, 1965.

7. Nishimura, J., "Theory of Cascade Showers," Handbuch Der Physik, 46/2, 1-114, Springen-Verlag, New York, 1967.

8. Peacock, D. S., J. C. Dutt, and T. Thambyahpillai, "Directional Measurements of the Cosmic-Ray Daily Variation at Vertical Depth of 60 M.W.E. in London," Can. J. Phys., 46, S788-S793, 1968.

9. Rossi, Bruno, High-Energy Particles, Prentice-Hall, Inc., Englewood Cliffs, N.J., 1952.

10. Simpson, J. A., "Cosmic-Radiation Neutron Intensity Monitor," Ann. IGY, 4, 351-373, 1957.

11. Vasilov, Yu. N., B. A. Nelepo, G. I. Pugacheva, and V. M. Fedonov, "Apparatus for Measuring the Intensity of Cosmic Rays at Great Depths," translated from Marine Hydrophysical Institute, Kiev, 36, 31-36, 1966.

# PART II

# SOLAR ELECTROMAGNETIC RADIATION

Prepared By

Charles D. Wende, Peter J. Havanac,
and Charles L. Marks

CONTENTS

# INTRODUCTION

The solar atmosphere is divided into three layers. The lowest of these is the cool, dense, weakly ionized photosphere. The highest is the hot, tenuous, almost fully ionized corona, of which the interplanetary plasma is the continuous extension. The 10,000-km-thick chromosphere serves as the transitional region. See Zirin (1966).

The interaction of the differentially rotating solar atmosphere with the solar magnetic field gives rise to solar active regions, which show statistically an 11-year periodicity in number and location. An individual active region may persist for several solar rotation periods (27 days); within an active region, enhancements of emissions called flares may last from seconds to hours. See Tandberg-Hanssen (1967).

Electromagnetic radiation emitted from the solar atmosphere consists of three components corresponding to the three solar activity time scales. The quiet sun component is that component observed when all contributions due to individual active regions have been deleted; coronal variations with the solar cycle are manifest in this component. The slowly varying component, which corresponds to a solar rotational period, is due to individual active regions. The burst component, associated with solar flares, has a time scale of seconds to hours.

There are four major periodicals that list solar data. Three of these are discussed in Part IX of this Handbook: Solar-Geophysical Data, Geophysics and Space Data Bulletin, and the Quarterly Bulletin on Solar Activity. The fourth source is the weekly Preliminary Report and Forecast of Solar-Geophysical Activity prepared by the Space Disturbance Forecast Center of the National Oceanic and Atmospheric Administration (NOAA) in Boulder, Colorado. This publication summarizes solar and geophysical events of the preceding week and forecasts solar related activity for the coming few weeks. Due to its preliminary nature, this publication is inappropriate for referencing in more definitive publications.

The remainder of this part is divided into sections based on the wavelength of the observed solar electromagnetic radiation. The wavelength range covered varies from radio wavelengths (kilometers to millimeters) to X-ray wavelengths (angstroms and less). Solar particle radiation is discussed in Part III in this Handbook.

## RADIO OBSERVATIONS

Solar radio emissions originate from both thermal and nonthermal processes in the solar atmosphere (chromosphere and corona). These emissions are divided into the three previously described components, the quiet sun and slowly varying components, both of which have primarily thermal origins, and the burst component, which has both nonthermal and thermal phases. A comprehensive review of solar radio astronomy is given by Kundu (1965). The instrumentation used to measure the solar radio emissions is described in Kraus (1966).

Observatories engaged in measuring solar radio emissions are listed in table 1. Because of their length, the tables referenced in this section on Radio Observations are included at the end of the section, beginning on page 23. The first line of each station listing gives the following information in the order and format listed: station name; alternate names; the International Astronomical Union abbreviation that is used in the Quarterly Bulletin on Solar Activity; other abbreviations; and the latitude, longitude, and observing hours in UT. The observing hours are given, where possible, for two time periods: the first and fourth quarters of the year and the second and third quarters.

The subsequent lines list: the frequency of observation in MHz; the type of observation (B = bursts are reported, F = flux measurements are reported, V = variability index is reported, P = polarization indices are reported, SS = one-dimensional strip scans are reported, MP = two-dimensional maps are given, and SP = spectrograms are given); the years that the apparatus was in operation (a year followed by a blank indicates that the apparatus is believed to be currently in operation, a '?' indicates that operation ceased at an unknown date); and the sources from which the data can be obtained. Data from Eastern Hemisphere stations did not appear in Solar-Geophysical Data before 1969. In the case of the Canary Islands, Carnarvon, and Houston stations, the data can be obtained only through the WDC-A for Upper Atmosphere Geophysics. The data are usually available in hard-copy form.

### Flux, Variability, and Polarization Measurements

Flux densities, in units of $10^{-22}$ watts meter$^{-2}$ Hz$^{-1}$, of the sum total of the radio emissions from the entire visible solar disk are measured at numerous frequencies by many observatories. These flux densities are measured instantaneously at solar meridian passage (local noon). If a burst occurs during meridian passage, the appropriate flux

is interpolated. The fluxes are useful as indices of the level of solar activity and reflect the flux level due to the quiet sun and slowly varying components. The fluxes can also be the mean solar flux densities observed during a specified interval of time, such as an observing day or a 3-hour observing period.

Additionally, some stations indicate the relative variability of the flux during the observing period. A scale of 0 to 3 is used, 0 indicating quiet conditions and 3 indicating violent variability.

Some stations also indicate the polarization of the observed solar radio flux. This polarization is described as being right- or left-handed (in the radioelectric sense, a clockwise rotating approaching wave is defined as left-handed) and having a magnitude of greater than 50%, less than 50%, or zero. The percent of polarization is defined as 100 times the difference of the right-handed and left-handed flux divided by the sum of the two components.

More detailed descriptions of the flux measurements are given by Fokker (1968) and in the descriptive text accompanying Solar-Geophysical Data. Calibration techniques used to determine the absolute flux values are described by Medd and Covington (1958) and Priese (1969).

Stations engaged in absolute flux measurements are listed in order of observing frequency on table 2. If parentheses enclose the station name, it is believed that the station is no longer in operation (no data published for 1968 or later). The letter P or V after a station name indicates that polarization (P) or variability (V) indices are given. Figure 2 illustrates the approximate coverage obtained by stations making solar flux observations since the IGY. Individual stations, although not identified on figure 2, may be identified by table 2. Since flux measurements are used to provide a background level of solar activity, the observing hours are not critical and hence are not illustrated.

Ottawa daily noon 10.7-cm flux values (1947 to the present) are available on the magnetic tape generated by the European Space Research Organization (ESRO) (Lenhart, 1968). This tape also contains geomagnetic and sunspot indices and is available from WDC-A, Boulder, WDC-A, Rockville, or NSSDC. Ottawa and Sagamore Hill data (January 1967 to the present) on punched cards are also available from WDC-A, Boulder.

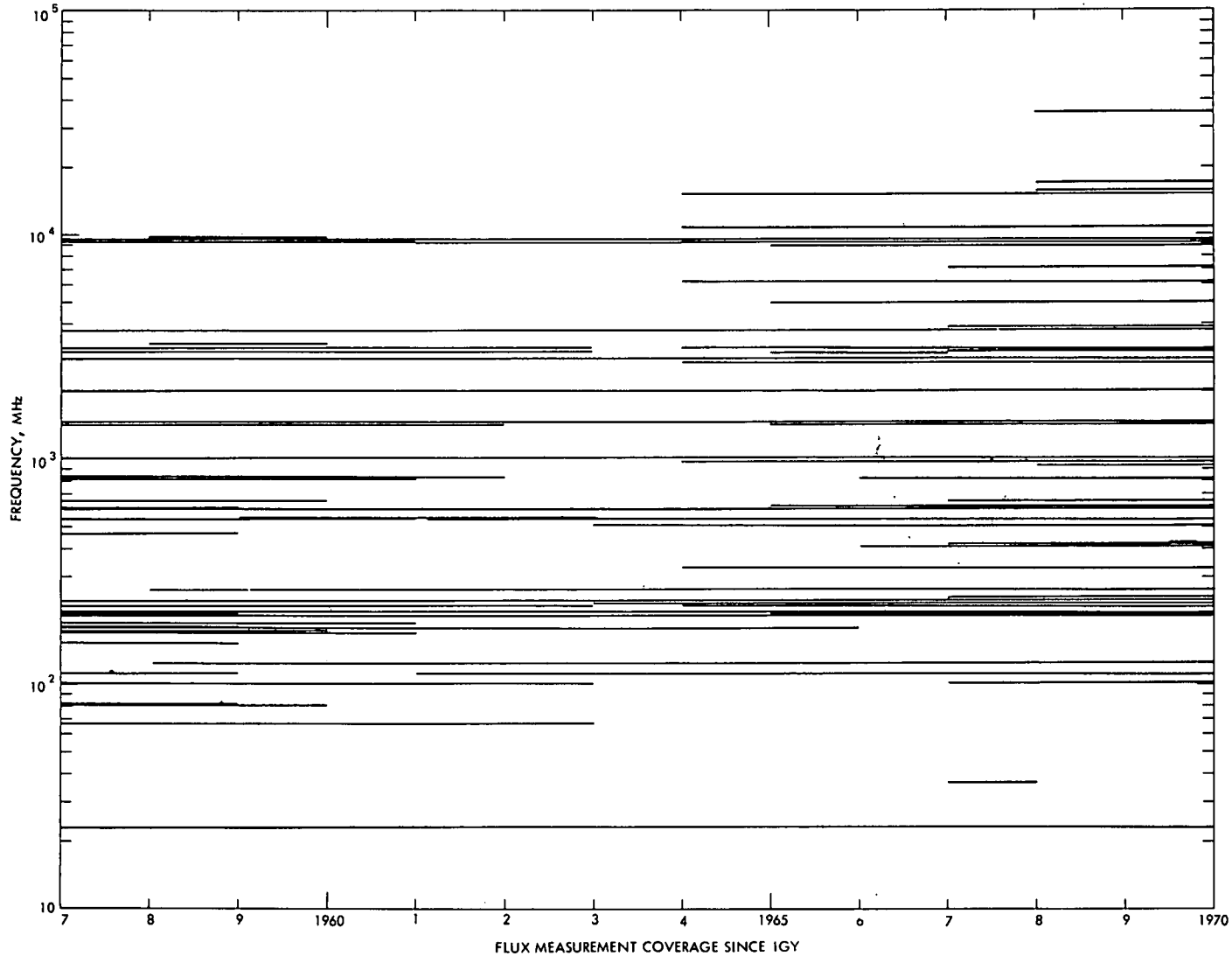


Figure 2. Approximate Coverage Obtained by Stations Making Solar Flux Observations Since the IGY

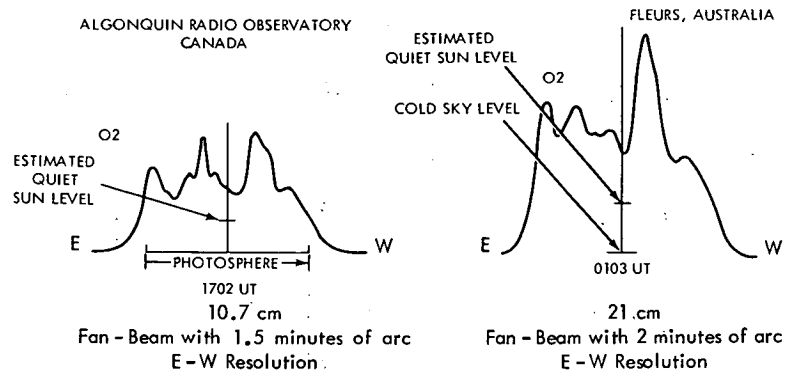


Figure 3. Example of a Strip Scan

## Daily Maps of the Sun

The distribution of sources on the solar disk is measured daily by several observatories. This distribution may be measured in only one dimension (typically requiring 4 minutes of observing time), as in a strip scan in which all sources lying in a line perpendicular to a point on the strip are summed. It may also be measured in two dimensions (typically requiring 1 hour of observing time), in which case the data are usually portrayed in the form of a map or a matrix. Examples of strip scans and solar maps are given in figures 3 and 4, respectively. Table 3 lists stations making one- or two-dimensional scans of the sun, ordered by frequency.

## Burst Observations

Increases in the intensity of solar radio emissions occur in conjunction with solar flares (Smith and Smith, 1963, and Wild et al., 1963). These solar emissions, called bursts, events, or radio flares, are classified by their spectral and temporal profiles. The character of bursts observed at meter wavelengths is markedly different from the character of the bursts observed at microwave wavelengths. Spectral information is most important in classifying solar bursts in the 5- to 500-MHz range (see figure 5), while the temporal profile alone is sufficient to classify the higher frequency microwave bursts. Further, the classification scheme used for microwave bursts is not universal. (See Fokker, 1968, and the "Descriptive Text" of Solar-Geophysical Data for high frequency microwave temporal profiles.)

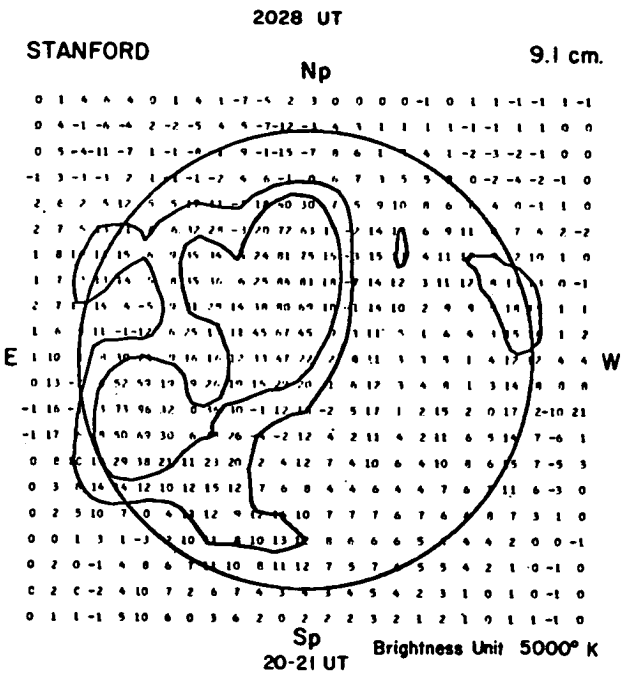


Figure 4. Map of the Distribution of Sources on the Solar Disk

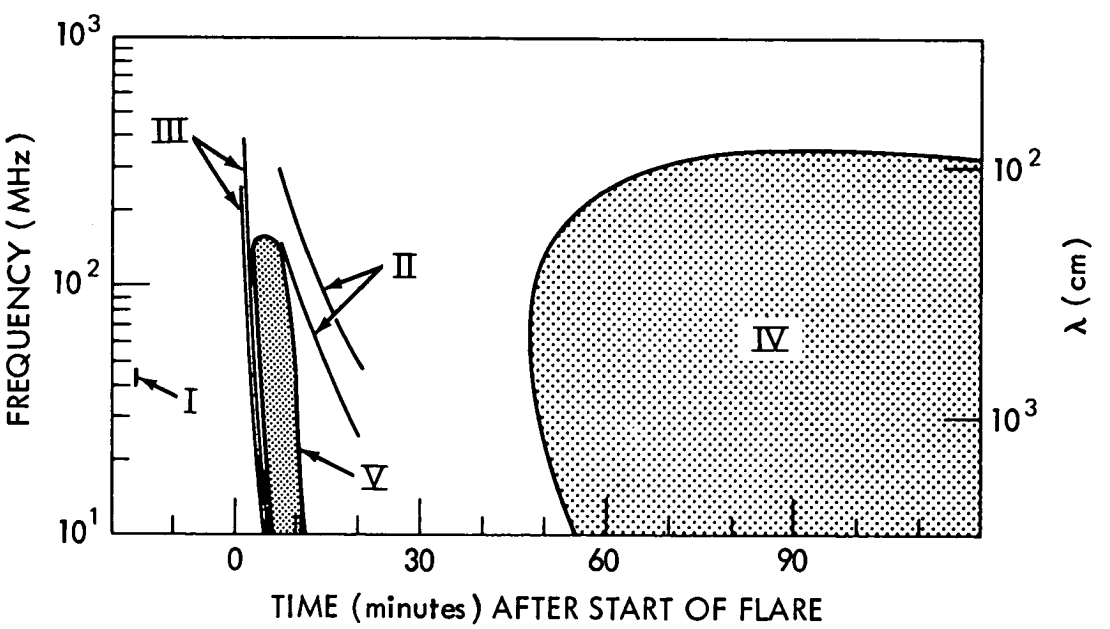


Figure 5. Spectra of Low-Frequency Bursts

## Single Frequency Burst Observations

Stations listing solar radio bursts are given on table 4, and the coverage obtained since the IGY is illustrated on figure 6. The observing hours currently covered are shown on figures 7a and 7b. The radio flare listings usually include the start time, the time of peak intensity, the end time or duration, the peak flux density, the average flux density, and an indication of the overall character of the event. Occasionally, temporal profiles are given for microwave bursts. In addition to the hard-copy data indicated in table 1, WDC-A, Boulder, holds single frequency burst data on punched cards from the following observatories: Ottawa (April 1966 to the present); Sagamore Hill (April 1966 to the present); Pennsylvania State University (April 1966 to the present); Boulder (April 1966 to July 1966, March 1967 to January 1968, July 1968 to the present); Washington State University (July 1966 to December 1967); Sao Paulo (October 1967 to the present); and San Miguel (October 1967 to the present).

## Burst Spectrograms

Spectral observations in the 5- to 500-MHz range are made by observatories equipped with receivers that sweep the frequency range of interest. These observatories are listed on table 5, and the coverage obtained is illustrated on figure 8. The data are in the form of tabular listings, but spectrograms may be available.

Recently, satellites have made possible radio burst observations at frequencies less than the lower limit imposed on ground-based observers by the earth's ionosphere (i.e., about 10 MHz). These observations are made with multichannel receivers. The only satellite data currently available are the data from the University of Michigan OGO 3 radio astronomy experiment, and these are available at the National Space Science Data Center on microfilm. They cover the frequency range of 2 to 4 MHz (3 to 4 MHz after October 1966) in the time period from June 1966 to September 1967. Data from the Goddard Space Flight Center experiment on the ATS 2 satellite covering .45 to 3.0 MHz in seven steps will be available soon at NSSDC. These data cover the period from April to July 1967.

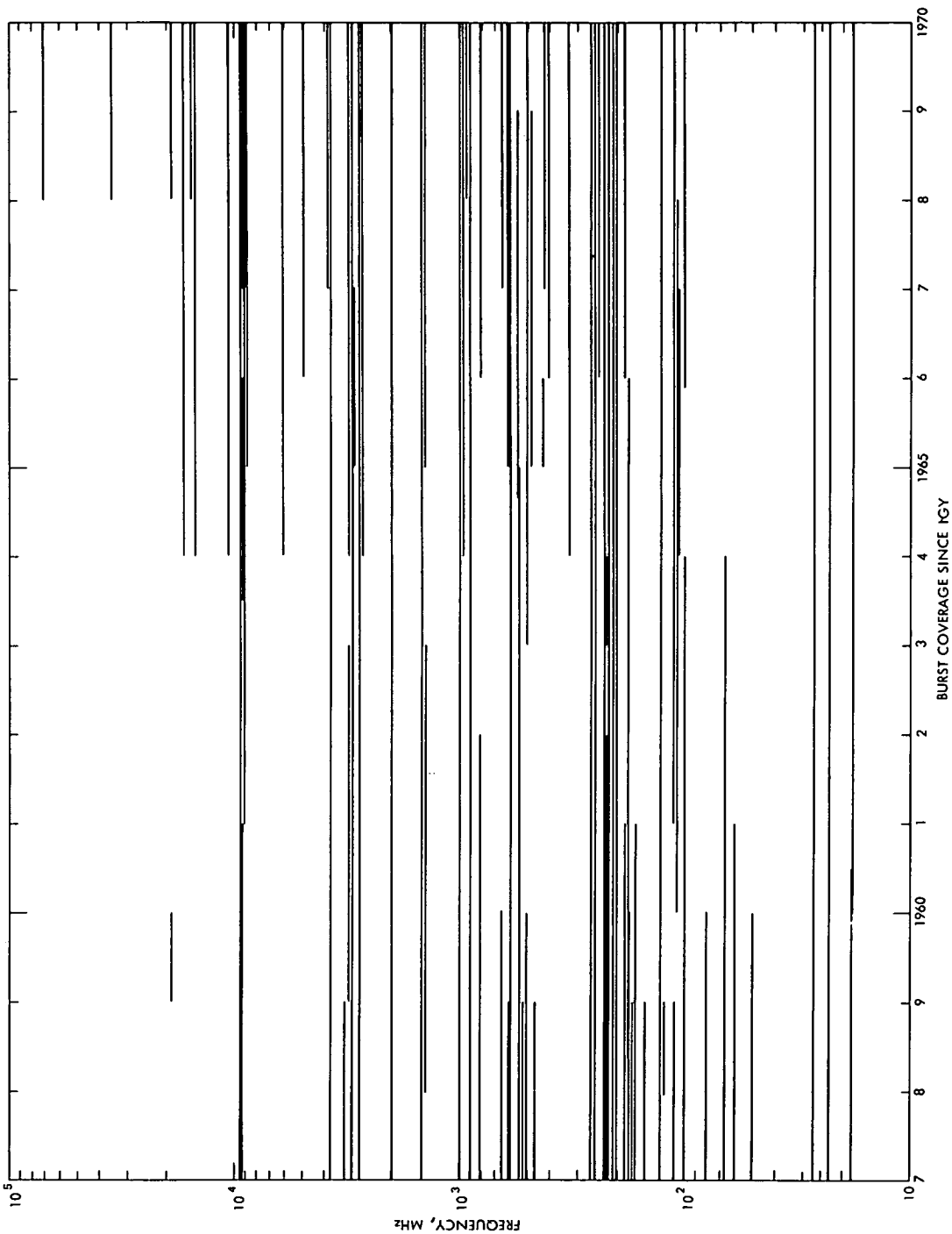


Figure 6. Solar Radio Burst Coverage Since the IGY

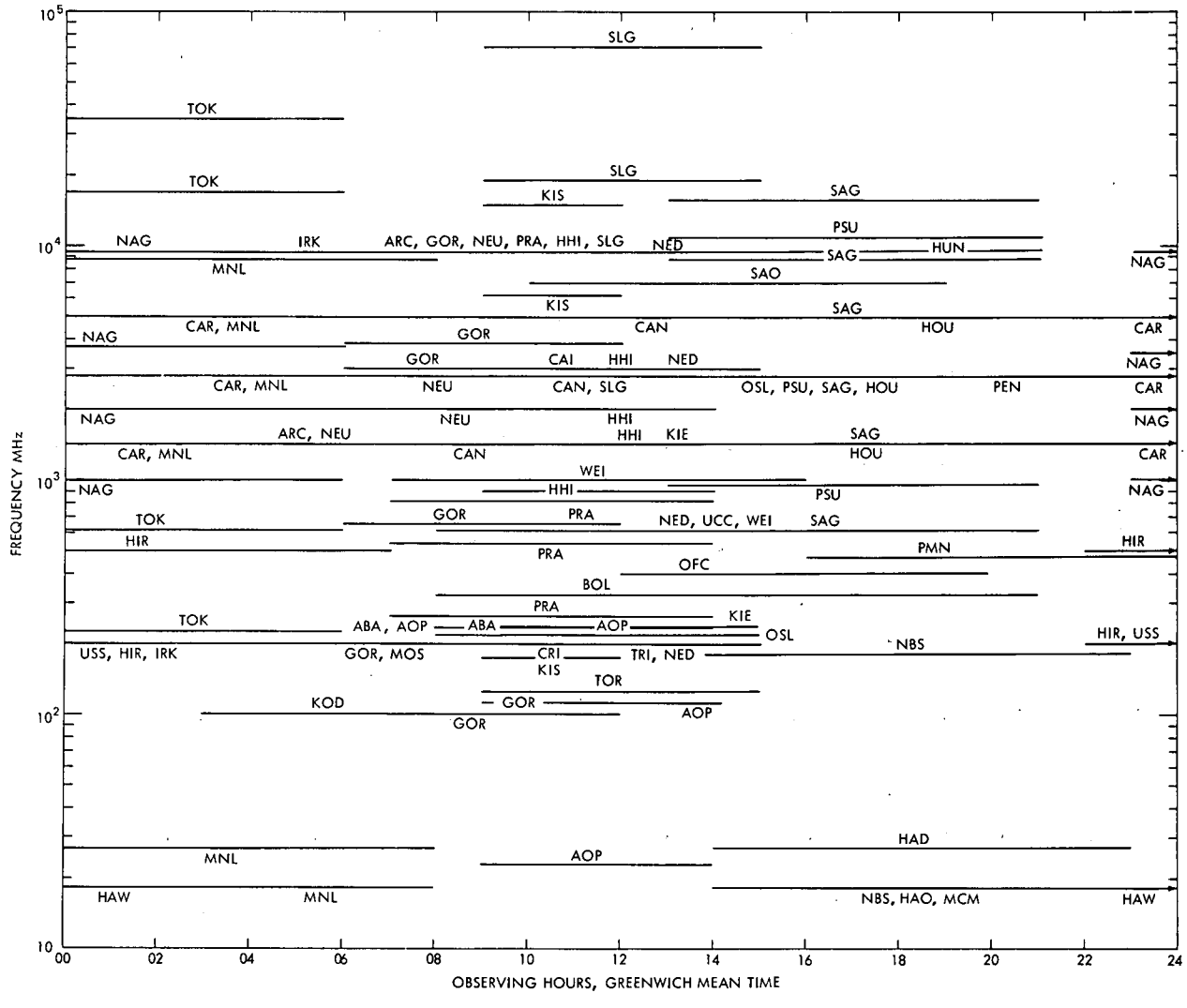


FIXED FREQUENCY SOLAR RADIO EVENTS, 1st & 4th QUARTERS

Figure 7a. Observing Hours Currently Covered

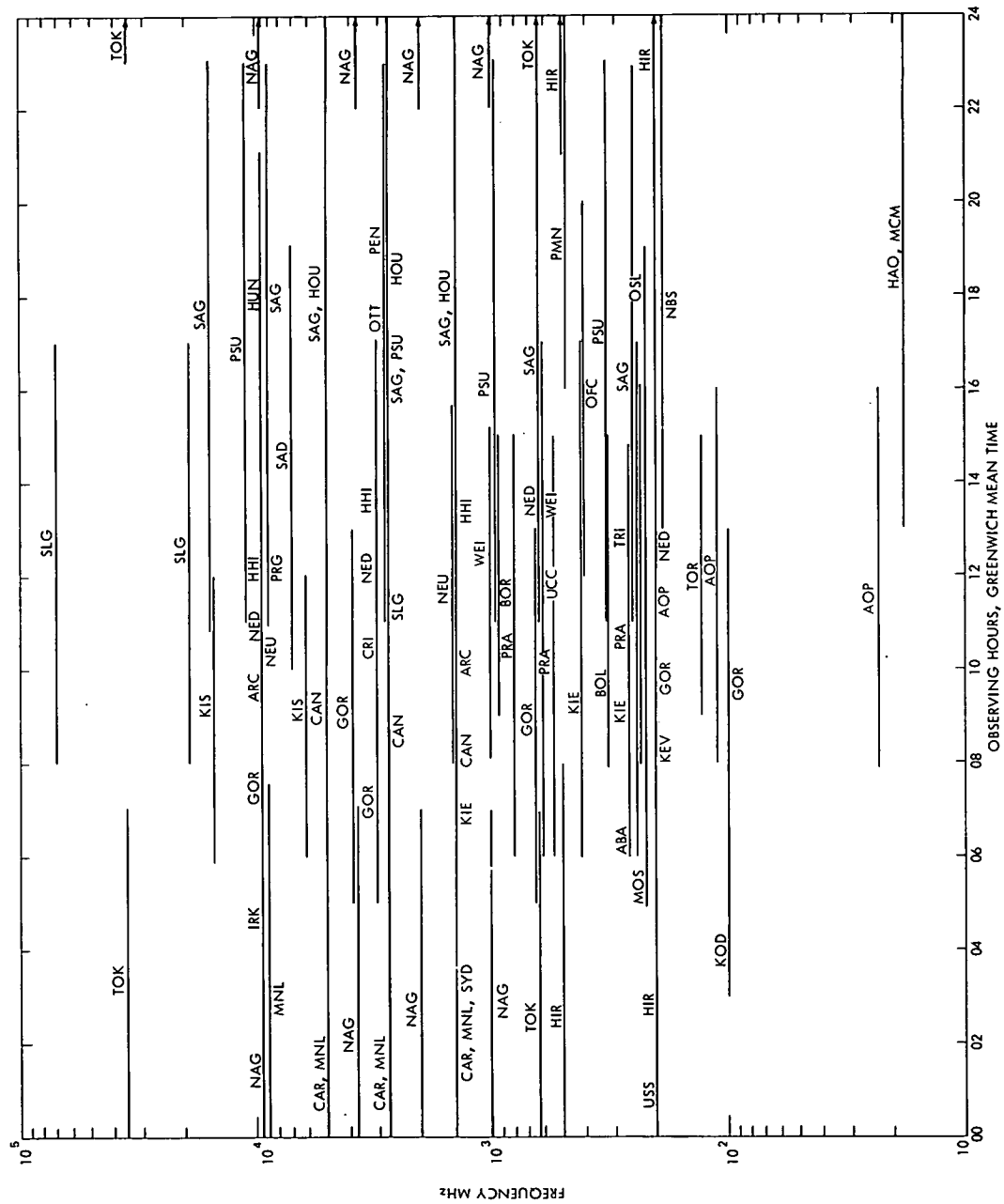


Figure 7b. Observing Hours Currently Covered

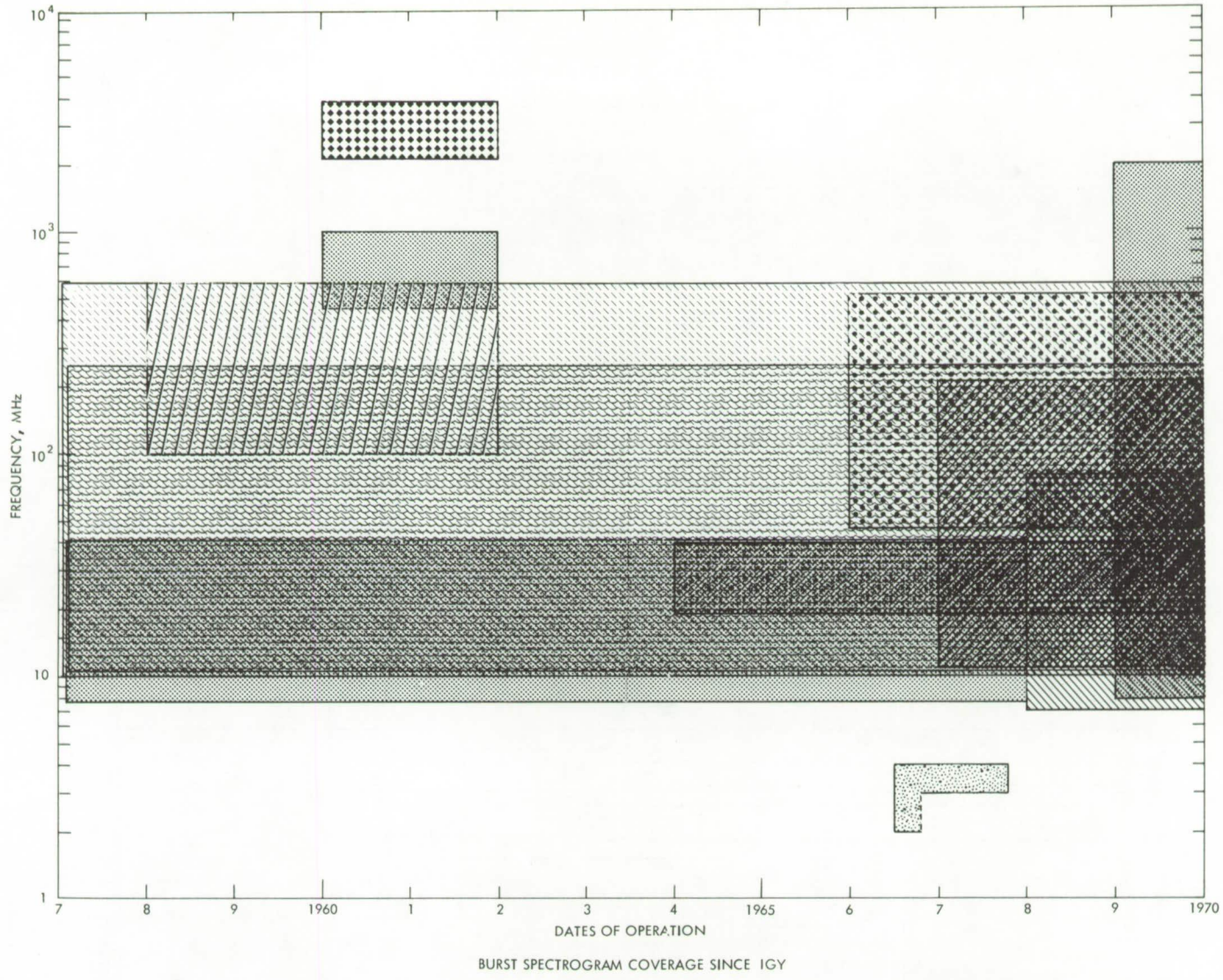


Figure 8. Burst Spectrogram Coverage

TABLE 1

OBSERVATORY LIST

Station Name / Alternate(s) / IAU Abbreviation(s) / Coordinates / Observing Hours

ABASTUMANI, Abastumany / ABA, ABST / 42N, 43E / 8-12, 6-12
221 (or 209) / B, F / 57-62, 64- / WDC-A, QBSA, SGD

Frequency(MHz) / Type of Observation / Years Observing / Sources

ABASTUMANI, Abastumany / ABA, ABST / 42N, 43E / 8-12, 6-12
221 (or 209) / B, F / 57-62, 64- / WDC-A, QBSA, SGD

ABASTUMANY, see ABASTUMANI

ALGONQUIN, see OTTAWA

ANN ARBOR, see McMATH-HULBERT

ARCETRI / ARC*, ARCE / 44N, 11E / 7-15**
186 / F / 57-60 / SGD 9285 / B / 69- / SGD
225 / F / 63-64 / SGD 1420 / B / 69- / SGD

ATHENS, Penteli, Pentili / ATH* / 38N, 24E / 7-15
2980 / B, F / 65-66 / G&SD, WDC-A

BERLIN-ADLERSHOF / BER, see HEINRICH HERTZ INSTITUTE

BIG PINE, Owens Valley / BPN* / 37N, 118W / 16-24**
450-1000 / SP / 60-61 / SGD, WDC-A

BJURAKAN (via Moscow IZMIRAN) / BJU / 40N, 44E / 6-9, 6-12
191, 203, or 209 / B, FV / 57-59 / QBSA, WDC-A

BLINDERN, see OSLO

BOEING, see SEATTLE

BOLOGNA / BOL / 44N, 11E / 8-15, 8-15
327 / B, F / 64- / QBSA, WDC-A

*Abbreviation assigned by NSSDC.
**Estimated by adding and subtracting 4 hours from the approximate time of solar meridian passage.

TABLE 1 (continued)

BONN, Stockert Rad. Obs., Eschweiler / BON* / 51N, 07E / 8-16**
36 / F / 67 / WDC-A
35,000 / B / 68 / WDC-A

BORDEAUX, Floirac / BOR, BORD / 44N, 01W / 8-16**
930 / B, F / 68- / WDC-A, SGD

BOULDER, see HIGH ALTITUDE OBSERVATORY and NOAA

BUENOS AIRES, see OSS. DI FISICA COSMICA

BUKAVU, see I.R.S.A.C.

CAMBRIDGE, see CAVENDISH

CANARY ISLANDS (via HOUSTON) / CAN* / 28N, 15W / 8-18
4995 / B / 67- / via WDC-A
2695 / B / 67- / via WDC-A
1420 / B / 67- / via WDC-A

CARNARVON (via HOUSTON) / CAR* / 25S, 114E / 23-9
4995 / B / 66- / via WDC-A
2695 / B / 66- / via WDC-A
1420 / B / 66- / via WDC-A

CAVENDISH, Cambridge / CAV / 52N, 00E / 10-15
178 / B, F / 57-58 / WDC-A
81 / B, F, V / 57-58 / WDC-A

CHALMERS INSTITUTE OF TECHNOLOGY, Onsala / CIT / 57N, 11E / 6-18, 6-18
150 / B, F, V / 57-58 / QBSA

COLORADO, UNIVERSITY OF, see HIGH ALTITUDE OBSERVATORY

CORNELL UNIVERSITY, Ithaca / COR / 42N, 76W / 14-21, 12-21
430 / B / 65 / WDC-A
201 / B, F, V / 57-58 / QBSA, SGD, WDC-A

CRACOW, Krakow / CRA / 50N, 19E / 9-12
810 / B, F, P / 57-60 / QBSA, WDC-A

*Abbreviation assigned by NSSDC.
**Estimated by adding and subtracting 4 hours from the approximate time of solar meridian passage.

TABLE 1 (continued)

CRIMEAN ASTROPHYS. OBS., Simferopol, Simeis / CRL, SIM, CRIM / 44N, 34E / 9-12
3100 / B, F / 59-62, 64- / QBSA, WDC-A, SGD
1000 / B, F / 66 / QBSA, WDC-A
208 / B, F, V / 57-62, 65-? / QBSA, WDC-A

CULGOORA / CUL* / 30S, 147E / 22-8
10-210 / SP / 67- / WDC-A
8-2000 / SP / 69- / SGD, WDC-A

DELHI, New Delhi / DEL* / 28N, 77E / 3-11**
2000 / F / 66- / WDC-A

DOMINION RADIO AST. OBS., see PENTICTON

DOURBES, see UCCLE

ESCHWEILER, see BONN

FLEURS, see SYDNEY

FLOIRAC, see BORDEAUX

FORT DAVIS, see HARVARD

GIZA / GIZ* / 30N, 31E / 6-14**

GORKY, Zimenki / GOR, GORK / 56N, 44E / 6-12, 5-13
19,000 / F, V / 59 / QBSA
9100 or 9375 / B, F / 57-60, 64-65, 67- / WDC-A, QBSA, SGD
3850 / B, F / 67- / QBSA, WDC-A, SGD
2950 or 3000 / B, F, V / 57-59, 67- / QBSA, WDC-A, SGD
650 / B, F, V / 57-59, 67- / QBSA, WDC-A, SGD
200 / B, F / 57-59, 67- / QBSA, WDC-A, SGD
100 / B, F, V / 67- / QBSA, WDC-A, SGD

GRAFTON, Troy, Rensselaer Polytechnic Inst. / GRA / 42N, 77W / 13-21**
18 / B / 57-62 / QBSA

GRAHAMSTOWN, see RHODES UNIV.

*Abbreviation assigned by NSSDC.
**Estimated by adding and subtracting 4 hours from the approximate time of solar meridian passage.

TABLE 1 (continued)

HALEAKALA, Hawaii / HAW / 20N, 156W / 17-28, 16-29
200 / B / 57-59 / QBSA, SGD, WDC-A
107 / B / 64-67 / QBSA, SGD, WDC-A
18 / B / 58-62, 64-66 / SGD, WDC-A (via ESSA)

HARESTUA, see OSLO

HARVARD, Fort Davis / HAR / 30N, 103W / 14-23, 13-24
10-580 / SP / 57- / SGD, QBSA, WDC-A
2100-3900 / SP / 60, 61 / WDC-A

HAWAII, see HALEAKALA

HEINRICH HERTZ INSTITUTE, Berlin-Adlershof / HHI, BER, BERL / 52N, 13E / 9-14, 8-15
9490 / B, F / 57- / WDC-A, QBSA, SGD
3000 / B / 57-62, 65- / QBSA, SGD
2000 / B / 57-64- ? / QBSA
1470 / B, F / 57- / WDC-A, QBSA, SGD
900 / B / 57- ? / WDC-A, QBSA

HIGH ALTITUDE OBSERVATORY, Univ. of Colorado / 40N, 105W / 14-23, 13-24
Boulder / HAO, BOUL
7.6-41 / SP / 59-68 / SGD, QBSA, WDC-A
7-80 / SP / 68- / SGD, QBSA, WDC-A
27 / B / 57- ? / WDC-A
18 / B / 57- / WDC-A, SGD

HIRAISO - HIR, HIRA / 36N, 400E / 22-7, 21-8
500 / B, F / 63- / QBSA, WDC-A, SGD
200 / B, F, V / 57- / QBSA, WDC-A, SGD

HOLLANDIA / HOL / 38, 141E / 21-8
500 / B, F / 57-62 / QBSA, WDC-A
200 / B, F / 57-62 / QBSA, WDC-A

HOUSTON, Manned Spacecraft Center / HOU* / 30N, 95W / 14-24
(operates NASA-SPAN, includes Canary Islands and Carnarvon)
4995 / B / 66- / WDC-A
2695 / B / 66- / via WDC-A
1420 / B / 66- / via WDC-A

*Abbreviation assigned by NSSDC.

TABLE 1 (continued)

HUANCAYO / HUN*, HUAN / 12S, 75W / 13-21**
9400 / B / 69- / SGD

HUMAIN, see UCCLE

HYDERABAD / HYD* / 17N, 78E / 3-11**
30 / B / 58 / WDC-A

IRKUTSK, Siberian IZMIRAN / IRK, IRKU / 52N, 104E / 2-9, 3-9
9500 or 9300 / B, F / 64- / QBSA, WDC-A, SGD
208 / B, F, V / 57-? / QBSA, WDC-A

I.R.S.A.C., Bukavu / IRS / / 6-15
169 / B, F, V / 57-59 / QBSA

ITHACA, see CORNELL UNIVERSITY

IZMIRAN, Moscow, Krasnaya Pakhra / IZM*, IZMI / 56N, 37E / 6-14**
(Institute of Terrestrial Magnetism,
Ionosphere, and Radio Wave Propagation -
coordinating agency for Abastumani,
Bjurakan, Cracow, Gorky, Kislovodsk,
Moscow, and Crimea)
202 / B, F / ? / SGD

JODRELL, Nuffield Rad. Ast. Lab, Manchester / JOD / 53N, 03W / 8-16**
3000 / B, F, P / 57-59 / QBSA, WDC-A
2000 / B, F / 57-59 / QBSA, WDC-A
200 / B, F / 57-59 / QBSA, WDC-A
80 / B, F, V / 57-59 / QBSA, WDC-A

KIEL / KIE*, KIEL / 54N, 10E / 8-15, 6-17
1420 / B, F / 67- / QBSA, WDC-A, SGD
420 / B, F / 67- / QBSA, WDC-A, SGD
240 / B, F / 67- / QBSA, WDC-A, SGD

KIEV / KEV*, KIEV / 50N, 30E / 6-14**
204 or 210 / F / 64- / WDC-A, SGD

*Abbreviation assigned by NSSDC.
**Estimated by adding and subtracting 4 hours from the approximate time of solar meridian passage.

TABLE 1 (continued)

KISLOVODSK, Kislovadak (via IZMIRAN) / KIS / 44N, 44E / 9-12, 6-12
15,000 / B, F, V / 64- / QBSA, WDC-A, SGD
6100 / B, F, P / 64- / QBSA, WDC-A, SGD
178 / B, F, V / 57-65 / QBSA, WDC-A

KODAIKANAL / KOD*, KODA / 10N, 77E / 3-11**
100 / B / 66- / WDC-A, SGD

KRAKOW, see CRACOW

KRASNAYA PAKHRA, see IZMIRAN

LWIRO / LWI* / 02S, 28E / 6-14**
169 / B, F / 57-59 / WDC-A

MACAO, Macau / MAC* / 22N, 113E / 0-8**

MACKENZIE, UNIVERSIDADE, see SAO PAULO

MANILA / MNL, MANI / 14N, 121E / 0-8**
8800 / B, F / 67- / G&SD, WDC-A, SGD
4995 / B, F / 67- / G&SD, WDC-A, SGD
2695 / B, F / 67- / G&SD, WDC-A, SGD
1415 / B, F / 67- / G&SD, WDC-A, SGD
27 / B / 62, 63, 67, 68 / WDC-A
18 / B / 62 / WDC-A

MANNED SPACECRAFT CENTER, see HOUSTON

MCMATH-HULBERT, Pontiac, Ann Arbor / MCM*, MCMA / 42N, 83W / 13-21**
100-580 / SP / 58-61 / WDC-A
18 / B / 57-62, 64- / WDC-A, SGD

MITAKA, see TOKYO

MOSCOW (via IZMIRAN) / MOS / 55N, 37E / 7-12, 6-12
600 / B, F, V / 57-58 / QBSA, WDC-A
545 / B, F, V / 59-62 / QBSA, WDC-A
208 or 202 / B, F, V / 57- / QBSA, WDC-A

*Abbreviation assigned by NSSDC.
**Estimated by adding and subtracting 4 hours from the approximate time of solar meridian passage.

TABLE 1 (continued)

NAGOYA, Toyokawa / NAG, TYKW / 35N, 137E / 23-6, 22-7
9400 / B, F / 57- / QBSA, WDC-A, SGD
4000 / SS / 57-68 / QBSA, WDC-A
3750 / B, F, P / 57-68 / QBSA, WDC-A, SGD
2000 / B, F, P / 57- / QBSA, WDC-A, SGD
1000 / B, F, P / 57-69 / QBSA, WDC-A, SGD

NANCAY / NAN / 47N, 02E / 11-13
408 / SS / 65- / QBSA, WDC-A
169 / SS / 57- / QBSA, WDC-A

NATIONAL BUREAU OF STANDARDS, see NOAA, / NBS

NAVAL RESEARCH LABORATORY / NRL* / 38N, 77W / 13-21**
9530 / B, F / 58-59 / SGD, WDC-A
3200 / B, F / 58-59 / SGD, WDC-A

NEDERHORST DEN BERG, see NETHERLANDS

NERA-UTRECHT, see NETHERLANDS

NETHERLANDS, Nederhorst Den Berg, NERA-Utrecht / NED, NERA / 52N, 5E / 8-15, 6-17
9500 / B / 59-63, 65- / QBSA, WDC-A, SGD
2980 / B / 57- / QBSA, WDC-A, SGD
610 / B / 65- / QBSA, WDC-A, SGD
545 / B / 57-65 / QBSA, WDC-A
250 / B / 57- ? / QBSA, WDC-A
252 / SS / 65-68 / WDC-A
200 / B, F, V, P / 57- / QBSA, WDC-A, SGD
136 / SS / 65- / WDC-A, QBSA

NEUSTRELITZ, Operated by Heinrich Hertz Institute / NEU* / 53N, 13E / 7-15**
9140 / B, F / 61- / WDC-A, SGD
2920 / B / 57-61, 65- ? / WDC-A
2000 / B, F / 64- ? / WDC-A
1490 / B, F / 60- / WDC-A, SGD

NEW COPERNICUS UNIVERSITY, see TORUN

NEW DELHI, see DELHI

*Abbreviation assigned by NSSDC.
**Estimated by adding and subtracting 4 hours from the approximate time of solar meridian passage.

TABLE 1 (continued)

NOAA, previously ESSA, Boulder / NBS, BOUL / 40N, 105W / 14-23, 13-24
460 or 470 / B, F / 57-58 / SGD, QBSA, WDC-A
184 / B / 66- / SGD, WDC-A, QBSA
167 / B, F, V / 57-60 / SGD, QBSA, WDC-A
180 / B / 60-67 / SGD, QBSA

NUFFIELD RADIO AST. LAB., see JODRELL

ONDREJOV, see PRAGUE

ONSALA, see CHALMERS INSTITUTE OF TECHNOLOGY

OSLO, Harestua, Blindern / OSL, HARS / 60N, 10E / 9-15, 5-19
225 or 215 / B, F, V / 57- / G&SD, QBSA, WDC-A, SGD
200 / B, F, V / 57-61 / QBSA

OSSERVATORIO DI FISICA COSMICA, San Miguel / OFC, SANM / 34S, 58W / 12-20*
408 / B, F / 66- / SGD, QBSA, WDC-A

OTTAWA, Algonquin / OTT, ARO, OTTA / 54N, 75W / 13-21, 11-23
2800 / SS / 68- / WDC-A
2800 / B, F / 57- / SGD, QBSA, WDC-A
500 / B / 57-59 / WDC-A
50 / B / 57-59 / WDC-A

OWENS VALLEY, see BIG PINE

PALO ALTO, see STANFORD

PARAMARIBO / PAR / 05N, 55W / 11-21
545 / B / 57-68 / QBSA, WDC-A
200 / B, F / 57-67 / QBSA, WDC-A

PENNSYLVANIA STATE UNIVERSITY, University Park / PSU, PENN / 41N, 78W / 13-21, 11-23
10,700 / B, F / 64- / SGD, QBSA, WDC-A
2690 / B, F / 64- / SGD, QBSA, WDC-A
960 / B, F / 64- / SGD, QBSA, WDC-A
328 / B, F / 65- / SGD, QBSA, WDC-A

PENTICTON, Dominion Radio Ast. Obs. / PENN, PENT / 49N, 120W / 16-24**
2700 / B, F / 64- / QBSA, WDC-A

*Abbreviation assigned by NSSDC.
**Estimated by adding and subtracting 4 hours from the approximate time of solar meridian passage.

TABLE 1 (continued)

PENTILI, see ATHENS

PIRKULI / PRK* / 40N, 48E / 5-13**
234 / B / 59-62 / WDC-A

PONTIAC, see MCMATH-HULBERT

POTSDAM, Tremsdorf / AOP, POTS / 52N, 13E / 9-14, 8-16
234 / B, F, V / 57- / QBSA, WDC-A, SGD
111 / B, F / -58, 61-- / QBSA, WDC-A, SGD
23 / B, F / 57- / QBSA, WDC-A, SGD

PRAGUE, Ondrejov / PRA, ONDR / 49N, 14E / 7-14, 6-15
9400 / B, F / 61-62, 66- / WDC-A, SGD
808 / B, F, P / 59-62, 66- / WDC-A, QBSA, SGD
536 / B, F, V / 57- / QBSA, WDC-A, SGD
261 / B, F / 58- / QBSA, WDC-A, SGD
231 / B, F, V / 58-61 / WDC-A, QBSA

PROSPECT HILL, Waltham / PRO* / 42N, 72W / 13-21**
35,000 / MP / 67- / G&SD, WDC-A

PULKOVO / PUL / 60N, 33E / 9-12
9375 / B, F / 57, 58 / QBSA, WDC-A

PULLMAN, Washington State University / PMN*, WASH / 47N, 117W / 16-24**
486 / B / 65-68 / SGD, WDC-A

RENSSELAER POLYTECHNIC INST., see GRAFTON

RHODES UNIVERSITY, Grahamstown / RHO / 33S, 26E / 6-14**
125 / B / 58 / QBSA, WDC-A

RIGA / RIG / 57N, 24E / 11-14, 12-15
220 / B, F / 57-60, 63-66 / QBSA, WDC-A

ROMA, see ROME

ROME, Roma / ROM* / 41N, 12E / 7-15**
27 / B / 63-66 / WDC-A
18 / B / 63-65 / WDC-A

*Abbreviation assigned by NSSDC.
**Estimated by adding and subtracting 4 hours from the approximate time of solar meridian passage.

TABLE 1 (continued)

SACRAMENTO PEAK, Sunspot / SAC* / 32N, 105W / 15-23**
18 / B / 57-61 / WDC-A

SAGAMORE HILL RADIO OBS., AFCRL / SAG, SGMR / 42N, 72W / 13-21, 11-23
Hamilton
15,400 / B, F / 68- / G&SD, SGD, QBSA, WDC-A
8800 / B, F / 65- / G&SD, SGD, QBSA, WDC-A
4995 / B, F / 65- / G&SD, SGD, QBSA, WDC-A
2695 / B, F / 65- / G&SD, SGD, QBSA, WDC-A
1415 / B, F / 65- / G&SD, SGD, QBSA, WDC-A
606 / B, F / 65- / G&SD, SGD, QBSA, WDC-A
245 / B, F / 69- / G&SD, SGD, WDC-A
19-41 / SP / 64- / G&SD, SGD, WDC-A

SAN MIGUEL, see OSS. DI FISICA COSMICA

SAO PAULO, Umuarama Obs., Univ. Mackenzie, / SAO, SAOP / 22S, 46W / 10-19
7000 / B, F / 67- / G&SD, SGD, QBSA, WDC-A

SEATTLE, Boeing / SEA / 47N, 122W / 16-2
221 / B / 62-63, 65 / QBSA, WDC-A
222 / SS / 62-65 / SGD

SIBERIAN IZMIRAN, see IRKUTSK

SIMEIS, see CRIMEAN ASTROPHYS. OBS.

SIMFEROPOL, see CRIMEAN ASTROPHYS. OBS.

SLOUGH / SLG, SLOU / 51N, 00E / 9-15, 8-17
71,000 / B / 68- / QBSA, WDC-A, SGD
19,000 / B / 68- / QBSA, WDC-A, SGD
9400 / B / 68- ? / QBSA, WDC-A
2800 / B / 68- / QBSA, WDC-A, SGD

STANFORD, Palo Alto / STN* / 37N, 122W / 20-21
2700 / MP / 60- / SGD, WDC-A

STOCKERT RADIO OBS., see BONN

SUNSPOT, see SACRAMENTO PEAK

*Abbreviation assigned by NSSDC.
**Estimated by adding and subtracting 4 hours from the approximate time of solar meridian passage.

TABLE 1 (continued)

SYDNEY, Fleurs / SYD / 36S, 151E / 23-5, 22-6
1420 / B, F / 57-61, 67-68 / QBSA
1420 / SS / 58-62 / QBSA
1420 / MP / 57-62, 64- / WDC-A, SGD
690 / SS / 65- / SGD, WDC-A, QBSA
600 / B, F / 57-58 / QBSA
10-250 / SP / 57-68 / QBSA, WDC-A

TOKYO, Mitaka / TOK, TOKO / 35N, 139E / -6, 23-7
35,000 / B, F / 68 / WDC-A
17,000 / B, F, P / 64- / QBSA, WDC-A, SGD
9500 / B, F, P / 57-64 / QBSA, WDC-A
3000 / B, F / 57-63 / QBSA, WDC-A
612 / B, F / 67, 69- / WDC-A, SGD
408 / B / 66-67 / WDC-A
326 / B / 66-67 / WDC-A
227 / B, F, V, P / 57-68 / QBSA, WDC-A
200 / B, F, V, P / 57-63 / QBSA
100 / B, F / 57-63 / QBSA, WDC-A
67 / B, F / 57-63 / QBSA, WDC-A

TORONTO / TTO* / 43N, 75W / 13-21**
520 / B / 57-59 / WDC-A

TORUN, New Copernicus Univ. / TOR / 53N, 18E / 6-14, 9-15
127 / B, F, V / 58- / QBSA, WDC-A

TOYOKAWA, see NAGOYA

TREMSDORF, see POTSDAM

TRIESTE / TRI, TRST / 45N, 13E / 10-14
239 / B, F / 66- / G&SD, QBSA, WDC-A, SGD

TROY, see GRAFTON

TUBINGEN, see WEISSENAU

UCCLE, Humain, Dourbes / UCC, UCCL / 50N, 4E / 8-15, 6-17
600 / B, F, V / 57- / QBSA, WDC-A, SGD
169 / B, F / 57-61 / QBSA, WDC-A

UMUARAMA, see SAO PAULO

*Abbreviation assigned by NSSDC.
**Estimated by adding and subtracting 4 hours from the approximate time of solar meridian passage.

TABLE 1 (continued)

UNIVERSITY PARK, see PENNSYLVANIA STATE UNIVERSITY

UPPER VAN NORMAN / UVN* / 34N, 118W / 16-24**
100,000 / MP / 67- / WDC-A

USSURIJSK, Ussurisk, Voroshilov / USS, VORO / 43N, 132E / 23-3
208 / B, F / 59- / QBSA, WDC-A, SGD

VILLA ELISA / VEL* / 34S, 58W / 12-20**
2695 / F / 67-68 / WDC-A
10-210 / SP / 66-67 / WDC-A

VOROSHILOV, see USSURIJSK

WALTHAM, see PROSPECT HILL

WASHINGTON STATE UNIVERSITY, see PULLMAN

WEISSENAU, Tubingen / WEI / 47N, 9E / 7-16, 8-15
1000 / B, F / 68- / WDC-A
611 / B, F / 68- / WDC-A
30-1000 / SP / 68- / SGD, WDC-A
46-540 / SP / 66-69 / QBSA, WDC-A

ZIMENKI, see GORKY

Abbreviations for Sources:

QBSA - Quarterly Bulletin on Solar Activity
SGD - Solar-Geophysical Data
WDC-A - World Data Center A Catalogue of Data on Solar-Terrestrial Physics
G&SD - Geophysics and Space Data Bulletin

*Abbreviation assigned by NSSDC.
**Estimated by adding and subtracting 4 hours from the approximate time of solar meridian passage.

TABLE 2

OBSERVATORIES MAKING FLUX MEASUREMENTS

| Frequency (MHz) | Observatory* |
|---|---|
| 35,000 | Tokyo |
| 19,000 | (Gorky-V) |
| 17,000 | Tokyo |
| 15,400 | Sagamore Hill |
| 15,000 | Kislovodsk-P |
| 10,700 | Pennsylvania State University |
| 9,530 | (Naval Research Laboratory) |
| 9,500 | Tokyo, Irkutsk-P |
| 9,490 | Heinrich Hertz Institute |
| 9,400 | Prague, Nagoya-P |
| 9,375 | (Pulkovo) |
| 9,140 | Neustrelitz |
| 9,100 | Gorky |
| 8,800 | Manila, Sagamore Hill |
| 7,000 | Sao Paulo |
| 6,100 | Kislovodsk-P |
| 4,995 | Manila, Sagamore Hill |
| 3,800 | Gorky |
| 3,750 | Nagoya-P |
| 3,200 | (Naval Research Laboratory) |
| 3,100 | Crimea |
| 3,000 | Tokyo, (Jodrell-V) |
| 2,980 | (Athens) |
| 2,950 | Gorky-V |
| 2,800 | Ottawa |
| 2,700 | Penticton |
| 2,695 | Manila, Sagamore Hill, Villa Elisa |
| 2,690 | Pennsylvania State University |
| 2,000 | Delhi, Nagoya-P, Neustrelitz, (Jodrell) |
| 1,490 | Heinrich Hertz Institute, Neustrelitz |
| 1,415 | Kiel, Manila, Sagamore Hill, (Sydney) |

*Stations in parentheses are not operational at present; P or V indicates polarization or variability indices given, respectively.

TABLE 2 (continued)

| Frequency (MHz) | Observatory* |
|---|---|
| 1,000 | Nagoya-P, Weissenau, (Crimea) |
| 960 | Pennsylvania State University |
| 930 | Bordeaux |
| 810 | (Cracow-V) |
| 808 | Prague-V |
| 650 | Gorky-V |
| 612 | Tokyo |
| 611 | Weissenau |
| 606 | Sagamore Hill |
| 600 | Uccle-V, (Moscow, Sydney) |
| 545 | (Moscow-V, Paramaribo) |
| 536 | Prague-V |
| 520 | (Toronto) |
| 500 | Hiraiso, (Hollandia) |
| 467 | (NBS, now NOAA) |
| 430 | (Cornell) |
| 420 | Kiel |
| 408 | Osservatorio di Fisica Cosmica |
| 328 | Pennsylvania State University |
| 327 | Bologna |
| 261 | Prague |
| 240 | Kiel |
| 239 | Trieste |
| 234 | Potsdam-V, (Pirkuli) |
| 231 | (Prague-V) |
| 227 | Tokyo-V, P |
| 225 | Oslo-V, (Arcetri) |
| 223 | Seattle |
| 221 | Abastumani |
| 220 | Crimea-V, (Riga) |

*Stations in parentheses are not operational at present; P or V indicates polarization or variability indices given, respectively.

TABLE 2 (continued)

| Frequency (MHz) | Observatory* |
|---|---|
| 210 | Kiev |
| 209 | Irkutsk-V, (Abastumani-V, Bjurakan) |
| 208 | Ussurijsk |
| 202 | Moscow-V |
| 201 | (Cornell-V) |
| 200 | Gorky, Hiraiso-V, Netherlands-V, P, (Jodrell, Hollandia), Paramaribo, Tokyo-V, P, Oslo-V |
| 191 | (Bjurakan-V) |
| 186 | (Arcetri) |
| 178 | Kislovodsk-V, (Cavendish) |
| 169 | (I.R.S.A.C.-V, Uccle, Lwiro) |
| 167 | (NBS, now NOAA) |
| 150 | (Chalmers Institute of Technology) |
| 127 | Torun-V |
| 111 | Potsdam |
| 100 | Gorky-V, (Tokyo) |
| 81 | (Cavendish-V) |
| 80 | (Jodrell-V) |
| 67 | (Tokyo) |
| 36 | (Bonn) |

*Stations in parentheses are not operational at present; P or V indicates polarization or variability indices given, respectively.

TABLE 3

OBSERVATORIES MAPPING THE SUN

| Type | Frequency (MHz) | Observatory |
|---|---|---|
| Strip scan | 4,000 | Nagoya |
| Strip scan | 2,800 | Ottawa |
| Strip scan | 1,420 | Sydney |
| Strip scan | 690 | Sydney |
| Strip scan | 408 | Nancay |
| Strip scan | 252 | Netherlands |
| Strip scan | 222 | Seattle |
| Strip scan | 169 | Nancay |
| Strip scan | 136 | Netherlands |
| Map | 100,000 | Upper Van Norman |
| Map | 35,000 | Prospect Hill |
| Map | 2,700 | Stanford |
| Map | 1,420 | Sydney |

TABLE 4

OBSERVATORIES LISTING SINGLE FREQUENCY BURSTS

| Frequency (MHz) | Observatory* |
|---|---|
| 71,000 | Slough |
| 35,000 | Bonn, Tokyo |
| 19,000 | Slough |
| 17,000 | Tokyo |
| 15,400 | Sagamore Hill |
| 15,000 | Kislovodsk |
| 10,700 | Pennsylvania State University |
| 9,530 | (Naval Research Laboratory) |
| 9,500 | Irkutsk, Netherlands, (Tokyo) |
| 9,490 | Heinrich Hertz Institute |
| 9,400 | Nagoya, Prague, Slough |
| 9,375 | (Pulkovo) |
| 9,140 | Neustrelitz |
| 9,100 | Gorky |
| 8,800 | Manila, Sagamore Hill |
| 7,000 | Sao Paulo |
| 6,100 | Kislovodsk |
| 4,995 | Canary Islands, Carnarvon, Houston, Manila, Sagamore Hill |
| 3,850 | Gorky |
| 3,750 | Nagoya |
| 3,200 | (Naval Research Laboratory) |
| 3,100 | Crimea |
| 3,000 | Heinrich Hertz Institute, Netherlands, (Tokyo, Jodrell) |
| 2,980 | (Athens) |
| 2,950 | Gorky |
| 2,920 | Neustrelitz |
| 2,800 | Ottawa, Slough |
| 2,700 | Penticton |
| 2,695 | Canary Islands, Carnarvon, Houston, Manila, Sagamore Hill |
| 2,690 | Pennsylvania State University |

*Stations in parentheses are not in operation.

TABLE 4 (continued)

| Frequency (MHz) | Observatory* |
|---|---|
| 2,000 | Heinrich Hertz Institute, Nagoya, Neustrelitz, (Jodrell) |
| 1,490 | Heinrich Hertz Institute |
| 1,420 | Canary Islands, Carnarvon, Houston, Kiel, Sydney |
| 1,415 | Manila, Sagamore Hill |
| 1,000 | Nagoya, Weissenau, (Crimea) |
| 960 | Pennsylvania State University |
| 930 | Bordeaux |
| 900 | (Heinrich Hertz Institute) |
| 810 | (Cracow) |
| 808 | Prague |
| 650 | Gorky |
| 612 | Tokyo |
| 611 | Weissenau |
| 610 | Netherlands |
| 606 | Sagamore Hill |
| 600 | Sydney, Uccle, (Moscow) |
| 545 | (Netherlands, Paramaribo, Moscow) |
| 536 | Prague |
| 500 | Hiraiso, (Hollandia, Ottawa, Toronto) |
| 486 | Washington State University |
| 467 | (NBS, now NOAA) |
| 430 | (Cornell) |
| 420 | Kiel |
| 408 | Osservatorio di Fisica Cosmica |
| 328 | Pennsylvania State University |
| 327 | Bologna |
| 326 | Tokyo |
| 320 | (Toronto) |
| 260 | Prague |
| 250 | Netherlands |
| 240 | Kiel |
| 239 | Trieste |
| 234 | Potsdam, (Pirkuli) |
| 231 | Prague |
| 227 | Tokyo |

*Stations in parentheses are not in operation.

TABLE 4 (continued)

| Frequency (MHz) | Observatory* |
|---|---|
| 225 | Oslo, (Arcetri) |
| 221 | Abastumani, Seattle |
| 220 | (Crimea), (Riga) |
| 208 | Crimea, Ussurijsk, (Irkutsk) |
| 202 | Moscow |
| 201 | (Cornell) |
| 200 | Hiraiso, Netherlands, Tokyo, (Hollandia, Honolulu, Jodrell, Paramaribo, Oslo) |
| 191 | (Bjurakan) |
| 186 | (Arcetri) |
| 184 | NOAA |
| 178 | (Cavendish, Kislovodsk) |
| 169 | (I.R.S.A.C., Lwiro, Uccle) |
| 167 | (NBS, now NOAA) |
| 150 | (Chalmers Institute of Technology |
| 127 | (Torun) |
| 125 | Rhodes University |
| 111 | Potsdam |
| 108 | (NOAA) |
| 107 | (Haleakala) |
| 100 | Gorky, Kodaikanal, (Tokyo) |
| 81 | (Cavendish, Giza) |
| 80 | (Jodrell) |
| 67 | (Tokyo) |
| 60 | (Macao) |
| 50 | (Ottawa) |
| 30 | (Hyderabad) |
| 27 | HAO, (Manila, Rome) |
| 23 | Potsdam |
| 18 | HAO, Manila, McMath-Hulbert, (Grafton, Haleakala, Rome, Sacramento Peak) |

*Stations in parentheses are not in operation.

TABLE 5

OBSERVATORIES MAKING BURST SPECTROGRAMS

| Frequency Band (MHz) | Observatory* |
|---|---|
| 3,900 - 2,100 | (Harvard) |
| 2,000 - 8 | Culgoora |
| 1,000 - 450 | (Big Pine) |
| 580 - 10 | Harvard |
| 580 - 100 | (McMath-Hulbert) |
| 540 - 46 | Weissenau |
| 250 - 10 | (Sydney) |
| 210 - 10 | Culgoora, Villa Elisa |
| 80 - 7 | HAO |
| 41 - 19 | Sagamore Hill |
| 41 - 7.6 | HAO |

*Stations in parentheses are not in operation.

## SOLAR OPTICAL DATA

The photosphere emits 99% of the total solar radiant flux with a black-body spectrum that peaks at 5500 A, near the center of the optical wavelength band. Weaker chromospheric and coronal optical emissions are observed either over the solar disk using a characteristic spectral line or over the limb in white light with the solar disk occulted. Extensive discussions of solar optical emissions and observational techniques are found in Zirin (1966). Ward (1956) gives a comprehensive discussion of solar optical phenomena and the various indices of solar activity.

Solar optical data are conveniently divided into six basic types associated with sunspots, plages, magnetic fields, flares, hydrogen $\alpha$ emission, and the corona. A worldwide network of observatories performs one or more of these observations. The WDC-A Catalogue of Data on Solar-Terrestrial Physics lists these observatories and their locations and normal temporal coverage since 1957. Figure 9 is a map that locates the observatories.

### Sunspots

Sunspots, first observed in the fourth century B.C., are optically dark photospheric regions of low temperature and high magnetic field. The occurrence and characteristics of sunspots exhibit an 11-year periodicity. Individual sunspots are frequent, but most spots appear in groups (solar active regions). Comprehensive discussions of sunspots and observational techniques are given by Bray and Loughhead (1965) and by Zirin (1966).

The most common index of solar activity throughout the history of solar observation is the sunspot number. The Wolf sunspot number was introduced in 1848 to give a quantitative measure of solar activity. The Wolf number was defined as $R = 10g+f$, where g is the number of spot groups observed and f is the number of individual spots observed. Despite the increase in the observing capability of modern telescopes, the current relative sunspot number definition assures continuity with the Wolf number. Relative sunspot numbers are now defined as $R = K(10g+f)$, where K is an observatory-dependent factor that effects the change of scale required to assure continuity.

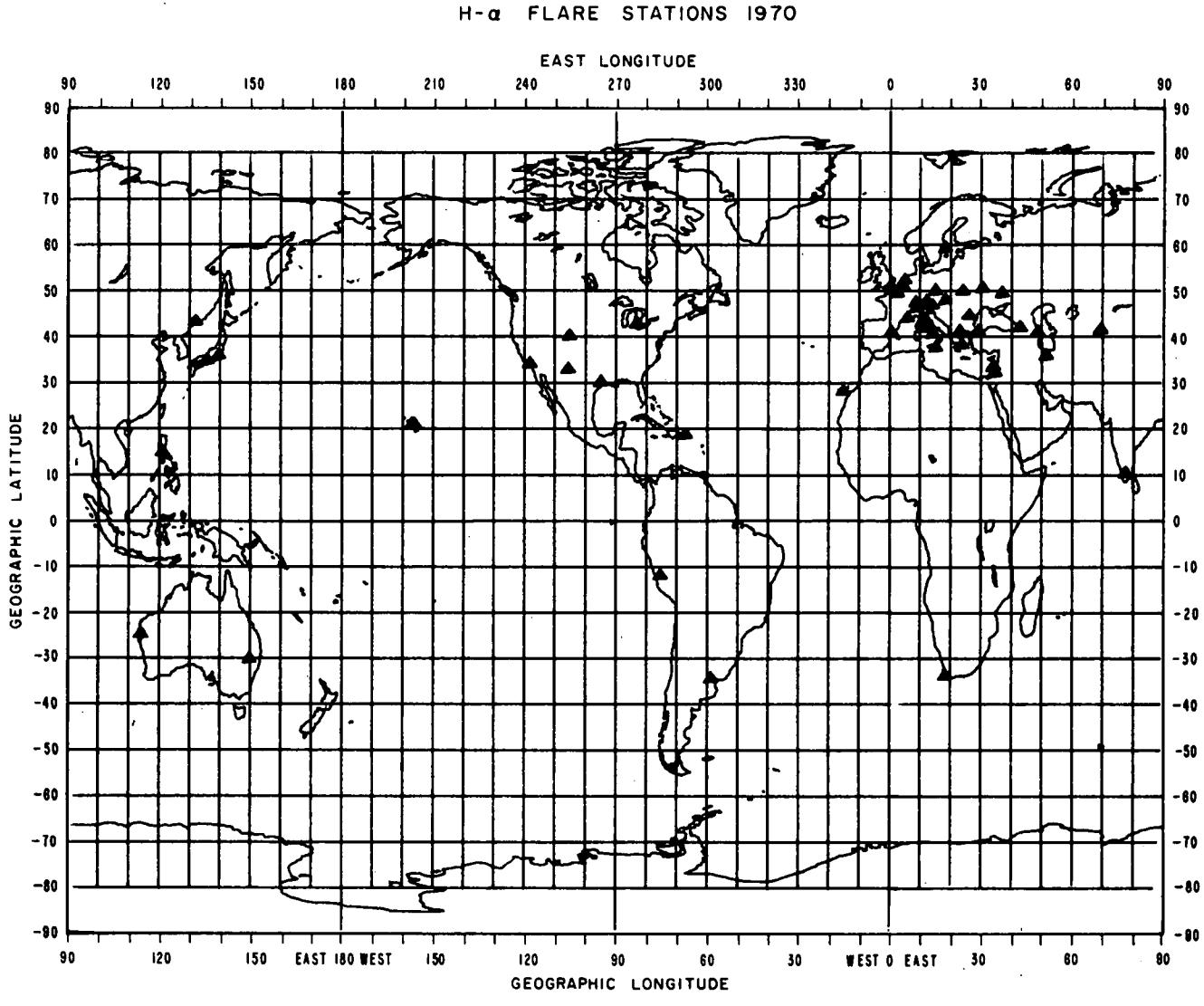


Figure 9. Map of Observatories for Solar Optical Data

The Zurich relative sunspot number, $R_z$, is the most widely used form of the normalized set of sunspot numbers. It is based principally on the observations of three sites of the Swiss Federal Observatory, and, when necessary, on data supplied by a number of international sites (Waldmeier, 1961).

Daily $R_z$ values are published in the IAU Quarterly Bulletin on Solar Activity and in Solar-Geophysical Data. These numbers are also available for the period 1932 to the present on the magnetic tape generated by the European Space Research Organization. This tape also contains many geomagnetic indices (Lenhart, 1968). Copies of this tape are held at WDC-A for Upper Atmosphere Geophysics, WDC-A for Geomagnetism, and at NSSDC. The relative sunspot numbers, as well as the sunspot area, published in the Quarterly Bulletin on Solar Activity from January 1957 to December 1967 are kept on 35-mm microfilm at NSSDC and are updated as new data become available. Daily values of $R_z$ and $R_A$ (the American relative sunspot number) are held on punched cards at WDC-A, Boulder, for the period October 1965 to the present.

Yearly and monthly means of Zurich relative sunspot numbers for the periods 1700 to 1960 and 1749 to 1960, respectively, are tabulated and plotted in Waldmeier (1961). This comprehensive work also contains tabulations and plots of daily sunspot numbers for the period 1818 to 1960 and epochs of minima and maxima of sunspot activity from 1610 to 1960. The remaining data (1960 to present) can be found, with a few exceptions, in Solar-Geophysical Data and in the Journal of Geophysical Research (until February 1969).

Daily sunspot numbers, obtained by 48 stations for various years between 1957 and the present, are kept on hard copy at WDC-A, Boulder. The complete station list and more detailed information on the availability and coverage of the data are given in the WDC-A Catalogue of Data on Solar-Terrestrial Physics.

In addition, 22 observatories provide tabulated data on the position, area, and classifications of sunspots. Two of these sites, Boulder and Mt. Wilson, also prepare daily solar hemisphere maps depicting the position and size of sunspot groups (figure 10). Both the tabulated data and the hemisphere maps, covering various years between 1957 and the present, are available on hard copy at WDC-A, Boulder. The WDC-A Catalogue of Data on Solar-Terrestrial Physics should be consulted to determine the coverage for each station. Some of the data from the 22 stations are selected to be published monthly in Solar-Geophysical Data and in the USSR Academy of Sciences Solar Data. Starting with January 1969, data on the solar active regions from Solar-Geophysical Data have been placed on magnetic tape and are available through WDC-A, Boulder. For the period February 1927 to December 1947, sunspot count,

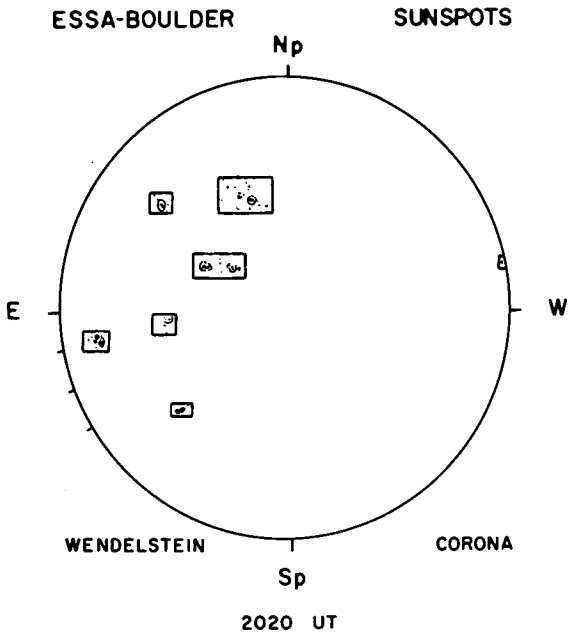


Figure 10. Daily Solar Hemisphere Map Depicting Position and Size of Sunspot Groups

position, and area data prepared by the U.S. Naval Observatory, Washington, D.C., were published in the Monthly Weather Review. From 1948 to the present, the "Positions, Areas, and Counts of Sunspots for (Month, Year)" reports were published by the U.S. Naval Observatory in the form of monthly circulars and can be obtained from the observatory or, through May 1969, from NSSDC.

Sunspot groups that meet certain criteria (maximum area during disk passage > 500 millionths of solar hemisphere, α or β magnetic classification, and/or associated with a major solar flare) have been isolated, and data on these groups have been published for the years 1954 to 1963 in the NASA/MSC Catalogue of Solar Activity. Some of the parameters, given in tabulated form, are the Mt. Wilson sunspot group identification number, the Greenwich sunspot group identification number, the McMath plage number, the sunspot group mean latitude and Carrington longitude during disk passage (see Coordinate Systems section, Part VIII, in this Handbook), the maximum area of the group in millionths of the solar hemisphere, the mean area of the group, the mean magnetic class and field strength, the Zurich and Mt. Wilson classifications for each day during disk passage, and the date on which the sunspot group was first observed.

Photographs of the solar disk taken by the White-Light Photographic Patrol at Sacramento Peak Observatory, New Mexico, are used to obtain information about sunspots and sunspot groups. These data are published in tabulated form in the Geophysics and Space Data Bulletin and cover the period 1964 to the present. Among the parameters given are the time of observation, the Zurich classification, the total number of spots in each group, the coordinates of the center of mass of each group under study, the ratio of total sunspot area (umbra + penumbra) to total umbral area, and the quality of the frame.

"Royal Observatory Bulletins," which are published annually in issues of Photoheliographic Results, give information about sunspots and sunspot groups as a function of solar rotation number. The bulletins give the daily positions and areas of sunspots, the compilations of sunspot group parameters (duration, area, and position), the daily total areas of sunspots and faculae by hemisphere, and the mean areas and latitudes of sunspots and faculae. WDC-A, Boulder, has copies of these publications covering the period 1951 to 1960.

The Solar Activity Summaries (1951-1959) and the Preliminary Reports of Solar Activity (1960 to the present), prepared by the High Altitude Observatory, Boulder, Colorado, give summaries of solar activity as a function of solar rotation number. The data, generally depicted on a Mercator-type map, include the location and size of sunspots and sunspot groups along with other parameters of solar activity.

In some reports the spot area and count of sunspot groups are tabulated along with such parameters as the flare index, the solar radio noise, the plage area, and the coronal emission for specific solar rotation numbers. Copies of these reports are kept at WDC-A, Boulder, and at NSSDC in hard-copy form.

Visual observations of the solar disk and drawings of the observed sunspot distribution are made by several different observatories; two of these, Boulder and Mt. Wilson, have already been mentioned. A third such site is the Fraunhöfer Institut in Germany, which publishes daily hemispheric maps of the solar disk depicting various phenomena, such as the location and size of sunspot groups associated with the active sun. Duplicates of these maps in hard-copy form for January 1957 to June 1961 and January 1962 to the present are available through WDC-A, Boulder.

The Trieste Astronomical Observatory in Italy prepares white-light visual sunspot drawings; the data, however, are extracted from these pictures before publication and given in tabulated form in the Geophysics and Space Data Bulletin. The parameters listed include the time and quality of observation, the total number of observed sunspot groups, the total number of spots observed, an adjusted (K = .91) relative sunspot number, and the sky conditions at the time of observation.

## Plages

The chromospheric fine structure around sunspots is marked by bright areas called flocculi or plages. When viewed using the K line of calcium, these areas are called calcium plages. Further details on plages, as well as details on observational techniques (spectroheliographs), may be found in Zirin (1966) and in Kuiper (1953).

Data from daily calcium plage observations made by the McMath-Hulbert Observatory are available through WDC-A, Boulder, and include the date of observation, the viewing quality, the wavelength used for the observation, the plage area number, a subjective activity index value, the complete position coordinates, the total area of the associated faculous region, the total area of sunspots in the active region, and an estimate of the plage intensity. WDC-A, Boulder, has data on 16-mm microfilm for January 1955 through 1967 and punched card data for 1962 to 1964 and for February 1968 to the present.

Monthly summaries of the McMath-Hulbert plage observations for 1962 to 1968 and January 1969 to the present can be obtained from WDC-A, Boulder, on punched cards and magnetic tape, respectively. The summaries, containing generally the same parameters as the daily reports, are also available in Solar-Geophysical Data for January 1955 to the present.

Data related to plage regions which meet specific criteria of size, intensity, and flare activity from 1954 through 1963 are given in the NASA/MSC Catalogue of Solar Activity. This publication lists, among other parameters, the McMath plage number, the plage category, the mean latitude during disk passage, the date first observed, the number of days visible, the average maximum area, the intensity on a 1 to 5 scale of the total number of flares during the disk passage of the plage, the Mt. Wilson sunspot group identification numbers of all spot groups covered by the plage, and the Mt. Wilson magnetic classification of the sunspot groups.

Visual observations of calcium plage distribution are made on a daily basis at McMath-Hulbert Observatory and are published as hemispheric maps (see figure 11) in Solar-Geophysical Data. Alongside each map is a listing of the plage regions (ordered according to region number), a subjective scaling of the plage intensity (1 to 5), the area in millionths of the solar disk, and the quality of the observation. When sky conditions have prevented the McMath-Hulbert Observatory from observing the plage regions, the Catania Astrophysical Observatory at Catania, Italy, has supplied available drawings. Similar but more complete maps of solar activity (including plages) are made by the Fraunhöfer Institut and are available through WDC-A, Boulder, for the periods from January 1957 to June 1961 and from January 1962 to the present. All of the above maps that are available from WDC-A are in hard-copy form.

Photographs taken in calcium K light (3933.7 A) on a daily basis by the Rome Astronomical Observatory and published in the Photographic Journal of the Sun are kept on 35-mm microfilm at WDC-A, Boulder. The pictures, cataloged according to solar rotation number, cover the period from January 1968 to the present.

Plage data from several other observing sites, while more irregular in coverage and availability, generally contain some of the more basic parameters; however, the formats vary widely. For complete details concerning the location of these sites and the availability of such data at WDC-A, Boulder, the user should refer to the WDC-A Catalogue of Data on Solar-Terrestrial Physics.

## Solar Magnetic Fields

The solar magnetic field is approximately dipolar at high latitudes and is highly irregular at middle and low latitudes. This field apparently gives rise to a coupling between solar differential rotation and the 11-year cycle of solar activity; the field also governs the evolution

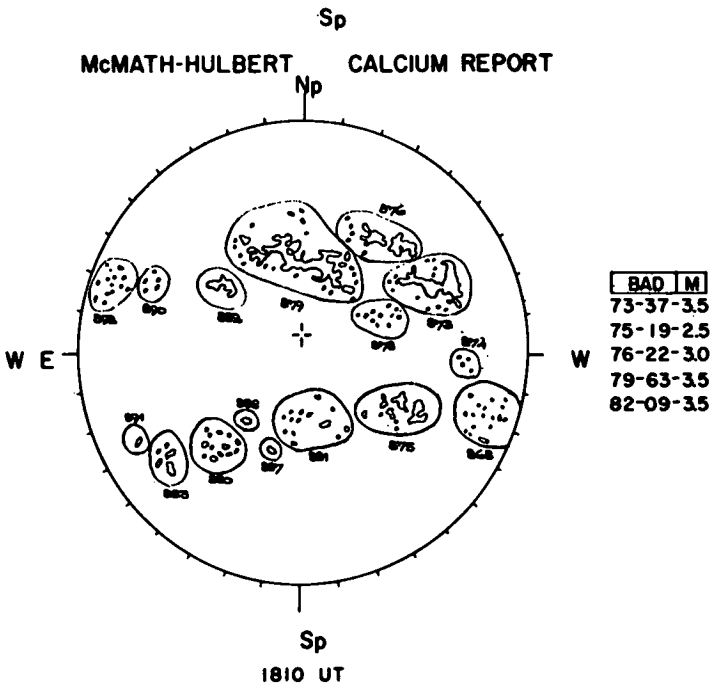


Figure 11. Sample of McMath-Hulbert Plage Data

of individual active regions. Field magnitudes range from a few gauss in quiet regions to a few thousand gauss in some active regions. Complete discussions of the solar magnetic fields appear in Bumba (1967) and Godoli (1967).

Longitudinal (line-of-sight) components of the solar magnetic field are measured by magnetographs which use the Zeeman effect. Magnetographs are discussed in von Klüber (1967) and in Zirin (1966).

The Mt. Wilson magnetograph uses the Fe(I) line ($\lambda$ 5250.216) and scans perpendicular to the solar central meridian with a resolution of 18 arc-seconds. A complete solar scan requires 1.5 hours. The results of these measurements are daily solar magnetograms, an example of which is shown in figure 12. These computer-plotted isogauss drawings use solid and dotted lines for positive and negative field polarities, respectively. (Magnitudes are read as shown.)

Since September 1966, daily Mt. Wilson magnetograms have been published in Solar-Geophysical Data; they are now being published 2 months after the time of observation. Large-scale (17-cm-diameter) copies of the daily magnetograms, as well as magnetic tapes containing the data from which the magnetograms are constructed, are available from WDC-A, Boulder.

## Flares

A flare is a short-lived sudden increase in the intensity of radiation emitted in the neighborhood of sunspots. It is best seen in H$\alpha$, and usually occurs in the chromosphere. Flares are characterized by a rise time of the order of minutes and a decay time of the order of tens of minutes. The total energy expended in a typical flare is about $10^{30}$ ergs; the magnetic field is extraordinarily high, reaching values of $10^2$ to $10^4$ gauss. Optical flares are usually accompanied by radio and X-ray bursts, or flares, and occasionally by high-energy particle emissions. The optical brightness and size of the flare are indicated by a two-character code called the importance. The first character, a number from 1 to 4, indicates the apparent area. For areas of less than 1, an "s" is used to designate a subflare. The second character indicates relative brightness: b for bright, n for normal, and f for faint. The most recent general discussion of solar flares is found in Smith and Smith (1963).

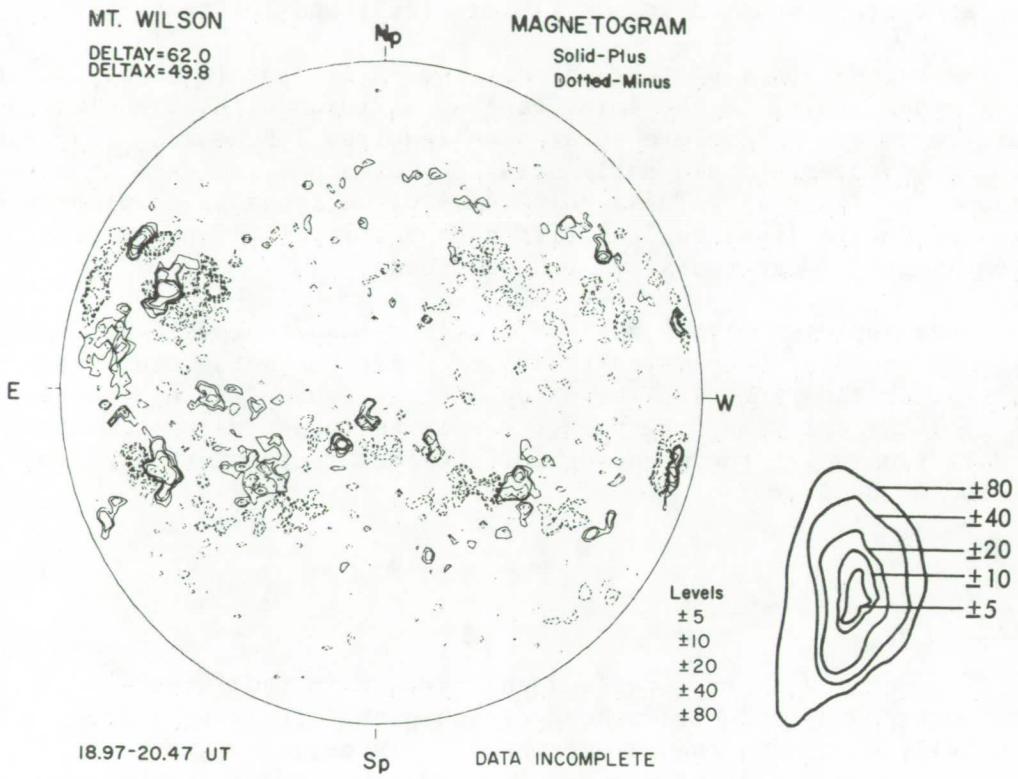


Figure 12. Daily Solar Magnetogram

Hydrogen-α solar flare data are collected by numerous solar patrol stations over the globe. The February 1970 Solar-Geophysical Data Descriptive Text lists 53 stations. Data from these stations are found in the Solar-Geophysical Data bulletin and in the IAU Quarterly Bulletin on Solar Activity.

The Solar-Geophysical Data bulletin contains two listings of solar flare reports--those published the month following the flare occurrence and those published 6 months after occurrence. The former list includes all reported flares of importance greater than one, giving the observatory, the date, the start time, the maximum and end times, the solar latitude and longitude, the McMath plage region, the duration in minutes, the importance, the observation condition and type, the area, and the maximum width of the Hα intensity. A 1-month listing of subflares is also provided indicating date, time, and location. A full discussion of these parameters is found in the Solar-Geophysical Data Descriptive Text which appears in February of each year.

The listing published in Solar-Geophysical Data 6 months after occurrence consists of those flare reports filtered according to a program used at the Observatoire de Paris, 92 Meudon, France, to produce the IAU Quarterly Bulletin on Solar Activity flare listing. The format of the 6-month listing is the same as that of the 1-month flare listing described above. The grouped flare data appearing in the 6-month listing are also available from WDC-A, Boulder, on punched cards and magnetic tape for the period 1955 to the present.

Written in French, the "Eruptions Chromospheriques" section of the IAU Quarterly Bulletin on Solar Activity contains flare data for approximately 14 months after flare occurrence.

## Hydrogen-Alpha Spectroheliograms

Hα spectroheliograms are generally taken with telescopes equipped with a half-angstrom bandwidth Halle filter as described in chapter 2 of Zirin (1966). Daily photographs of solar disk images 15 cm in diameter and sequence photographs of the same type taken at approximately 10-second intervals can be obtained from the World Data Center A for Upper Atmosphere Geophysics, which has taken over data formerly distributed by NASA's Solar Particle Alert Network.

## Solar Corona

The corona, the outer layer of the sun's atmosphere, is a hot plasma (1 to 2 million degrees K) consisting mainly of fully ionized hydrogen and helium with smaller amounts of heavier, highly ionized atoms. The high temperatures are apparently caused by the dissipation of sound waves and hydromagnetic waves generated below the corona.

There are three major spectroscopic components of importance in the corona. The first is the L or E (emission) component, which consists of 31 major emission lines lying between 3328 A and 10,728 A. Coexisting with this emission spectrum is a weak, continuous spectrum composed of two components: the K (electron) component and the F (dust) component. The E component, however, is the most widely used in determining coronal properties.

The various lines that comprise the emission component are generally divided into three classes based on the degree of excitation. Class I consists of the lowest excitation lines, which are most prominent near sunspot minimum and in regions of low activity. Class II lines are intense near plages and sunspots, particularly at sunspot maximum. The lines of Class III are less frequently seen, appearing only in regions of very high ionization such as around loop prominences and directly above large sunspots.

In practice, only the Class I red Fe X line ($\lambda$ 6374 A) and the Class II green Fe XIV line ($\lambda$ 5303 A) are observed on a regular basis by coronagraph stations. The distributions of the above two lines, as well as of the Class III yellow Ca XV line ($\lambda$ 5694 A) when bright enough, are studied throughout the entire solar cycle to obtain information on temperature variations in the corona.

More detailed accounts of the solar corona and its properties can be found in Shklovskii (1965), Rosch (1967), and Zirin (1966).

The coronagraph, which is used to observe the coronal emission lines, consists of a special telescope with an occulting disk placed at the focus of the objective lens to block out the direct light of the sun. For a comprehensive treatment of the theory and operation of the coronagraph refer to Zirin (1966), McMath (1953), and Evans (1953).

The World Data Center A, Boulder, has daily maps of the sun's corona, supplied by the Fraunhöfer Institut, for January 1957 through the present. In addition, WDC-A has the following coronal data available: numerous HAO reports that list coronal emission line intensities

as a function of solar rotation number for a variety of periods from 1961 to 1965, the IAU Quarterly Bulletin on Solar Activity from January 1957 to June 1966 (giving daily intensities and isophotes of coronal activity) and from July 1957 through December 1959 (giving coronal indices), and coronal line indices in Solar-Geophysical Data for July 1957 through December 1958 and daily charts with three intensity levels from January 1969 to the present.

Spectrographic coronal observations from 1964 to 1969 are given in the Geophysics and Space Data Bulletin.

## SOLAR X RAYS

Solar X-ray emissions, like solar radio emissions, originate from both thermal and nonthermal processes that take place primarily in the solar corona. Solar X-ray emissions can be divided into three components: the quiet sun component, the slowly varying component, and the burst component. Nonthermal X-ray emissions occur only in the hard X-ray emissions (photon energies greater than about 10 kev or wavelengths less than about 1 A) accompanying solar flares. Solar X-ray astronomy has been reviewed by Mandelshtam (1965), Underwood (1968), and Krimigis and Wende (1970).

Solar X rays are directly observed with satellite-borne detectors and indirectly observed through their effects on the ionosphere. The occurrences of solar X-ray bursts are indicated by the sudden ionospheric disturbances (SID) discussed in Part V of this Handbook.

Patrol types of solar X-ray measurements must be carried out using instruments flown on satellites. The resulting data that are available are listed on table 6. (All figures and tables for this section are included here beginning on page 61.) The first line of each experiment listing gives the satellite common name and the experimenter's affiliation. The second line gives the wavelength passband, in angstroms; the type of observations (B = burst listings, F = flux measurement listing, PL = flux plotted, and MAP = two-dimensional mapping); the years the experiment was operational (a blank after a year indicates that the apparatus is believed to be currently in operation); and the sources of the data. Some of the quoted passbands have recently been questioned (Wende, 1970). Because solar X-ray instrumentation must be flown on satellites, the data quite often contain periodic and significant time intervals when no data were obtained due to the satellite's being eclipsed.

Ion chambers, proportional counters, Geiger tubes, and scintillators are used to measure the integral solar X-ray flux within specific wavelength or energy passbands. A review of such instrumentation is given by Boyd (1965) and Neupert (1969), and some calibration techniques are discussed by Wende (1969).

## Flux Measurements

Solar X-ray fluxes, integrated over the entire solar disk in units of ergs $cm^{-2}$ $sec^{-1}$ over a specified passband, have been obtained from several satellites. These measurements are listed in table 7 ordered by passband, and the coverage is illustrated in figure 13. These data are occasionally presented in the form of plots of the X-ray flux as a function of time (e.g., Drake et al., 1969). These data are listed in table 8, and the coverage available is listed in figure 14. The X-ray fluxes are useful and sensitive indicators of the level of solar activity.

## Daily Maps of the X-Ray Sun

As of August 1969, X-ray spectroheliograms taken in the 9.1- to 10.50-A passband by an OSO 5 experiment have been printed with a 2-month lag time in Solar-Geophysical Data (Prompt Reports) by the University of Leicester/University College, London. A soft X-ray telescope of the type described by Giacconi and Rossi (1960) is being used, and a period of 5 minutes is required to scan the sun (32 arc-minutes in diameter) with an inherent spatial resolution of 1.6 arc-minutes. An example of such a spectroheliogram is given in figure 15.

## Burst Observations

Information on X-ray burst observations is given in table 9, and the coverage is illustrated in figure 16. X-ray burst data are presented in a manner similar to that of radio bursts. The data lists usually include the start time, the time of peak intensity, the end time or duration, and the maximum flux or ratio of peak flux to background flux, as well as descriptive remarks. Lists of observing times are given when there are significant time gaps in the data.

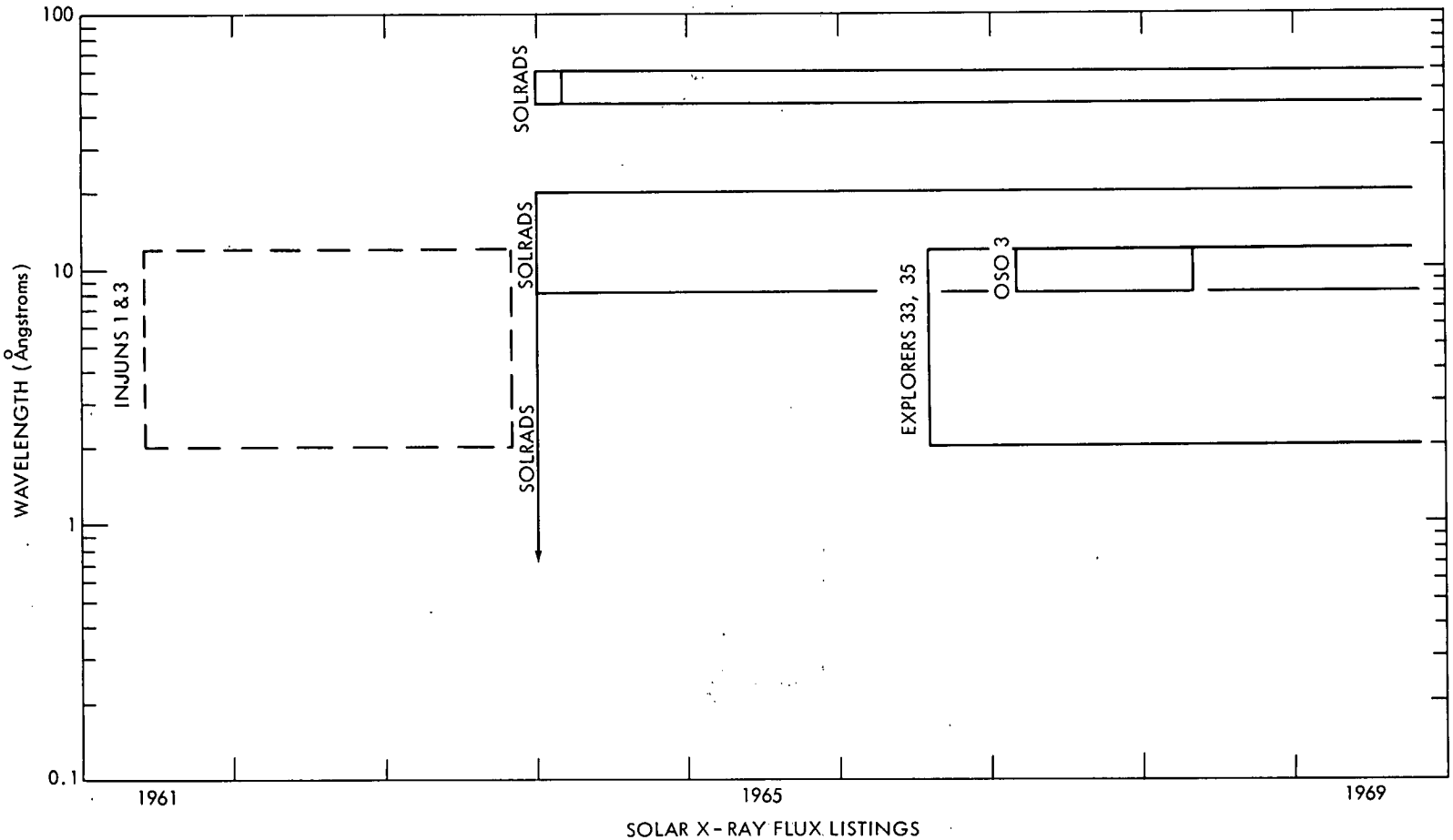


Figure 13. Solar X-Ray Flux Coverage

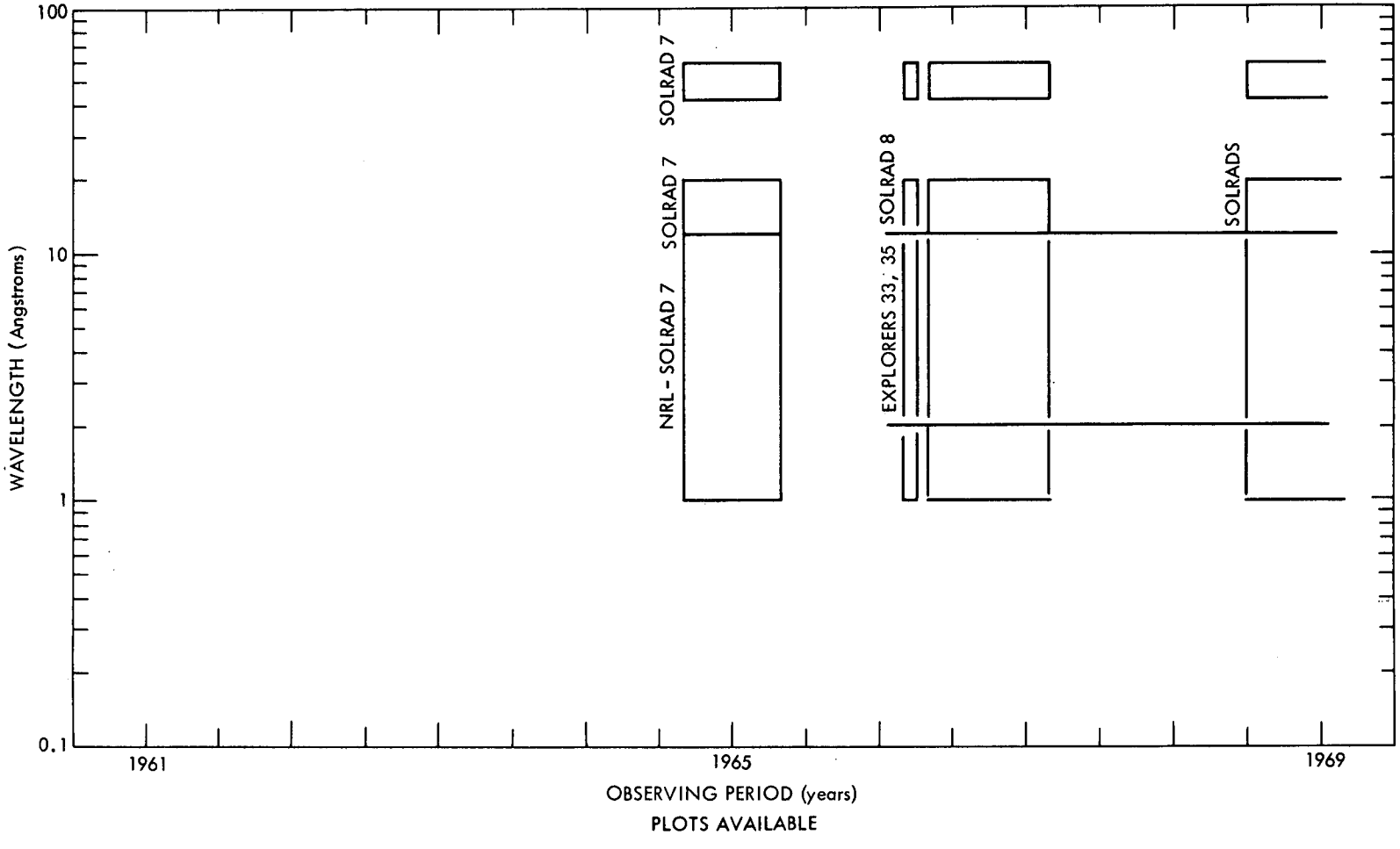


Figure 14. Coverage of Flux Plots

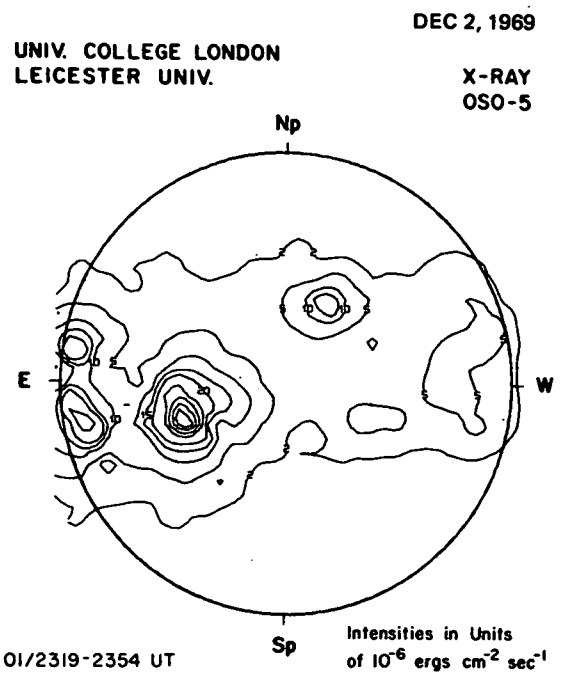


Figure 15. Example of a Spectroheliogram

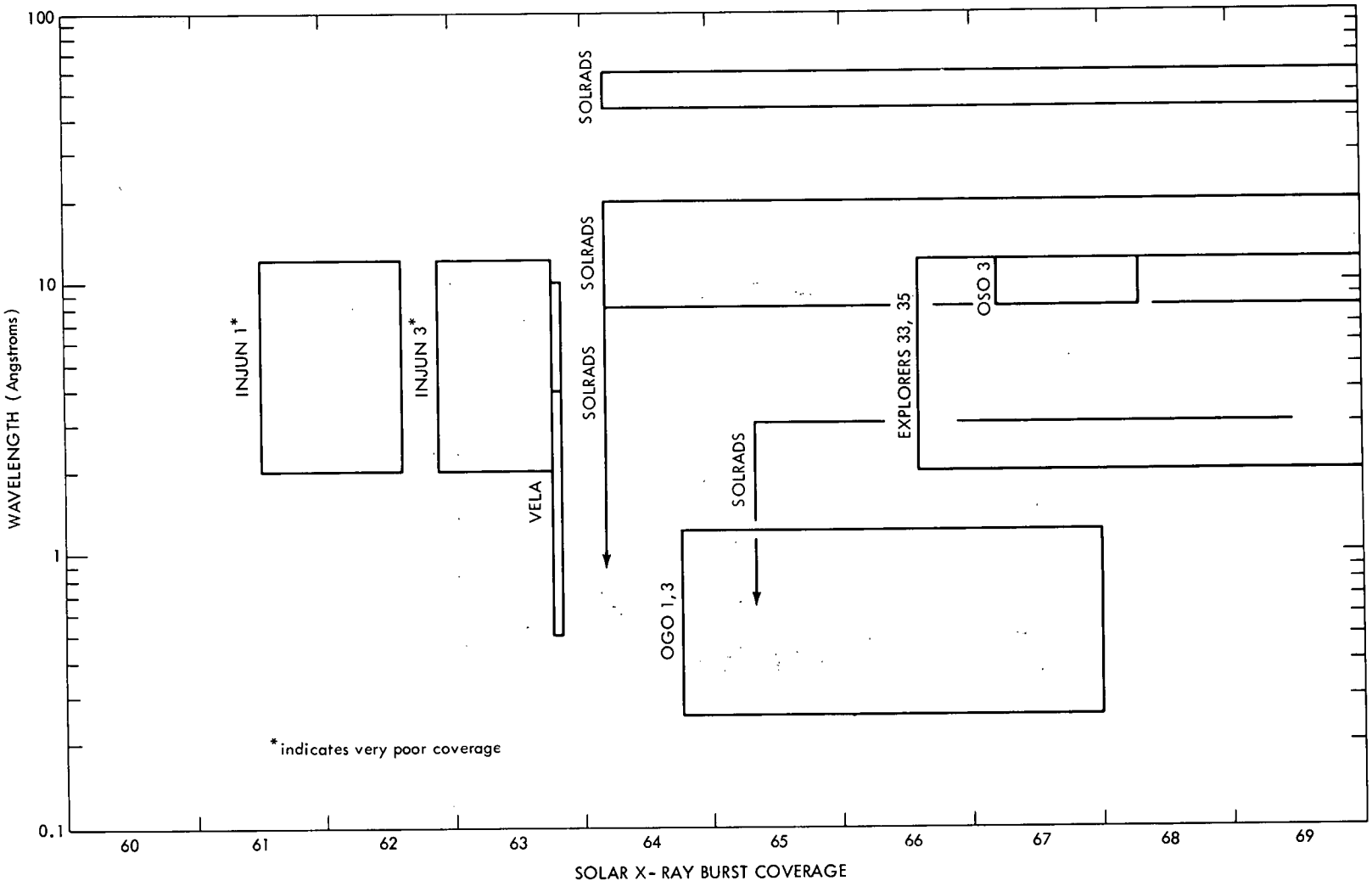


Figure 16. Coverage of X-Ray Burst Observations

TABLE 6

SOLAR X-RAY PATROLS

Spacecraft — Experimenter

EXPLORER 33, EXPLORER 35, UNIVERSITY OF IOWA
2-12 / B, F, PL / 7/66- / NSSDC, SGD (B only), WDC-A

Wavelength (A) — Type of Observation — Dates — Sources

EXPLORER 33, EXPLORER 35, UNIVERSITY OF IOWA
2-12 / B, F, PL / 7/66- / NSSDC, SGD (B only), WDC-A

INJUN 1, INJUN 3, UNIVERSITY OF IOWA
2-12 / F* / 6/61 - 10/63 / NSSDC, WDC-A

OGO 1, OGO 3, UNIVERSITY OF MINNESOTA
0.25-1.2 / B / 9/64 - 12/67 / NSSDC, WDC-A

OSO 3, UNIVERSITY OF MICHIGAN
8-12 / B, F / 3/67 - 4/68 / NSSDC, WDC-A (B only)

OSO 5, UNIVERSITY OF LEICESTER, UNIVERSITY COLLEGE, LONDON
9-10 / MAP / 9/69 / SGD, WDC-A

SOLRAD Series, NAVAL RESEARCH LABORATORY
44-60 / B, F, PL / 64- / SGD, WDC-A
8-20 / B, F, PL / 64- / SGD, WDC-A
0- 8 / B, F, PL / 64- / SGD, WDC-A
0- 3 / B / 65- / SGD

VELA 1, LOS ALAMOS SCIENTIFIC LABORATORY
0.5-4 / B / 8/63 / SGD, WDC-A
0.5-10 / B / 8/63 / SGD, WDC-A

*Data coverage very poor.

Sources:

WDC-A - World Data Center A for Upper Atmosphere Geophysics
NSSDC - National Space Science Data Center
SGD - Solar-Geophysical Data

TABLE 7

SOLAR X-RAY FLUX MEASUREMENTS
(Single Points or Time Averages)

| WAVELENGTH RANGE (ANGSTROMS) | SPACECRAFT, EXPERIMENT SPONSOR |
|---|---|
| 0 - 8 | SOLRADS, Naval Research Laboratory |
| 2 - 12 | Injuns 1 & 3, University of Iowa |
| 2 - 12 | Explorers 33 & 35, University of Iowa |
| 8 - 12 | OSO 3, University of Michigan |
| 8 - 20 | SOLRADS, Naval Research Laboratory |
| 44 - 60 | SOLRADS, Naval Research Laboratory |

TABLE 8

PLOTS OF SOLAR X-RAY FLUXES

| WAVELENGTH RANGE (ANGSTROMS) | SPACECRAFT, EXPERIMENT SPONSOR |
|---|---|
| 0 - 8 | SOLRADS, Naval Research Laboratory |
| 2 - 12 | Explorers 33 & 35, University of Iowa |
| 8 - 20 | SOLRADS, Naval Research Laboratory |
| 44 - 60 | SOLRADS, Naval Research Laboratory |

TABLE 9

SOLAR X-RAY BURST OBSERVATIONS

| WAVELENGTH RANGE (ANGSTROMS) | SPACECRAFT, EXPERIMENT SPONSOR |
|---|---|
| 0 - 3 | SOLRADS, Naval Research Laboratory |
| 0 - 8 | SOLRADS, Naval Research Laboratory |
| 0.25 - 1.2 | OGO 1 & 3, University of Minnesota |
| 0.5 - 4 | VELA, Los Alamos Scientific Laboratory |
| 0.5 - 10 | VELA, Los Alamos Scientific Laboratory |
| 2 - 12 | Explorers 33 & 35, University of Iowa |
| 8 - 12 | OSO 3, University of Michigan |
| 8 - 20 | SOLRADS, Naval Research Laboratory |
| 44 - 60 | SOLRADS, Naval Research Laboratory |

## REFERENCES


1. Boyd, R. L. F., "Techniques for the Measurement of Extraterrestrial Soft X-Radiation," Space Science Reviews, 4, 35-90, 1965.

2. Bray, B. J., and R. E. Loughhead, Sunspots, John Wiley and Sons, New York, 1965.

3. Bumba, V., "Observations of Solar Magnetic and Velocity Fields," Plasma Astrophysics, ed. P. A. Sturrock, Academic Press, New York, 77-120, 1967.

4. Drake, J. F., J. Gibson, and J. A. Van Allen, "Iowa Catalog of Solar X-Ray Flux (2-12A)," Solar Physics, 10, 433-459, 1969.

5. Evans, J. W., "The Coronagraph," The Sun, ed. G. Kuiper, University of Chicago Press, Chicago, 635-644, 1953.

6. Fokker, A. D., Ann. IQSY, 1, 31-39, 1968.

7. Giacconi, R., and E. Rossi, "Telescope for Soft X-Ray Astronomy," J. Geophys. Res., 65, 773-775, 1960.

8. Godoli, G., "On the Sun's Polar Magnetic Fields," Solar Physics, ed. J. N. Xanthakis, Interscience Publishers, London, 305-323, 1967.

9. Kraus, J. D., Radio Astronomy, McGraw-Hill, New York, 1966.

10. Krimigis, S. M., and C. D. Wende, "X-Ray Emissions from the Sun," Solar Eclipses and the Ionosphere, ed. M. Anastassiades, Plenum Press, New York, 1970.

11. Kuiper, G. P., ed., The Sun, University of Chicago Press, Chicago, 1953.

12. Kundu, M. R., Solar Radio Astronomy, Interscience Publishers, London, 1965.

13. Lenhart, K. G., "Geomagnetic and Solar Data for Use with Digital Computers," Trans. A.G.U., 49, 463-464, 1968.

14. Mandelshtam, L., "X-Ray Emission of the Sun," Space Science Reviews, 4, 587-665, 1965.

15. McMath, R. R., "Tower Telescopes and Accessories," The Sun, ed. G. Kuiper, University of Chicago Press, Chicago, 605-626, 1953.

16. Medd, W. J., and A. E. Covington, "Discussion of 10.7-cm Solar Radio Flux Measurements and an Evaluation of the Accuracy of Observations," Proc. IRE, 46, 112, 1958.

17. Neupert, W. M., "X-Rays from the Sun," Annual Reviews of Astron. and Astrophys., 7, 121-148, 1969.

18. Priese, J., "Absolute Calibration Method and Techniques of the Daily Patrol of the Flux Density at 1470 MHz," Solar Physics, 9, 235-240, 1969.

19. Rosch, J., "The Solar Corona," Solar Physics, ed. J. N. Xanthakis, Interscience Publishers, London, 423-445, 1967.

20. Shklovskii, I. S., Physics of the Solar Corona, Addison-Wesley Publishing Co., Inc., Reading, Mass., 1965.

21. Smith, H. J., and P. Smith, Solar Flares, Macmillan Co., New York, 1963.

22. Tandberg-Hanssen, E., Solar Activity, Blaisdell Publishing Co., Waltham, Mass., 1967.

23. Underwood, J. H., "Solar X-Rays," Science, 159, 383-390, 1968.

24. Von Klüber, H., "Spectroscopic Determinations of Solar Magnetic Fields," Solar Physics, ed. J. N. Xanthakis, Interscience Publishers, London, 255-304, 1967.

25. Waldmeier, M., The Sunspot Activity in the Years 1610-1960, Sculthess and Co., Zurich, 1961.

26. Ward, F. W., "Solar, Geomagnetic and Ionospheric Phenomena as Indices of Solar Activity," Geophysical Research Paper No. 54, AFCRL CR-56-213, Nov. 1956.

27. Wende, C. D., "Correlation of Solar Microwave and Soft X-Ray Radiation, 1, The Solar Cycle and Slowly Varying Components," J. Geophys. Res., 74, 4649-4660, 1969.

28. Wende, C. D., "The Normalization of Solar X-Ray Data from Many Experiments," EOS, 51, 820, 1970.

29. Wild, J. P., S. F. Smerd, and A. A. Weiss, "Solar Bursts," Annual Reviews of Astron. and Astrophys., 1, 291-366, 1963.

30. Zirin, H., The Solar Atmosphere, Blaisdell Publishing Co., Waltham, Mass., 1966.

# PART III

# SOLAR PROTONS

Prepared By

Joseph H. King and
Julius J. Brecht

CONTENTS

## INTRODUCTION

Significant numbers of charged particles, mainly electrons and protons, are accelerated at the sun during many solar flares. Some of these particles are subsequently detected within the interplanetary medium and at the earth. These particles serve as useful indicators of solar, terrestrial, and interplanetary conditions. Often, effects from these various regions are not separable, but in certain events they are. (See, for example, Cline and McDonald, 1968.) A recent review paper with extensive references is that of Kavanagh et al. (1970).

In addition to their relevance to scientific studies, particles with energies above about 10 Mev are also of interest because sufficiently large fluxes pose radiation hazards to space systems, particularly manned systems.

## SATELLITE OBSERVATIONS

### Solar Proton Monitoring Experiment

A series of Solar Proton Monitoring Experiments (SPME), initiated by scientists at Johns Hopkins University/Applied Physics Laboratory and at NASA Goddard Space Flight Center, is intended to provide reliable flux and spectral measurements of solar protons over at least half a solar cycle and over a wide flux range. Each SPME consists of an array of solid-state detectors that measure the combined counting rate due to fluxes of protons and alpha particles in each of the three energy ranges: $\geq$ 10 Mev/nucleon, $\geq$ 30 Mev/nucleon, and $\geq$ 60 Mev/nucleon. The alpha particle component is usually very small and may be thought of as introducing an ambiguity of less than 10% into the proton count rate. Further discussions of this point and of the SPME in general can be found in Kohl (1968) and in the "Descriptive Text" of Solar-Geophysical Data (February 1970).

The SPME packages have been successfully flown on the highly eccentric orbit Explorers 34 (IMP-F, May 24, 1967, to May 3, 1969) and 41 (IMP-G, June 21, 1969, to present, Oct. 1970) and on the 1100-km-altitude polar orbiting ITOS 1 (January 23, 1970, to present, Oct. 1970). These packages measure omnidirectional fluxes. A similar package is scheduled for launch on IMP-I (highly eccentric orbit) in early 1971.

From IMP data, hourly averaged fluxes are generated using up to 22 "good" data points for the $\geq$ 60-Mev and $\geq$ 30-Mev channels and up to 44 "good" data points for the $\geq$ 10-Mev channel. These hourly averages are published monthly in Solar-Geophysical Data, with a 6-month time lag. The data appear in the forms of plots and tabular listings.

## Pioneers 6 and 7

The counting rates of the galactic and solar cosmic-ray protons observed by the University of Chicago experiments (Fan et al., 1968) on Pioneers 6 and 7 (launched December 12, 1965, and August 11, 1966, respectively) have been published since April 1969, with a 1-month lag, in Solar-Geophysical Data. The rates are typically given once per day for each of three energy channels: 0.6 to 13 Mev, 13 to 175 Mev, and > 175 Mev. A letter flag indicates whether the flux was rising(R), steady(S), or falling(F) at the time when the fluxes were monitored. Information on geometrical factors and quiescent counting rates and on the effects of electron and alpha particle contamination is given as footnotes to the tabular data listing.

## Pioneers 8 and 9

The counting rates of the galactic and solar cosmic-ray protons observed by University of New Hampshire detectors on Pioneers 8 and 9 (launched December 13, 1967, and November 8, 1968, respectively) have been published since January 1970, with a 1-month lag, in Solar-Geophysical Data. Solid-state telescopes are used to measure protons above 13.9 Mev and 64 Mev on Pioneer 8 and above 13.9 Mev and 40 Mev on Pioneer 9. Typically, count rates are given about four times per day in a tabular listing.

In addition, hourly and daily averaged count rates are available in hard-copy form from Space Science Center, University of New Hampshire, Durham, New Hampshire. The time period of available data extends from launch until at least as recently as 1 year prior to the current date.

## ATS 1

Three Li-drifted cubical silicon detectors, designed by Aerospace Corporation personnel, separately measure omnidirectional electron and proton fluxes on ATS 1. The ATS 1 satellite was launched in December 1966 and placed into a geostationary orbit at 6.6 earth radii (geocentric) at 150° W longitude. The experiment is further described in Blake et al. (1968) and in the descriptive text of Solar-Geophysical Data.

Beginning in February 1970, Solar-Geophysical Data has published a tabular listing of the hourly averaged flux values, with a 1-month lag, for each of the two proton energy channels observed (5 to 21 Mev and 21 to 70 Mev).

# GROUND-BASED DATA

Solar protons reaching the polar cap regions cause enhanced ionization which in turn leads to enhanced radio wave absorption. Such events are referred to as Polar Cap Absorption (PCA) events. From a knowledge of the absorption characteristics, both qualitative and quantitative information about the incident solar protons can be gained. Techniques used in studying relevant ionization enhancements are described below.

## Riometer

The riometer detector is described in Part V of this Handbook. Polar cap riometer absorption is usually associated with incident solar proton flux (Adams and Masley, 1966). There are models relating riometer absorption readings for daytime polar cap absorption events to the corresponding particle flux above a given threshold energy. For example, Juday and Adams (1969) give the relationship between omnidirectional particle flux, $J(cm^{-2}sec^{-1})$, and riometer absorption reading, A, (in decibels) as

$$J(> 11 \text{ Mev}) \simeq 295\ A^2 \ (30 \text{ MHz})$$

for daytime measurements with essentially zero magnetic cutoff. The value of this proportionality constant has recently been called into question for early phases (through maximum) of events (Smart and Shea, 1970).

Several riometer stations are actively sending data to WDC-A for Upper Atmosphere Geophysics at Boulder, Colorado. The data are available in the form of strip charts or film copies of strip charts for the time periods from 1957 to present. The stations cover geographic latitudes from 54° N to 80° N and 66° S to 90° S and are listed in the WDC-A Catalogue of Data on Solar-Terrestrial Physics.

## Ionospheric Vertical Incidence Soundings

The ionospheric vertical incidence sounding experiments and resultant f-plots are described in Part V in the section on Ionosondes. The f-plots (especially f-min) can be used to indicate the presence of solar protons as Polar Cap Absorption events (Bailey, 1964). Data are available from WDC-A, Boulder, for the time period from 1957 to the present. The stations cover geographic latitudes from 58° N to 87° N and 66° S to 90° S. A list of the stations is given in the WDC-A data catalog, which also includes an indication of the completeness of time coverage from each station.

## VHF Forward Scatter

Information on the energy spectrum and temporal variations of incident protons and relativistic electrons can be derived from an analysis of the temporal and magnetic latitude dependences of the intensity of scattered radio waves (Bailey, 1964). See Part V of this Handbook for a more detailed explanation of the forward scatter technique. The WDC-A data catalog contains information about the very limited amount of forward scatter data available.

## REFERENCES


1. Adams, W., and A. J. Masley, "Theoretical Study of Cosmic Noise Absorption Due to Solar Cosmic Radiation," Planet. Space Sci., 14, 277-290, 1966.

2. Bailey, D. K., "Polar Cap Absorption," Planet. Space Sci., 12, 495-541, 1964.

3. Blake, J. B., G. A. Paulikas, and S. C. Freden, "Latitude-Intensity Structure and Pitch-Angle Distributions of Low-Energy Solar Cosmic Rays at Low Altitude," J. Geophys. Res., 73, 4927-4934, 1968.

4. Cline, T. L., and F. B. McDonald, "Relativistic Electrons from Solar Flares," Solar Physics, 5, 507-530, 1968.

5. Fan, C. Y., M. Pick, R. Pyle, J. A. Simpson, and D. R. Smith, "Protons Associated with Centers of Solar Activity and Their Propagation in Interplanetary Magnetic Field Regions Corotating with the Sun," J. Geophys. Res., 73, 1555-1582, 1968.

6. Juday, R. D., and G. W. Adams, "Relationships Between Riometer Absorption and Proton Intensity," Planet. Space Sci., 17, 1313-1319, 1969.

7. Kavanagh, L. D., Jr., A. W. Schardt, and E. C. Roelof, "Solar Wind and Solar Energetic Particles: Properties and Interactions," Reviews of Geophysics and Space Physics, 8, 389-460, 1970.

8. Kohl, J. W., "Solar Proton Monitoring," A.P.L. Technical Digest, 8, 2-9, Sept.-Oct. 1968.

9. Smart, D. F., and M. A. Shea, AFCRL, private communication, 1970.

# PART IV

# GEOMAGNETISM

Prepared By

Joseph H. King

CONTENTS

## INTRODUCTION

Large-scale current systems, mainly internal to and secondarily exterior to the earth, give rise to the geomagnetic field. These current systems possess temporal variability, which is reflected in geomagnetic variations. Extensive discussions of geomagnetism can be found in Sugiura and Heppner (1968), in Matsushita and Campbell (1967), and in Chapman and Bartels (1940).

## MAGNETOGRAMS, DIGITIZATIONS

Surface observations of the geomagnetic field and of its temporal variations have been made by a large number of observatories. A 269-member observatory list, containing geographic and geomagnetic coordinates of each station active for at least part of the 1957 to present time period, may be found in the WDC-A Catalogue of Data on Solar-Terrestrial Physics. A map of stations (figure 17) is included here to show the geographic extent of data coverage. By using the techniques discussed in McComb (1952), components of the geomagnetic field are measured by magnetographs and are exhibited as functions of time on

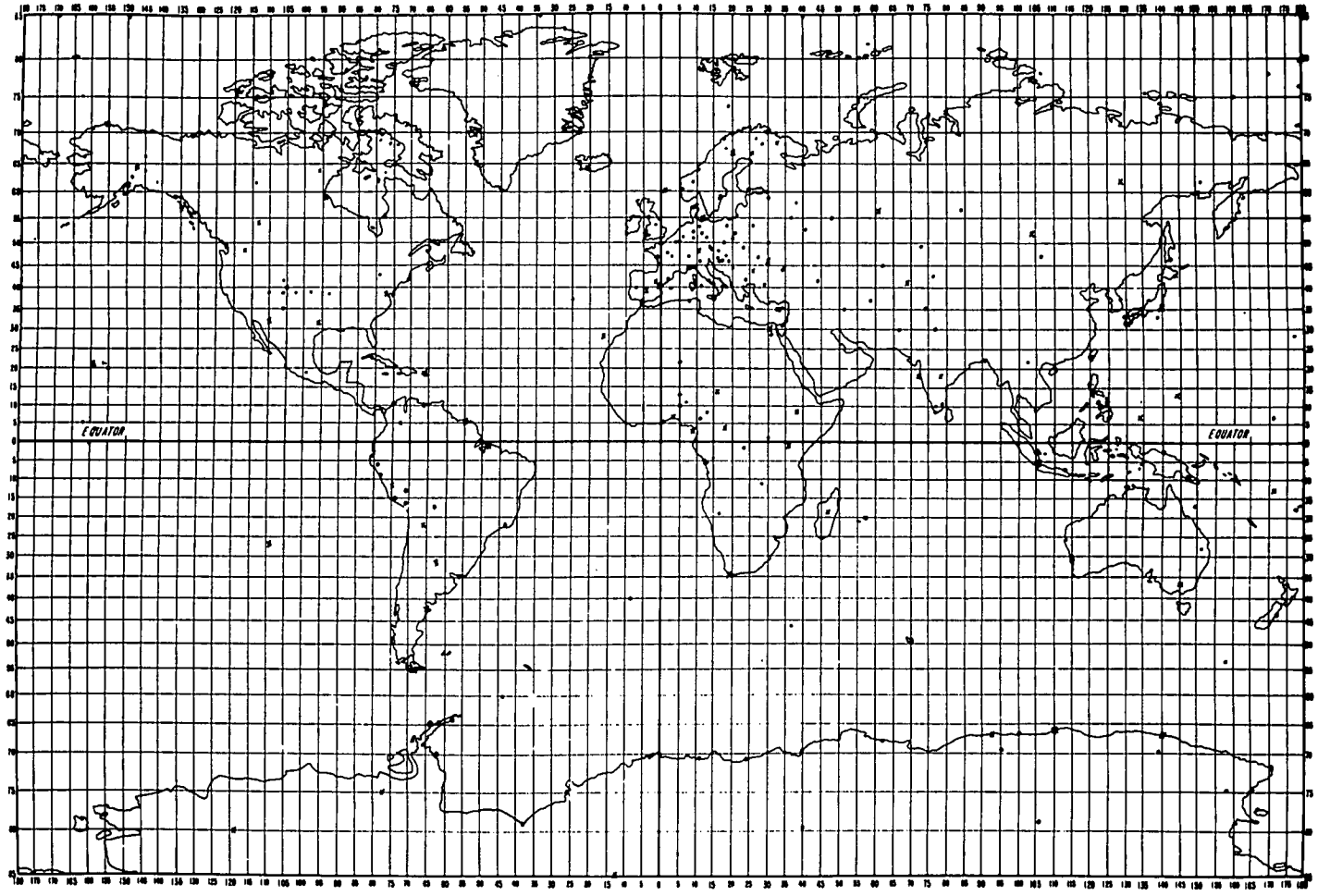


NOTE: Crosses indicate those stations whose magnetograms have been digitized, at least in part.

Figure 17. Map of Stations Making Geomagnetic Observations

magnetograms; a sample magnetogram is shown in figure 18. The magnetic components are defined using the local coordinate system shown in figure 19. In figure 19, F is the total magnetic vector, Z is its vertical component, H is its total horizontal component, D is its declination angle, and I is its inclination angle. The less often used X and Y are the horizontal north and east components, respectively, of H.

In the traces for each of the three components, fields arising from different sources can be distinguished. For example, the horizontal component H(t) can be written as

$$H = H_0 + Sq(H) + L(H) + D(H),$$

where $H_0$ is the main field with its secular variation, Sq(H) is the quiet daily solar variation in H, L is the quiet lunar variation in H (usually insignificant), and D(H) is the irregular variation in H (or the disturbance field H component). These variations and the subclassifications are well described in Chapman (1964).

Using station magnetograms, hourly averaged values of the magnetic components have been generated at some stations. Further, 2.5-minute digitized values of magnetic components are being generated from some station magnetograms at the National Oceanic and Atmospheric Administration/U.S. Coast and Geodetic Survey (NOAA)/(USCGS) as a joint undertaking of that organization and NASA (Cain et al., 1966). Annual means are also available.

WDC-A for Geomagnetism at Rockville, Maryland, has extensive holdings on microfilm of normal-run magnetograms (recording speed = 20 mm/hr), rapid-run magnetograms (4 mm/min), hourly averages, and station K indices described later in this part of the Handbook. WDC-A for Geomagnetism also holds magnetic tapes containing the 2.5-minute digitizations, hourly averages, and annual means. NSSDC holds copies of a subset of the WDC-A microfilms and copies of all of the tapes.

Lists of the available data since 1957 held by WDC-A for Geomagnetism are given by station in the WDC-A Catalogue of Data on Solar-Terrestrial Physics. Updated availability lists on the 2.5-minute digitizations are generated monthly and are available from Mr. Carl Absten, Geomagnetic Division, U.S. Coast and Geodetic Survey, NOAA, Washington Science Center, Rockville, Maryland 20852 (phone 301-496-8168). A list of data available from NSSDC will be provided on request. The actual data on either microfilm or tape can be obtained by writing Mr. William Paulishak, World Data Center A for Geomagnetism, Environmental Data Service, NOAA, Rockville, Maryland 20852 (phone 301-496-8160).

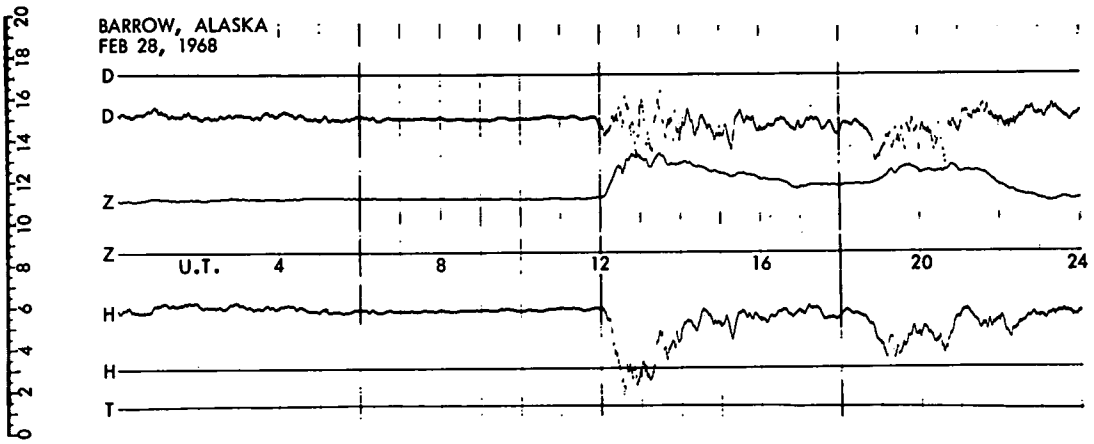


NOTE: Magnetogram generated at Point Barrow, Alaska, on February 28, 1968. The required scaling information is provided elsewhere on the microfilm from which this magnetogram was taken.

Figure 18. Sample Magnetogram

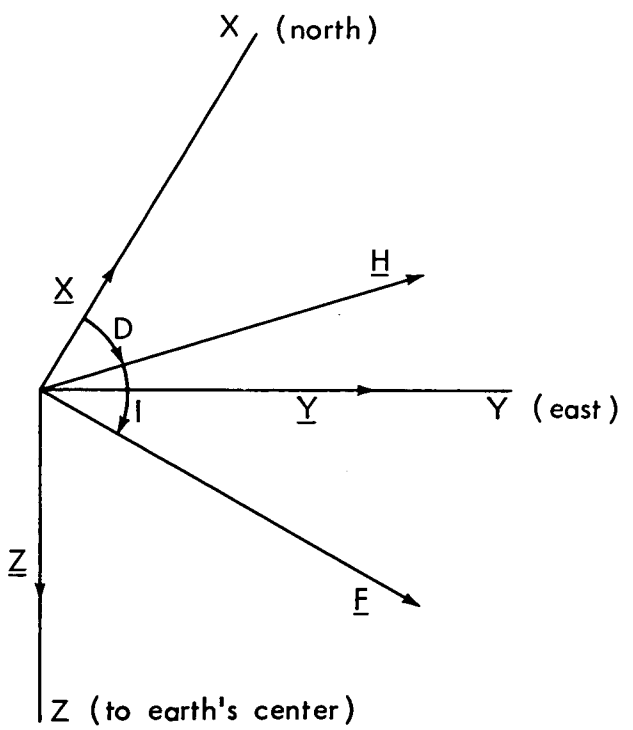


Figure 19. Local Coordinate System

# INDICES

A number of activity indices have been defined to facilitate the study of geomagnetic activity. Local indices are determined at individual geomagnetic observatories from station magnetograms. Planetary indices are obtained by performing appropriate worldwide averages of local indices. Detailed descriptions of many of the indices and their histories are given in Bartels (1957), Lincoln (1967), and Dwarkin and Mescher (1967). A functional diagram taken from Dwarkin and Mescher (1967), illustrating the relationships among some of the various geomagnetic activity indices, is given in figure 20.

## K Index

The K index, adopted in 1939, is intended to measure the geomagnetic effect of solar particle flux. The index is determined at individual stations for each 3-hour interval (UT) by using the magnetic trace from station magnetograms after subtracting the effects of the quiet daily solar variation (Sq), lunar variation (L), solar flare effects (Sqa), and the aftereffects of the disturbance field (DR; R for ring current).

For each field component in each 3-hour interval, a range, R, in gammas, is defined as the difference between the maximum and minimum values of the adjusted magnitude of the component observed in that time interval. McComb (1952) contains an equation by which the "component" D is converted from angular measure into a specified number of gammas. Then K is defined in terms of the largest of the three R values (two R values after 1964, the Z component being specifically excluded in this determination). The relation between R and K is defined by one of about 10 loosely logarithmic scales, in each of which K runs between 0 and 9. The appropriate scale is determined by the station latitude so that all stations will report a similar K value for a given event. The scale appropriate to each station is characterized by the lower limit of R (between 300$\gamma$ and 2800$\gamma$) for K = 9, and is given for most stations in each issue of the IAGA Bulletin No. 12 series. As an example, at a mid-latitude station, if R in gammas is between

| | 0-5 | 5-10 | 10-20 | 20-40 | 40-70 | 70-120 | 120-200 | 200-330 | 330-500 | >500, |
|---|---|---|---|---|---|---|---|---|---|---|
| then K = | 0 | 1 | 2 | 3 | 4 | 5 | 6 | 7 | 8 | 9. |

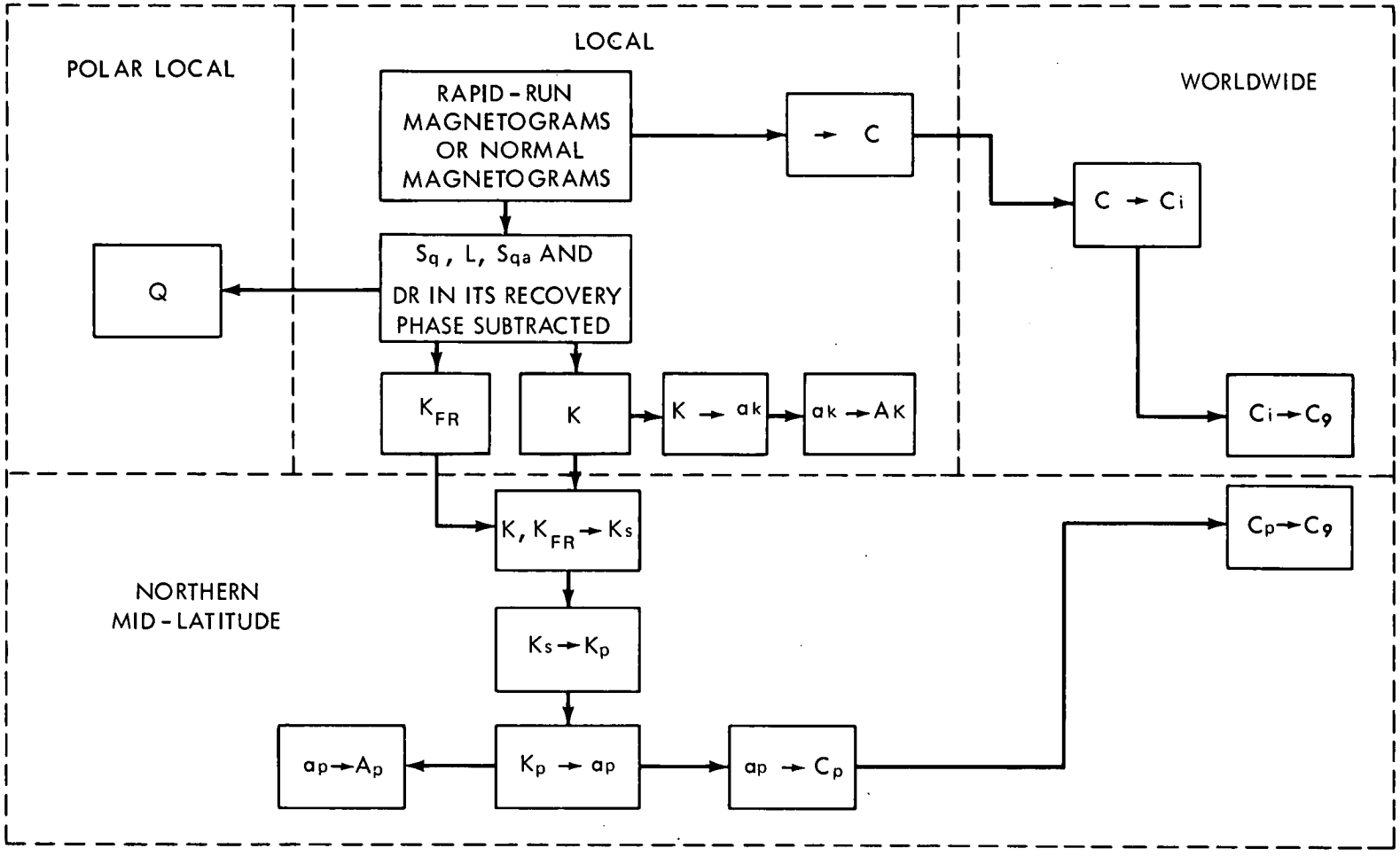


Figure 20. Functional Diagram of Relationships Among Geomagnetic Activity Indices

The World Data Center A for Geomagnetism maintains the K values for many observatories on microfilm. The catalog of data issued by WDC-A contains information on the availability of K values listed by station since 1957. The K values themselves for the year 3 years prior to publication are given in the IAGA Bulletin No. 12 series.

## $K_{FR}$ - Fredericksburg K Index

The Fredericksburg K index obtained in Fredericksburg, Virginia, has been the standard of geomagnetic activity for the United States. Between January 1957 and February 1969, the $K_{FR}$ values were given in the Journal of Geophysical Research for the month 5 months prior to publication. Prior to 1957, the K index derived from the Cheltenham, Maryland, magnetic records was also published in the Journal of Geophysical Research. $K_{FR}$ values are currently listed only in the "Preliminary Report and Forecast of Solar Geophysical Activity" prepared by the Space Disturbance Forecast Center of NOAA, Boulder, Colorado.

## Ks - Standardized K Index

The standardized K index, Ks, is obtained from K by using a scale dependent upon both station and local time. The Ks index was originated to remove local effects from the K indices. The Ks index runs from 0 to 9. It is expressed in thirds of an integer; e.g., the interval 1.5 to 2.5 is divided into thirds and denoted $2_-$, $2_o$, $2_+$.

The Ks index is used almost exclusively for determining the Kp index.

## Kp - Planetary 3-Hour Range Index

The planetary Kp index is determined by arithmetically averaging Ks for 12 stations located at geomagnetic latitudes between 48° and 63°. As with Ks, Kp can assume 28 values as follows:

$$0_o,\ 0_+,\ 1_-,\ 1_o \ \ldots\ 8_+,\ 9_-,\ 9_o.$$

Note that $0_0$ and $9_0$ denote one-sixth of a unit interval, while the other values denote one-third of a unit interval.

Values of Kp are available from numerous sources, including:

1. A BCD magnetic tape generated by the European Space Research Organization (ESRO), copies of which are held at WDC-A for Geomagnetism, Rockville, Md., and at NSSDC, for the time period from 1932 until 1 month prior to the most recent update. See Lenhart (1968). Currently, one update is issued every 3 months.

2. Solar-Geophysical Data for the month 2 months prior to publication.

3. The IUGG/IAGA Three-monthly Bulletin on Geomagnetic Indices and Rapid Variations for the 3-month period about 8 months prior to publication. These bulletins may be obtained from the International Service of Geomagnetic Indices, Royal Netherlands Meteorological Institute, DeBilt, The Netherlands.

4. IAGA Bulletin No. 12 for the 3 years prior to publication and IAGA Bulletin No. 18 for the period 1932 to 1961.

5. Journal of Geophysical Research for the month 5 months prior to publication, but only between 1951 and February 1969.

6. "Abbreviated Calendar Records" (see Miscellaneous Data section).

In addition, monthly and annual mean values of Kp, for the period 1932 to 1962, and daily mean values of Kp, for the period 1957 to 1962, are published in the Handbook of Geophysics and Space Environments (Shea L. Valley, ed., AFCRL-USAF, 1965).

## Kn, Ks, Km Indices

To reflect the differences in geomagnetic activity occurring in the earth's Northern and Southern Hemispheres, planetary indices Kn and Ks have been derived using data obtained by Northern and Southern Hemisphere observatories, respectively. Km is a mean value and is usually very close in magnitude to Kp. More detailed discussions of

these indices and a listing of their numerical values for the time period 1964 to 1967 are given in Mayaud (1968). The little used Southern Hemisphere Ks index is not to be confused with the previously discussed standardized station index Ks; the context in which Ks is used should make clear which meaning is intended.

## ak, Ak Indices

The ak and Ak indices, introduced in 1951, are determined from the K index in a way that they are linearly related to the geomagnetic disturbance amplitude. As such, they are more appropriate in performing many statistical averages than are the K indices themselves.

The ak values are determined from K according to

| K = | 0 | 1 | 2 | 3 | 4 | 5 | 6 | 7 | 8 | 9 |
|---|---|---|---|---|---|---|---|---|---|---|
| ak = | 0 | 3 | 7 | 15 | 27 | 48 | 60 | 140 | 240 | 400 |

The ak index may also be considered an equivalent range of the most disturbed component, given in units fγ where the factor f is the ratio of the station lower limit for K = 9, to 250. For example, if the range is R = 100γ while the lower limit for K = 9 is 500, then K = 5, and, by the conversion scale, ak = 48. The factor f is now 2, so that ak = 96γ gives an equivalent range.

The Ak index is called the equivalent daily amplitude and is the arithmetic average of the eight ak values per Greenwich day for a given observatory. Neither ak nor Ak values are published on a regular basis.

## ap, Ap Indices

The 3-hour planetary index, ap, is determined from the Kp index according to the following table:

| Kp = | $0_o$ | $0_+$ | $1_-$ | $1_o$ | $1_+$ | $2_-$ | $2_o$ | $2_+$ | $3_-$ | $3_o$ | $3_+$ | $4_-$ | $4_o$ | $4_+$ | $5_-$ | $5_o$ | $5_+$ | $6_-$ | $6_o$ | $6_+$ |
|---|---|---|---|---|---|---|---|---|---|---|---|---|---|---|---|---|---|---|---|---|
| ap = | 0 | 2 | 3 | 4 | 5 | 6 | 7 | 9 | 11 | 15 | 18 | 22 | 27 | 32 | 39 | 48 | 56 | 67 | 80 | 94 |

| Kp = | $7_-$ | $7_o$ | $7_+$ | $8_-$ | $8_o$ | $8_+$ | $9_-$ | $9_o$ |
|---|---|---|---|---|---|---|---|---|
| ap = | 111 | 132 | 154 | 179 | 207 | 236 | 300 | 400 |

The arithmetic average of the eight ap values per Greenwich day is Ap, the daily equivalent planetary amplitude. Since ap and Ap are linearly related to disturbance amplitude while Kp is logarithmically related, the use of ap and Ap in statistical averaging is recommended over the use of Kp or of daily sums of Kp.

Sources of Ap values are the same as those for the Kp indices, except that Ap values do not appear in the IUGG/IAGA Three-monthly Bulletin on Geomagnetic Indices and Rapid Variations. Values of ap are found on the ESRO tape and in IAGA Bulletin No. 12 and IAGA Bulletin No. 18, with the same respective time coverages as for Kp values.

## C - Daily Magnetic Character Index

The C index is a daily measure of magnetic activity assigned for each magnetic observatory. For a given station, C = 0, 1, or 2 according to whether the Greenwich day is quiet, moderately disturbed, or highly disturbed. Some stations have fixed range limits for C = 1. These stations and the limits are listed in the IAGA Bulletin No. 12 series. Each Bulletin in the series also contains daily C values listed by station for the year 3 years prior to publication.

## Ci - International Daily Character Figure

The Ci index is the arithmetic mean of the C values reported by individual observatories for each Greenwich day. The Ci values are available from 1884 to the present.

Monthly and annual mean values of Ci are available from 1884 to 1964 in the AFCRL Handbook of Geophysics and Space Environments. Daily values for Ci, also given in that document, are cited for the period 1957 to 1963. Daily values are also available in the IUGG/IAGA Three-monthly Bulletin on Geomagnetic Indices and Rapid Variations for the 3-month period about 8 months prior to publication, in Solar-Geophysical Data for the month 2 months prior to publication, in the Journal of Geophysical Research (prior to February 1969) for the month 5 months prior to publication, and in the IAGA Bulletin No. 12 series for the year 3 years prior to publication. The IAGA Bulletin No. 12 series also lists the monthly and annual mean values since 1900, with a cutoff date of 3 years prior to publication.

## Cp - Daily Planetary Character Figure

The Cp index is a measure of magnetic activity that is determined for each Greenwich day from the sum of the eight ap values for that day according to:

| | | | | | | | | | | | | |
|---|---|---|---|---|---|---|---|---|---|---|---|---|
| 8Ap = Σap < | 22 | 34 | 44 | 55 | 66 | 78 | 90 | 104 | 120 | 139 | 164 | 190 |
| Cp = | 0.0 | 0.1 | 0.2 | 0.3 | 0.4 | 0.5 | 0.6 | 0.7 | 0.8 | 0.9 | 1.0 | 1.1 |
| Σap < 228 | 273 | 320 | 379 | 453 | 561 | 729 | 1101 | 1399 | 1699 | 1999 | 2399 | 3200 |
| Cp = 1.2 | 1.3 | 1.4 | 1.5 | 1.6 | 1.7 | 1.8 | 1.9 | 2.0 | 2.1 | 2.2 | 2.4 | 2.5 |

Although daily values of Ci and Cp rarely differ by more than 0.2, Cp is more reliable (Dwarkin and Mescher, 1967). Sources of Cp values are the same as those for the Kp indices, except that Cp values do not appear in IUGG/IAGA Three-monthly Bulletin on Geomagnetic Indices and Rapid Variations or in the "Abbreviated Calendar Records."

## $C_9$ Index

The $C_9$ index expresses the daily geomagnetic activity by a single digit. The values for Ci and Cp are contracted to form the $C_9$ values as follows:

| | | | | | | | | | | |
|---|---|---|---|---|---|---|---|---|---|---|
| Ci or Cp = | 0.0 to 0.1 | 0.2 to 0.3 | 0.4 to 0.5 | 0.6 to 0.7 | 0.8 to 0.9 | 1.0 to 1.1 | 1.2 to 1.4 | 1.5 to 1.8 | 1.9 | 2.0 to 2.5 |
| $C_9$ | 0 | 1 | 2 | 3 | 4 | 5 | 6 | 7 | 8 | 9 |

Values of $C_9$ appear occasionally in Solar-Geophysical Data (e.g., the period 1965 to 1968 is covered in Solar-Geophysical Data, 294, Feb. 1969). $C_9$ values are also found on the ESRO tape (see discussion in Kp section) for the interval 1932 until 1 month prior to the most recent update.

## Dst - Axisymmetric Component of Geomagnetic Disturbance

A Dst(X; t) field may be defined for any field component, X, as the average of the D(X; t) field values as observed by stations of similar geomagnetic latitude but varying geomagnetic longitude. In practice, only Dst for the horizontal field, Dst(H; t) has been considered. At a given station Ds(H; t) ≡ D(H; t) - Dst(H; t).

The Dst index, the magnitude of the Dst(H) field, is intended primarily to indicate the effect of magnetospheric ring currents, especially during magnetic storms. Thus, observatories used for the determination of Dst are distributed as uniformly as possible in longitude and lie at low, but not equatorial, latitude. The low latitudes minimize auroral zone effects. Equatorial latitudes are avoided to minimize equatorial electrojet effects.

A more detailed discussion of the Dst(H) index and its derivation are presented in Sugiura (1964). This reference also contains a list of hourly Dst(H) values for the IGY (July 1957 to December 1958) and a list of the eight stations from which these Dst(H) values were determined. Hourly Dst(H) values have been generated using data from Hermanus, Honolulu, and San Juan; these values are found in Sugiura and Hendricks (1967) for the years 1961 through 1963, in Sugiura and Cain (1969) for the years 1964 through 1967, and in Sugiura and Cain (1970) for 1968.* No Dst values have yet been generated for the 1959/1960 time interval. Copies of these documents can be obtained from the authors or through NSSDC. The Dst values are also available on a BCD magnetic tape, copies of which are kept at WDC-A, Rockville, and at NSSDC.

## U, u, $u_1$ Measures

The U, u, and $u_1$ measures are the older indices related to ring current effects. Their use has largely been superseded by the use of the Dst index. At a given station, the U measure is the absolute magnitude of the difference of the daily mean values of the H component for two successive days as assigned to the second day. These U values are geometrically reduced to equivalent equatorial u values. The $u_1$ measure is related to the u measure in a nonlinear fashion such that the larger values of u are deemphasized; $u_1$ correlates well with sunspot numbers.

Values for $u_1$ related to u are as follows:

| | | | | | | | | | |
|---|---|---|---|---|---|---|---|---|---|
| u | = 0.3 | 0.5 | 0.7 | 0.9 | 1.2 | 1.8 | 2.1 | 2.7 | 3.6 |
| $u_1$ | = 0 | 20 | 40 | 57 | 79 | 108 | 108 | 132 | 140 |

(u in units of 10γ)

*Post deadline note: Dst through 7/70 now available through NSSDC.

Published values of the u measure are based on averages of values of one to six near-equator equatorial stations. Monthly and annual mean values for U are given in the AFCRL Handbook of Geophysics and Space Environments for the years 1872 to 1949. In Terrestrial Magnetism and Atmospheric Electricity, 37, 1-52, 1932, the following values are listed:

U - monthly and annual means for the years 1872 to 1930.
u - annual means for the years 1835 to 1871.
$u_1$ - monthly and annual means for the years 1872 to 1930.

AE - Auroral Electrojet Activity Index

The AE index is a direct measure of the amplitude of the auroral electrojet and is obtained as follows. A $\Delta H(t)$ is determined at selected auroral zone stations as the difference between the observed H(t) and the quiet time H(t). The $\Delta H(t)$ values for all observatories are plotted versus time on a single graph. The AU and AL curves are then drawn versus time through the maximum and minimum $\Delta H$ values, respectively. At each point in time, AE is defined as AE = AU - AL. Another index, Ao, is defined by (AU + AL)/2, and is the displacement of the midpoint between AU and AL from the reference level.

The significance of AE and a more detailed discussion of the method of derivation are given by Davis and Sugiura (1966).

Hourly values of AE have been computed from magnetic data gathered at 11 stations (10 for 1957) fairly well distributed in geomagnetic longitude and located mainly in the Northern Hemisphere. These computations have been done for the period from July 1957 to December 1964 by T. N. Davis et al. at the University of Alaska. The results have been published in the University of Alaska Geophysical Institute Report (UAG-R) No. 192, 194, 195, 196, 197, 198, 199, and 200. The reports contain plots of the AE index and tabulations of AE, AU, AL, and Ao.

WDC-A for Geomagnetism currently has available one IBM 7094 binary tape per calendar year containing 2.5-minute AE values for the period from September 1964 through December 1968 and one BCD tape containing hourly AE values for the period from July 1957 through December 1968. The 2.5-minute AE values are computed at NSSDC (in cooperation with D. Fairfield) and are based on available Northern Hemisphere 2.5-minute digitized magnetogram data. The hourly AE values are based on hourly

averages of the 2.5-minute digitized data. At present, 11 stations fairly well distributed in geomagnetic longitude are represented in the AE values for 1964 and 1965. For 1966 and 1967, data from six stations, four of which lie in the longitude range 256 to 347 degrees geomagnetic, have been used. For 1968, four stations in the preceding longitude range and one outside the range have been used. As additional 2.5-minute digitizations become available, these AE values will be updated and extended forward in time.

In addition to these AE values on magnetic tape, WDC-A also has plots and tabulations of these AE values on microfilm and AU and AL values on both magnetic tape and microfilm. NSSDC also has copies of these data.

## Q Index

The Q index is a measure of geomagnetic activity assigned by high latitude (geomagnetic latitude $> 58°$) magnetic observatories for each 15-minute interval centered around 00, 15, 30, and 45 minutes past the hour. The index is designed to study auroral and ionospheric phenomena over a time scale smaller than that possible with Kp. The Q scale is loosely logarithmic, with possible values from 0 to 11.

The index is defined as the sum of the maximum positive deviation from the normal nondisturbance curve and the absolute value of the maximum negative deviation. The more disturbed of the two horizontal elements is chosen for this determination. As an example, if the extreme deviations from normal are +200γ and +50γ, the K index would be based on a range of 150γ, whereas Q is based on the 200γ maximum deviation from normal. (The negative deviation is zero in this case.) The uniform conversion scale for all stations is:

| | | | | | | | | | | | | |
|---|---|---|---|---|---|---|---|---|---|---|---|---|
| $S \leq$ | 10 | 20 | 40 | 80 | 140 | 240 | 400 | 660 | 1000 | 1500 | 2000 | $\infty$ (γ) |
| $Q =$ | 0 | 1 | 2 | 3 | 4 | 5 | 6 | 7 | 8 | 9 | 10 | 11 |

(S = sum of absolute values of positive and negative deviations.)

The Q indices are available from WDC-A for Geomagnetism. The availability information since 1957 is listed by station in the WDC-A Catalogue of Data on Solar-Terrestrial Physics.

## SELECTED DAYS

For many studies, a selection of magnetically quiet or disturbed days is necessary. For each month, the five most disturbed days, the five least disturbed days, and the 10 least disturbed days are selected by IAGA personnel using criteria described in Lincoln (1967).

Sources of selected days are the same as for Kp indices, except that selected days are not listed on the ESRO tape or in IAGA Bulletin No. 18.

## EVENTS

In addition to being used for the generation of indices, magnetogram records are used to identify individual events. These events include magnetic storms, sudden impulses, polar magnetic substorms, micropulsations, and solar flare effects.

The reader may wish to refer to the previous section on magnetograms for availability information. Some geomagnetic activity information (especially on storms) is distributed on a real-time basis as part of the International Ursigram and World Days Service (IUWDS) effort (see discussion in Miscellaneous Information, Part VIII).

### Geomagnetic Storm

A geomagnetic storm is a worldwide transient variation in the geomagnetic field. In mid and low latitudes, four distinct phases in a typical storm can be distinguished. The storm sudden commencement (sc or ssc) phase is the nearly simultaneous worldwide increase in H, typically by a few tens of gammas. This state of enhanced H may persist for a few tens of minutes and is called the initial phase. During the following main phase, H is depressed below its prestorm value typically by several tens to a few hundred gammas for many hours. The recovery phase, or return to the prestorm state, usually requires a few days.

The sudden commencement and initial phases are manifestations of magnetospheric compression due to enhanced solar wind pressure, while the main and recovery phases are due to the great enhancement and gradual decay of the diamagnetic ring current found within the magnetosphere. Further discussions of geomagnetic storms may be found in Sugiura and Heppner (1968).

Since 1961, the IAGA Bulletin No. 12 series has published for the year 4 years prior to publication a storm sudden commencement list using an "occurrence format." That is, for a given event, characterized by a given start time, reporting stations are separated into six classes according to whether the event in that station's magnetogram was: (1) very distinct; (2) fair, ordinary, but unmistakable; (3) doubtful; (4) not recorded despite satisfactory magnetogram records; (5) not discerned due to heavy disturbance; (6) missing because the magnetogram itself was missing. No event morphology information is given in these lists.

The Three-monthly Bulletin on Geomagnetic Indices and Rapid Variations of IUGG/IAGA lists the same information for the 3-month period about 8 months prior to publication.

Until January 1967, the Journal of Geophysical Research published a monthly listing of storms, grouped by station, that had occurred about 6 months earlier. The begin and end times of storms, the types of sudden commencement, the magnetic amplitude of each field component during initial and main phase, and the maximum associated K index were all presented. Since February 1967, this information, grouped by event, has appeared in ESSA's Solar-Geophysical Data for the month 2 months prior to publication. Beginning April 1969, storm magnetograms for a few events for selected observatories are presented in Solar-Geophysical Data.

## Sudden Impulse

Transient magnetic disturbances are similar to storm sudden commencements, but they tend to be of smaller amplitude and of less abruptness than the ssc's. These sudden impulses (s.i.) appear to result from sudden magnetospheric compressions and expansions associated with shock waves and other discontinuities in the interplanetary medium (Burlaga, 1970), but they are not followed by main phase storms. Incomplete lists of sudden impulses appear in the IUGG/IAGA Three-monthly Bulletin on Geomagnetic Indices and Rapid Variations, for the 3-month interval about 8 months prior to publication, and in IAGA Bulletin No. 12 for the year 4 years prior to publication. The "occurrence format"

described in the preceding Geomagnetic Storm subsection is used in both sources. Three-month lists have also appeared in Solar-Geophysical Data, with varying time lags, since January 1966.

## Polar Magnetic Substorm

A polar magnetic substorm (formerly called a magnetic bay) is a predominantly night-side variation, often superposed on a worldwide geomagnetic storm. The magnetic deviation, which may be positive (usually pre-midnight) or negative (usually post-midnight), can have an amplitude of hundreds of gammas at auroral latitudes and a significantly reduced amplitude away from the auroral zones. Each event usually lasts between 1 and 6 hours.

Recent reviews of polar magnetic substorms and of their relations to auroras and to magnetospheric dynamics are given in Hultqvist (1969) and in Feldstein (1969).

Lists of magnetic bays are given in the IUGG/IAGA Three-monthly Bulletin on Geomagnetic Indices and Rapid Variations, for the 3-month interval about 8 months prior to publication, and in IAGA Bulletin No. 12 for the year 4 years prior to publication. The "occurrence format" described in the Geomagnetic Storm subsection is used in both sources. The type of bay (calm or stormy time, sharp or gradual beginning, associated pulsations or not) is also indicated.

## Micropulsations

Small amplitude, quasi-periodic magnetic fluctuations are found occasionally in both ground and satellite magnetometer records. Occurrence frequencies and amplitude depend on geomagnetic latitude and longitude, radial distance, and the fluctuation frequency. Pulsations lasting for considerable lengths of time are classed as Pc1 (Pc - continuous pulsation), Pc2, Pc3, Pc4, or Pc5 according to whether the fluctuation periods lie within the respective ranges: 0.2 to 5 seconds, 5 to 10 seconds, 10 to 45 seconds, 45 to 150 seconds, 150 to 600 seconds. Typically, the smaller period waves have amplitudes of a fraction of a gamma, while the Pc5 wave may have amplitudes of hundreds of gammas, especially in the auroral zones. One class of Pc1 waves is referred to as pearls, or hydromagnetic emissions.

Review papers on the subject include those by Troitskaya (1964) and Saito (1969). The relationship between magnetic pulsations and polar magnetic substorms is discussed in Gendrin (1970). A recent paper by Liemohn (1969), which contains a discussion of magnetospheric ELF signals (periodicities 0.002 to 5 sec), presents a 148-member list of stations making micropulsation observations. Station location, frequency range observed, and the name of an analyst are given.

Lists of stations observing Pc4 and Pc5 micropulsations in their normal magnetograms and lists of stations observing micropulsations of all Pc classes in their rapid-run magnetograms are given in the IUGG/IAGA Three-monthly Bulletin on Geomagnetic Indices and Rapid Variations for the 3-month interval about 8 months prior to publication. Start and stop times for each occurrence are given.

In addition to the continuous micropulsations, irregular pulsations are also observed. Trains of pulsations, Pt, with periods of 40 to 100 seconds are closely associated with magnetic bays. Pt occurrence data are published in conjunction with magnetic bay data.

Other irregular pulsations are classed as Pi1 and Pi2 according to whether the periods lie within the ranges 1 to 40 seconds and 40 to 150 seconds, respectively. Pulsations of unusually large amplitude are denoted as Pg (giant pulsations). Lists of stations observing Pi2 and Pg pulsations in their normal magnetograms and lists of stations observing Pi1, Pi2, and Pg pulsations in their rapid-run magnetograms are given in the IUGG/IAGA Three-monthly Bulletin on Geomagnetic Indices and Rapid Variations. Again, start and stop times for each occurrence are given.

A survey of magnetospheric micropulsations observed by OGO 3 and OGO 5 can be found in Heppner et al. (1969).

## Solar Flare Effects

Enhanced lower-ionospheric ionization resulting from solar flare X rays causes an enhancement of the dayside Sq current, which in turn results in geomagnetic variations. The occurrence of this effect is listed by observing station in the monthly letter issued by the International Service of Geomagnetic Indices, Royal Netherlands Meteorological Institute, DeBilt, The Netherlands. Quarter-yearly lists, with varying time lags, have appeared in Solar-Geophysical Data since January 1966.

## TELLURIGRAMS

Temporal changes in the geomagnetic field induce electric fields and currents in the earth's crust. For changes (pulsations) with periods between tenths of a second to tens of minutes, the induced telluric currents are measured directly at a number of stations, largely (75%) in the Soviet Union. A more detailed discussion of the concepts involved is given in Chapman and Bartels (1940) and in Troitskaya (1957); the latter reference also contains a description of experimental techniques.

Each station generates a tellurigram daily; each tellurigram gives magnitude of current versus time. World Data Center A for Geomagnetism, Rockville, has a number of these tellurigrams on microfilm. The station list and the availability of the tellurigrams, given by station and by year since 1957, are listed in the WDC-A Catalogue of Data on Solar-Terrestrial Physics (June 1970).

## GEOMAGNETIC FIELD MODELS

For many reasons it is useful to have an analytical representation of the steady component of the geomagnetic field. In regions of no magnetic sources (i.e., no currents), a static magnetic field, $\underline{B}$, may be represented by

$$\underline{B} = -\nabla V$$

where the scalar potential V is given by

$$V = a \sum_{n=1}^{\infty} \sum_{m=0}^{n} \left\{ \left[ \left(\frac{a}{r}\right)^{n+1} g_n^m + \left(\frac{r}{a}\right)^n A_n^m \right] \cos m\phi + \left[ \left(\frac{a}{r}\right)^{n+1} h_n^m + \left(\frac{r}{a}\right)^n B_n^m \right] \sin m\phi \right\} P_n^m (\cos \theta)$$

Here, a is the earth's effective radius, $P_n^m(\cos\theta)$ is a Schmidt normalized Legendre polynomial, and $g_n^m$, $h_n^m$, $A_n^m$, and $B_n^m$ are coefficients whose specification defines a field model. Different coordinate systems for $\theta$ and $\phi$ have been used in differing models.

There have been two basically different types of models generated in the past. The first type of model is based on data gathered at or near the earth's surface; in this type, sources exterior to the earth are neglected, and $A_n^m = B_n^m = 0$ (all n and m). The second type of field model takes into account external sources in the form of model current systems such as those associated with the magnetopause and the geomagnetic tail. The earth's core field in this type model is taken to be dipolar so that $g_1^0 \neq 0$, while $g_n^m = h_n^m = 0$ (all other n and m).

## Models Based on Near-Earth Data

Models based on near-earth data are defined by the specification of a finite number of the coefficients $g_n^m$ and $h_n^m$. The early history of these models is given in Chapman and Bartels (1940) and Vestine (1960). References to more recent representations (some of which present time derivatives of the coefficients) are given in Cain and Cain (1968) and Zmuda (1970).

Within the framework of the international effort named the World Magnetic Survey, as outlined by Heppner (1963) and Zmuda (1970), input data for recent models have been collected by surface observatories (annual means of magnetogram records), ships, aircraft, and low-altitude satellites (e.g., OGO 2, OGO 4, 1964-83C, and Cosmos 49).

As is detailed in Cain and Cain (1968), IAGA (1969), and Zmuda (1970), some recent models have been appropriately weighted to yield the International Geomagnetic Reference Field [IGRF 1965.0] for epoch 1965. The IGRF specifies $g_n^m$ and $h_n^m$ through n = m = 8 and was developed to provide a standard field model where the long duration of validity (1960 to 1969) outweighs the advantages of high accuracy. The 80 non-zero IGRF (1965.0) coefficients and their first time derivatives are listed for geographic coordinates in IAGA (1969), Cain and Cain (1968), Zmuda (1970), and Fabiano and Peddie (1969) and are also shown in table 10. Also contained in Fabiano and Peddie are tables of the total magnetic field intensity and its annual change at every 2° grid intersection of geographic latitude and longitude for the earth's surface. Mead (1970) has transformed the coefficients and their time derivatives to values applicable in geomagnetic dipolar coordinates (see the section on Coordinate Systems in Part VIII of this Handbook).

TABLE 10

Spherical Harmonic Coefficients--IGRF--1965

| n | m | Main Field $g_n^m$ | Main Field $h_n^m$ | Secular Change $\dot{g}_n^m$ | Secular Change $\dot{h}_n^m$ |
|---|---|---|---|---|---|
| | | γ | γ | γ/yr | γ/yr |
| 0 | 0 | 0 | 0 | 0.0 | 0.0 |
| 1 | 0 | -30339 | 0 | 15.3 | 0.0 |
| 1 | 1 | -2123 | 5758 | 8.7 | -2.3 |
| 2 | 0 | -1654 | 0 | -24.4 | 0.0 |
| 2 | 1 | 2994 | -2006 | 0.3 | -11.8 |
| 2 | 2 | 1567 | 130 | -1.6 | -16.7 |
| 3 | 0 | 1297 | 0 | 0.2 | 0.0 |
| 3 | 1 | -2036 | -403 | -10.8 | 4.2 |
| 3 | 2 | 1289 | 242 | 0.7 | 0.7 |
| 3 | 3 | 843 | -176 | -3.8 | -7.7 |
| 4 | 0 | 958 | 0 | -0.7 | 0.0 |
| 4 | 1 | 805 | 149 | 0.2 | -0.1 |
| 4 | 2 | 492 | -280 | -3.0 | 1.6 |
| 4 | 3 | -392 | 8 | -0.1 | 2.9 |
| 4 | 4 | 256 | -265 | -2.1 | -4.2 |
| 5 | 0 | -223 | 0 | 1.9 | 0.0 |
| 5 | 1 | 357 | 16 | 1.1 | 2.3 |
| 5 | 2 | 246 | 125 | 2.9 | 1.7 |
| 5 | 3 | -26 | -123 | 0.6 | -2.4 |
| 5 | 4 | -161 | -107 | 0.0 | 0.8 |
| 5 | 5 | -51 | 77 | 1.3 | -0.3 |
| 6 | 0 | 47 | 0 | -0.1 | 0.0 |
| 6 | 1 | 60 | -14 | -0.3 | -0.9 |
| 6 | 2 | 4 | 106 | 1.1 | -0.4 |
| 6 | 3 | -229 | 68 | 1.9 | 2.0 |
| 6 | 4 | 3 | -32 | -0.4 | -1.1 |
| 6 | 5 | -4 | -10 | -0.4 | 0.1 |
| 6 | 6 | -112 | -13 | -0.2 | 0.9 |
| 7 | 0 | 71 | 0 | -0.5 | 0.0 |
| 7 | 1 | -54 | -57 | -0.3 | -1.1 |
| 7 | 2 | 0 | -27 | -0.7 | 0.3 |
| 7 | 3 | 12 | -8 | -0.5 | 0.4 |
| 7 | 4 | -25 | 9 | 0.3 | 0.2 |
| 7 | 5 | -9 | 23 | 0.0 | 0.4 |
| 7 | 6 | 13 | -19 | -0.2 | 0.2 |
| 7 | 7 | -2 | -17 | -0.6 | 0.3 |

TABLE 10 (continued)

| n | m | Main Field $g_n^m$ | Main Field $h_n^m$ | Secular Change $\dot{g}_n^m$ | Secular Change $\dot{h}_n^m$ |
|---|---|---|---|---|---|
| | | γ | γ | γ/yr | γ/yr |
| 8 | 0 | 10 | 0 | 0.1 | 0.0 |
| 8 | 1 | 9 | 3 | 0.4 | 0.1 |
| 8 | 2 | -3 | -13 | 0.6 | -0.2 |
| 8 | 3 | -12 | 5 | 0.0 | -0.3 |
| 8 | 4 | -4 | -17 | 0.0 | -0.2 |
| 8 | 5 | 7 | 4 | -0.1 | -0.3 |
| 8 | 6 | -5 | 22 | 0.3 | -0.4 |
| 8 | 7 | 12 | -3 | -0.3 | -0.3 |
| 8 | 8 | 6 | -16 | -0.5 | -0.3 |

The POGO (10/68) and POGO (8/69) models generated by J. C. Cain from OGO 2 and OGO 4 data provide greater accuracy for the post-1965 period than does the IGRF (1965.0) field (Cain and Sweeney, 1970). Of course all models become progressively less accurate as one moves in time away from the model epoch date. Future models will be generated as the need arises. It is suggested that the potential user of any model field consider his accuracy requirements in determining which of the available field models to use.

IBM card decks containing the GSFC (12/66), POGO (10/68), POGO (8/69), and IGRF (1965.0) model coefficients for use with geodetic coordinates are available at NSSDC. A deck containing IGRF (1965.0) coefficients for use with geomagnetic dipolar coordinates is also available at NSSDC.

The standard FORTRAN program used to generate the actual magnetic field at a fixed point in space from any of the field models is available on cards at NSSDC. Also available is a fast, comprehensive FORTRAN routine (ALLMAG) that condenses six selected, time dependent models into one operational assembly, permitting a multiple successive selection of models and/or time periods during a single program execution. This routine was developed by Stassinopoulos et al. (1970) and contains, in addition to four models mentioned above, the GSFC (9/65) model and that of Leaton et al. (1965).

The field computation programs are compatible with the programs, also available at NSSDC, used to evaluate the B, L coordinates of a spatial point (refer to section on Coordinate Systems) and to trace out field lines.

WDC-A, Rockville, has card decks for the 80 IGRF (1965.0) model coefficients and for the 168 World Magnetic Chart coefficients for 1970. World Magnetic Chart coefficients are computed from extensive ground-based data by personnel at the United States Coast and Geodetic Survey (Rockville, Maryland) under the direction of E. B. Fabiano, and are used in the generation of the World Magnetic Charts issued every 5 years by the Naval Oceanographic Office, Suitland, Maryland. WDC-A also has the program decks required to compute field values from either of these sets of coefficients.

## Models with External Sources

As mentioned, there are field models that take into account current systems exterior to the earth. These models involve a specification of the coefficients $A_n^m$ and $B_n^m$ and are valid only at distances interior to the location of the current systems. Early versions of such models

assume that the geomagnetic dipole axis is perpendicular to the incident solar wind flow. Two early models that include the effects of currents located on the magnetospheric boundary are given in Mead (1964) and Midgley (1964).

One of these (Mead, 1964) postulates a model magnetopause current system and computes numerical values of the resultant magnetic field at 273 points within the magnetosphere. Least-squares fitting to the computed field values is used to determine the coefficients $A_n^m$ and $B_n^m$. A parameter, $r_b$, which depends on the solar wind pressure and which scales the magnetosphere, is the subsolar geocentric magnetopause distance. Mead presents two sets of numbers for the products $A_n^m r_b^{n+2}$ ($B = 0$ by symmetry, all n and m) for $n \leq 6$ and for $n \leq 2$, respectively. Use of the coefficients with values of n up to 2 (only $A_1^0$ and $A_2^1$ are non-zero) yields a fit with only 3% inaccuracy for geocentric distances less than $0.7\ r_b$.

Using different techniques but the same general approach as Mead, Midgley (1964) also presents a model with coefficients having values of n up to 6. Midgley's results are not significantly different from those of Mead.

An early model in which a magnetic field due to a model geomagnetic tail current is superposed on the dipolar core field and magnetopause-current field is that of Williams and Mead (1965). The postulated tail current lies in a semi-infinite sheet in the earth's equatorial plane, at distances between 10 and 40 earth radii at local midnight, and flows everywhere perpendicular to the midnight meridian. The field adjacent to the current sheet is 40 gammas. This model was generated to explain satellite (1963-38C) particle observations near the noon-midnight meridian plane. No Gaussian coefficients $A_n^m$ and $B_n^m$ are presented.

A more recent field model that includes the effect of magnetopause and magnetotail currents is that of Olson (1970). This model is distinguished from earlier models in that the geomagnetic dipole axis is tilted with respect to the incident solar wind; the angle between the geomagnetic dipole axis and the earth-sun vector is $90° - \mu$. This model also incorporates a cylindrical geomagnetic tail in which current flows across the neutral sheet and returns across the two halves of the cylindrical boundary. The neutral sheet typically lies outside the solar magnetospheric equatorial plane and contains a current density that is a function of geocentric distance.

To facilitate the computation of the magnetic fields resulting from the postulated current systems, the effects of magnetopause and magnetotail currents are considered separately. As such, two scalar potentials are involved and two sets of Gaussian coefficients are specified. Due to the linearity of all relevant equations, linear superposition of the fields (addition of coefficients for given n and m) is possible.

As in Mead's original model, there is a parameter, $r_{ref}$, that depends on the solar wind pressure and that scales the magnetosphere. For a given solar wind pressure, $r_{ref}$ also depends on the tilt angle, $\mu$. Values of $r_{ref}$ for eight equispaced values of $\mu$ between 0° and 35° are presented for constant solar wind pressure.

For solar magnetospheric coordinates and for solar magnetic coordinates separately and for four discrete values of $\mu$ (0°, 10°, 20°, 30°), numerical values of $A_n^m r_{ref}^{n+2}$ are given for the fields due to the magnetopause ($0 \leq n \leq 6$) and magnetotail ($0 \leq n \leq 4$) current systems. $B_n^m = 0$ for all n and m due to symmetry. Further, $A_n^m r_{ref}^{n+2}$ is expanded as a power series in $\mu$: $A_n^m r_{ref}^{n+2} = a_1 + a_2\mu + a_3\mu^2$. For the field due to magnetopause currents ($0 \leq n \leq 6$) and for the field due to magnetotail currents ($0 \leq n \leq 4$) and for each n and m, values of $a_1$, $a_2$, and $a_3$ are presented for each coordinate system.

IBM card decks containing the coefficients ($A_n^m r_{ref}^{n+2}$) for certain tilt angles and the fit coefficients ($a_1$, $a_2$, $a_3$), as well as a program deck for the computation of the magnetic field at any point in space, are available at NSSDC.

## REFERENCES


1. Bartels, J., "The Geomagnetic Measures for the Time Variations of Solar Corpuscular Radiation, Described for Use in Correlation Studies in Other Geophysical Fields," Ann. IGY, 4, 227-236, 1957.

2. Burlaga, L. F., "Discontinuities and Shock Waves in the Interplanetary Medium and Their Interaction with the Magnetosphere," presented at the International STP Symposium, Leningrad, May 1970, NASA/GSFC X-692-70-154, April 1970.

3. Cain, J. C., and S. J. Cain, "Derivation of the International Geomagnetic Reference Field (IGRF 10/68)," NASA/GSFC X-612-68-501, 1968.

4. Cain, J. C., F. Eleman, S. J. Hendricks, H. Meyers, W. Paulishak, and K. L. Svendsen, "U.S. Coast and Geodetic Survey - NASA Geomagnetic Data Reduction Program," NASA-GSFC X-612-66-11, Jan. 1966.

5. Cain, J. C., and R. E. Sweeney, "Magnetic Field Mapping of the Inner Magnetosphere," J. Geophys. Res., 75, 4360-4362, 1970.

6. Chapman, S., Solar Plasma, Geomagnetism, and Aeronomy, Gordon and Breach Science Publishers, Inc., New York, 1964.

7. Chapman, S., and J. Bartels, Geomagnetism, Oxford University Press, London, 1940.

8. Davis, T. N., and M. Sugiura, "Auroral Electrojet Activity Index AE and Its Universal Time Variations," J. Geophys. Res., 71, 785-802, 1966.

9. Dwarkin, M. L., and E. J. Mescher, "Solar-Terrestrial Activity Indices," The Johns Hopkins University Applied Physics Laboratory, SIP-239-67, 1967, to be published in STP Notes.

10. Fabiano, E. B., and N. W. Peddie, "Grid Values of Total Magnetic Intensity IGRF - 1965," ESSA Technical Report C & GS 38, 1969.

11. Feldstein, Y. I., "Polar Auroras, Polar Substorms, and Their Relationships with the Dynamics of the Magnetosphere," Reviews of Geophysics, 7, 179-218, 1969.

12. Gendrin, R., "Substorm Aspects of Magnetic Pulsations," Space Science Reviews, 11, 54-130, 1970.

13. Heppner, J. P., "The World Magnetic Survey," Space Science Reviews, 2, 315-354, 1963.

14. Heppner, J. P., B. J. Ledley, T. L. Skillman, and M. Sugiura, "A Preliminary Survey of the Distribution of Micropulsations in the Magnetosphere from OGOs 3 and 5," NASA/GSFC X-612-69-429, 1969, (to be published in Annales de Geophysique).

15. Hultqvist, B., "Auroras and Polar Substorms," Reviews of Geophysics, 7, 129-177, 1969.

16. IAGA Commission 2 Working Group 4, Analysis of the Geomagnetic Field, "International Geomagnetic Reference Field 1965.0," J. Geophys. Res., 74, 4407-4408, 1969.

17. Leaton, B. R., S. R. C. Malin, and M. J. Evans, "An Analytical Representation of the Estimated Geomagnetic Field and Its Secular Change for Epoch 1965.0," J. Geomag. Geoelec., 17, 187-194, 1965.

18. Lenhart, K. G., "Geomagnetic and Solar Data for Use with Digital Computers," Trans. A.G.U., 49, 463-464, 1968.

19. Liemohn, H. B., "ELF Propagation and Emission in the Magnetosphere," Proceedings of URSI, XVIth General Assembly, Ottawa, Canada, Aug. 18-28, 1969, to be published, (also Boeing Report D1-82-0890).

20. Lincoln, J. Virginia, "Geomagnetic Indices," Physics of Geomagnetic Phenomena, 1, 67-100, 1967.

21. Matsushita, S., and W. H. Campbell, eds., Physics of Geomagnetic Phenomena, Academic Press, New York, 1967, 2 volumes.

22. Mayaud, P. N., "Indices Kn, Ks, et Km, 1964-1967," Editions du Centre National de la Recherche Scientifique, 1968.

23. McComb, H. E., "Magnetic Observatory Manual," U.S. Department of Commerce Special Publication 283, U.S. Government Printing Office, 1952.

24. Mead, G. D., "Deformation of the Geomagnetic Field by the Solar Wind," J. Geophys. Res., 69, 1181-1195, 1964.

25. Mead, G. D., "The International Geomagnetic Reference Field 1965.0 in Dipole Coordinates," NASA/GSFC X-641-70-198, May 1970, and J. Geophys. Res., 75, 4372-4374, 1970.

26. Midgley, J. E., "Perturbation of the Geomagnetic Field - A Spherical Harmonic Expansion," J. Geophys. Res., 69, 1197-1200, 1964.

27. Olson, W. P., "A Scalar Potential Representation of the Tilted Magnetopause and Neutral Sheet Magnetic Fields," MDAC paper WD 1332, Mar. 1970, to be submitted to J. Geophys. Res.

28. Saito, T., "Geomagnetic Pulsations," Space Science Reviews, 10, 319-412, 1969.

29. Stassinopoulos, E. G., G. D. Mead, and A. R. Geelhaar, "ALLMAG: An Operational Assembly of Selected, Current, Time Dependent, Geomagnetic Field Models," to be published, 1971.

30. Sugiura, M., "Hourly Values of Equatorial Dst for the International Geophysical Year," Ann. IGY, 35, 9-45, Pergamon Press, Oxford, 1964.

31. Sugiura, M., and S. J. Cain, "Provisional Hourly Values of Equatorial Dst for 1964, 1965, 1966, and 1967," NASA/GSFC X-612-69-20, Feb. 1969.

32. Sugiura, M., and S. J. Cain, "Provisional Hourly Values of Equatorial Dst for 1968," NASA/GSFC X-612-70-3, Jan. 1970.

33. Sugiura, M., and S. Hendricks, "Provisional Hourly Values of Equatorial Dst for 1961, 1962, and 1963," NASA Technical Note TN D-4047, Aug. 1967.

34. Sugiura, M., and J. P. Heppner, "The Earth's Magnetic Field," Introduction to Space Science, ed. W. N. Hess and G. D. Mead, Gordon and Breach Science Publishers, Inc., New York, 1968.

35. Troitskaya, J., "Earth-Current Installations at the Stations of the U.S.S.R.," Ann. IGY, 4, 322-329, 1957.

36. Troitskaya, V. A., "Rapid Variations of the Electromagnetic Field of the Earth," Research in Geophysics, ed. Hugh Odishaw, MIT Press, Cambridge, Mass., 1964.

37. Vestine, E. H., "The Survey of the Geomagnetic Field in Space," Trans. A.G.U., 41, 4-21, 1960.

38. Williams, D. J., and G. D. Mead, "Nightside Magnetosphere Configuration as Obtained from Trapped Electrons at 1100 Kilometers," J. Geophys. Res., 70, 3017-3029, 1965.

39. Zmuda, A. J., ed., "World Magnetic Survey, 1957-1969," IAGA Bulletin No. 28, to be published by IUGG/IAGA in late 1970, see also Trans. A.G.U. (EOS), 52, No. 2, 60-67, Feb. 1971.

# PART V

# IONOSPHERE

Prepared By

Leland L. Dubach and
Francis J. Hagan

CONTENTS

## INTRODUCTION

The ionosphere is the ionized part of the earth's atmosphere that results mainly from the ionizing effect of solar electromagnetic radiation on the earth's atmosphere. For poleward latitudes, the ionizing effect of incident energetic particles is also significant. Traditionally, the following ionospheric regions and their approximate height ranges have been designated: D region (60-90 km); E region (90-150 km); F1 region (150-250 km); and F2 region (above 250 km). Recent discussions of the ionosphere are those of Davies et al. (1968), Hines et al. (1965), and Rishbeth and Garriott (1969).

Of principal interest for ionospheric studies are observations of electron density, ionic composition, and temperatures, and the dependence of these parameters on position and time.

Much useful information about these quantities has been obtained indirectly by analysis of the effects of the ionospheric plasma on the propagation of electromagnetic waves. The presence of the plasma leads to wave group velocities less than that of light in a vacuum. Collisions between neutral and charged particles yield absorption of wave energy. The geomagnetic field splits a wave into two waves of different polarization (birefringence); these two waves generally propagate along different paths.

Full wave reflection in the ordinary polarization mode occurs when a wave of a given frequency reaches that spatial position in the plasma at which the plasma frequency [$f_p$, related to electron density N according to $N(cm^{-3}) = 1.25 \times 10^{-8} f_p^2(Hz)$] is equal to the wave frequency. Partial reflections, such as those associated with sporadic E, may occur when a wave encounters thin layers of enhanced ionization, steep gradients in electron density, or localized scattering irregularities. For more complete discussions of absorption, geomagnetic effects, and reflection, see the previously cited general references. A recent paper contrasting ionospheric measuring techniques and indicating the relative advantages of each is that of Booker and Smith (1970).

## IONOSONDES

Ionosondes utilize the radio wave-reflecting properties of the ionosphere. The product of the speed of light in a vacuum (c) and

half the elapsed time (t) between vertical transmission of a single-frequency electromagnetic wave and reception of the reflected wave at the transmitting location is defined as the virtual range ($h'$) for that frequency (f):

$$h'(f) = c\,t(f)/2$$

A sweep-frequency ionogram is a plot of virtual range versus frequency and is recorded as nearly instantaneously as possible. A fixed-frequency ionogram is a plot of virtual range for a single frequency versus time.

In the ionospheric plasma, there is normally a primary maximum in the electron density between 200 km and 400 km (F2 maximum). Except for weak backscattering, waves with frequencies greater than the plasma frequency associated with this density maximum are not reflected but continue propagating through the atmosphere. Thus, the ionosphere is divided into two regions, bottomside and topside, relative to the layer of maximum density. These two regions can be studied using normal ionograms observed only below or above this layer, respectively.

In addition, sweep- and-fixed-frequency ionograms are distinguished according to whether they are A-scan or B-scan ionograms. A-scan ionograms contain information that indicates the strength of the returned signal and hence information about the effects of absorption and partial transmission. A-scan ionograms are not produced on a routine basis because they are more cumbersome; i.e., they are longer records and more difficult to read. The common B-scan ionograms do not normally contain signal-amplitude information.

## Bottomside Soundings

### Sweep-Frequency Soundings

A sample daytime bottomside B-scan sweep-frequency ionogram is shown in figure 21. (The ordinate is usually called "virtual height" instead of "virtual range" for bottomside ionograms.) Such ionograms have been obtained with the ionosonde techniques and equipment described in Wright, Knecht, and Davies (1957) and by the network of ground-based stations listed and illustrated in the WDC-A Catalogue of Data on Solar-Terrestrial Physics. A given station typically generates a sweep-frequency ionogram in about 2 minutes. Five ionograms are normally taken per hour, two on the hour, and one at each quarter hour. Microfilmed copies of these ionograms and information on time coverage of data of individual observatories are available from WDC-A for Upper Atmosphere Geophysics, Boulder, Colorado.

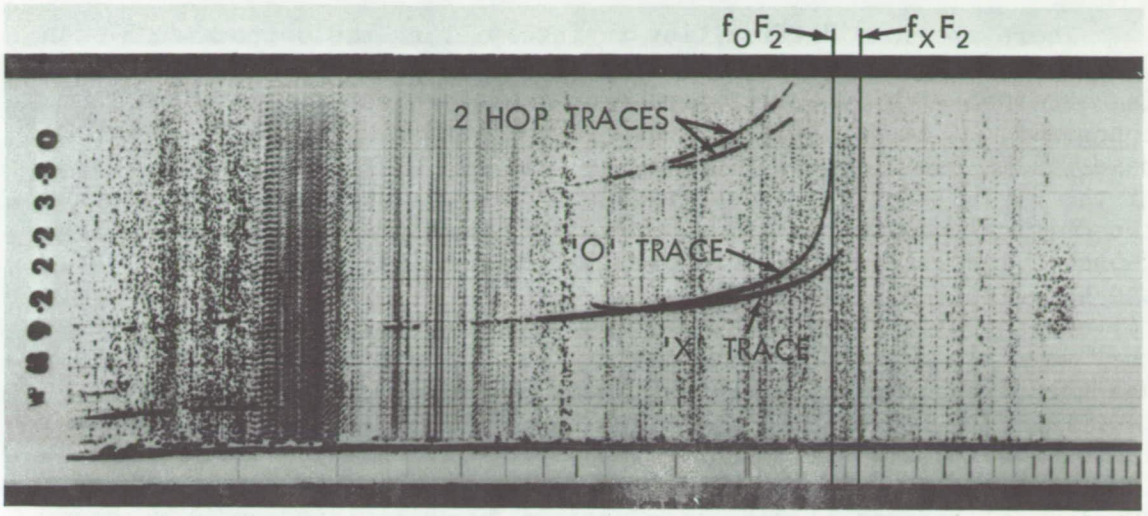


NIGHTTIME

Bottomside nighttime 'B' scan ionogram from Wallops Island, Va. The bottomside enhanced regions are normally absent at night. The two hop traces result from pulses reflected twice from the ionosphere and once from the ground.

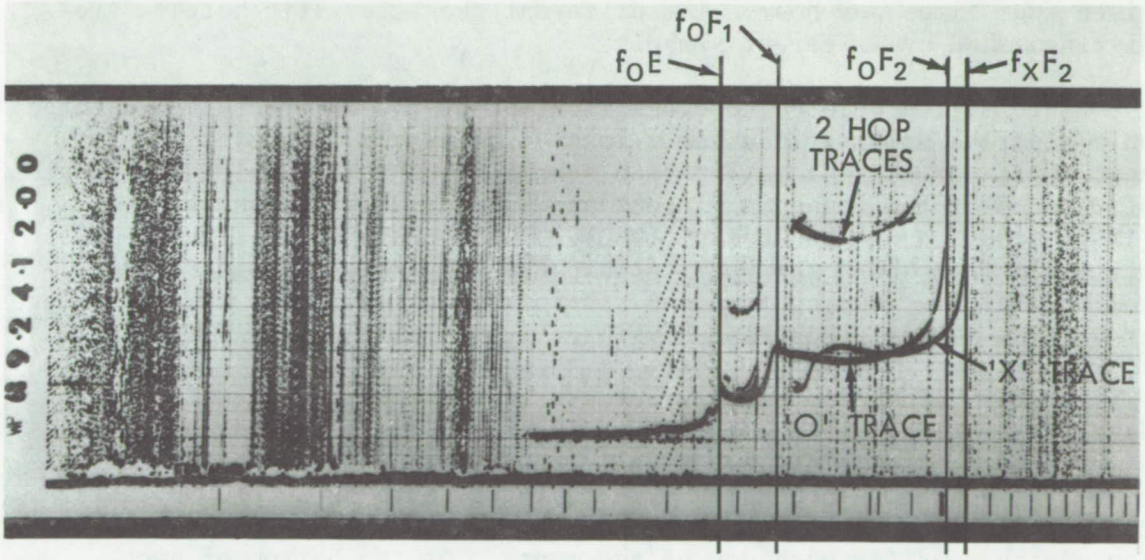


DAYTIME

Bottomside daytime 'B' scan ionogram from Wallops Island, Va. The E, $F_1$, and $F_2$ critical frequencies are indicated. An 'O' (ordinary) and 'X' (extraordinary) mode of propagation can usually be identified.

Figure 21. Sample Bottomside B-Scan Sweep-Frequency Ionograms

There are some difficulties in interpreting the bottomside B-scan sweep-frequency ionograms, and a considerable portion of the literature is concerned with interpretation of particular features noted on the ionograms. (See Wright, 1967, and Piggott and Rawer, 1961). In most cases, some useful quantities may be obtained directly from the shape of the virtual height versus frequency curve. These quantities include the critical frequencies foF2, foF1, foE, and foEs (ordinary wave frequencies just large enough to permit transmission through the F2, F1, and E regions; a slightly different definition applies to the partially reflecting Es level), the blanketing frequency fbEs (the lowest ordinary wave frequency at which echo traces are observed on the ionogram), and the virtual heights h'F, h'Es, and h'E associated with local electron density enhancements or maxima. MUF (Maximum Usable Frequency) factors, which are useful for oblique propagation computations, can be immediately derived from the critical frequencies (Piggott and Rawer, 1961). Collections illustrating various types of ionograms have been made by Wright and Knecht (1957) and by Shapley (1970).

F-Plots - Many of the characteristics digitized (scaled) from bottomside sweep-frequency ionograms are presented in a graphical format called f-plots. For a given station for a given day, the reflection heights for a number of characteristic frequencies are presented on a single plot. The heights for each characteristic frequency are typically given four times per hour. The different characteristic heights are distinguished by different symbols.

Information related to classification of the Es trace is presented on a separate small grid usually located below the main plot. A full description of this classification scheme and a more complete discussion of the f-plot are found in Piggott and Rawer (1961), Wright et al. (1957), and Piggott and Bossy (1963). The f-plots are available on microfilm from WDC-A for Upper Atmosphere Geophysics, Boulder. Availability information, by time and station, is given in the WDC-A Catalogue of Data on Solar-Terrestrial Physics.

Hourly Values and Monthly Summary Tabulations - Scaled ionosonde data are available in tabular form. Each table presents data taken at one station; data points are usually read from the ionograms taken nearest the hour. An hourly value table presents data for one characteristic. The table presents the data in columns for each of the 24 hours with rows for each day of the month. At the bottom of each column, monthly summaries of median and quartile values and the number of hourly values from which these values were obtained are often presented. These monthly summaries are usually available separately in tables using columns for each hour of the day and rows across the tables for the various characteristics. Qualifying and descriptive letters used in the hourly value and monthly summary are defined and discussed in Piggott and Rawer (1961) and are often contained in brief form in the introductions to published tables of data.

These digitized ionospheric data tables are available for more than 200 sounding stations. For recent years, tables for over 100 stations are available. The most complete and convenient source for these tables (in both hard-copy and microfilmed forms) is WDC-A for Upper Atmosphere Geophysics, Boulder. Data on magnetic tape for over 60 stations are also available from the same source. Detailed availability information is given in the WDC-A Catalogue of Data on Solar-Terrestrial Physics. WDC-A personnel can often be of assistance in obtaining data that are not currently available in their files.

Electron Density Profiles - Profiles of electron density (N) versus real (geocentric) height can be calculated from ionograms using the equation defining virtual height [$h'(f)$],

$$h'(f) = \int_0^{h_R} n'[N(h), f, B(h), \theta(h) \nu]dh$$

where $h'$ and $h_R$ are virtual and real heights of reflection of the wave with frequency (f). The group index of refraction is designated by $n'$; N(h) is the electron density, B(h) is magnetic field magnitude, $\theta(h)$ is the angle between the magnetic field direction and the wave propagation direction, and $\nu$ is the collision frequency. When the changes in magnetic field strength along the propagation path are small and the collision frequency is small (true above the D region), the equation can be simplified to

$$h'(f) = \int_0^{h_R} n'[N(h), f]dh.$$

A vertical propagation path is usually assumed.

There are several techniques for solving this equation to obtain the N(h) profile from observed values of $h'$. The frequently used lamination technique involves a step-by-step procedure. It is assumed

that N(h) is known for $h \leq h_1$. For a wave frequency $f_2$, reflected from a known electron density level at a small but unknown distance $\Delta h$ above $h_1$, the virtual height is

$$h'(f_2) = \int_0^{h_1} n'[f_1, N(h)]dh + \int_{h_1}^{h_1+\Delta h} n'[f_2, N(h)]dh.$$

The quantity $h'(f_2)$ is read off the ionogram, and the first integral is known because N(h) is known for $\leq h_1$. In the second integral, both $N(h_1)$ and $N(h_1 + \Delta h)$ are known, although $\Delta h$ is not itself known. By assuming a functional form for the variation of N(h) with h in the small height interval $h_1$ to $h_1 + \Delta h$, $\Delta h$ may be determined as that value yielding the required equality. This completes a given step.

Complicating effects in this approach are: (1) low level absorption, which results in having to assume a value for $h_1$ for the first step; (2) an E region electron density maximum; and (3) determination of $h'$ at the absolute density maximum where the $h'(f)$ curve becomes asymptotic to the vertical. A much more complete discussion of these effects and of details describing other reduction techniques can be found in "Special Issue on Analysis of Ionograms for Electron Density Profiles," Radio Science, volume 2 (new series) #10, October 1967. An extensive bibliography on profile calculation is included in this issue.

In addition to the generation of N(h) profiles from individual ionograms, a composite N(h) profile can be generated from a "median ionogram." Twenty-four median ionograms are generated (one for each hour) for a given station each month.

For a given N(h) profile, a number of parameters have been defined (Wright, 1967, and Piggott and Rawer, 1961). These include:

1. $h_c$ (height of the maximum) - real height of the F layer maximum assuming a parabolic profile near the maximum (same as the more commonly used $h_m$, $h_{max}$, or HMAX).

2. $q_c$ (quarter thickness) - half the height difference between $h_c$ and the two points at which the electron density is three-quarters of that at $h_c$.

3. SCAT - same as $q_c$; also called characteristic thickness.

4. HMIN, HMAX - true heights from which the minimum and maximum frequencies are reflected.

5. NMAX - electron density at $h_c$.

6. SHMAX - total electron content (TEC) downward from $h_c$.

7. SHINF - TEC from the ground to infinity, assuming a Chapman layer density profile above the density maximum.

8. RATIO - ratio of TEC to SHMAX.

Hard-copy tabular data, which contain ionogram station and time information, electron densities, virtual and true heights, total columnar content below given heights, and some of the parameters listed above, are available at WDC-A, Boulder. The WDC-A Catalogue of Data on Solar-Terrestrial Physics includes the station list, data availability, and sample formats. These tables have been prepared by the Institute for Telecommunication Sciences and Aeronomy (ITSA), NOAA, from ionograms (individual and median) of 41 stations for various periods of time since 1956. The format of the tables is given in a paper by Wright and McKinnis (undated). This paper is available from the authors or from NSSDC.

## Oblique Soundings

The oblique incidence sweep-frequency ionospheric sounding technique uses the same principle of operation as the vertical incidence sounder (Davies, 1964). The primary difference is that the transmitter and receiver are located at different places so that the signal is reflected at an angle. The most common use of these sounders is to operationally investigate optimum conditions for radio propagation. According to Rawer (1969), no attempts are known to have been made to compute electron density versus height profiles from oblique incidence ionograms. These oblique incidence soundings do not adequately substitute for the vertical soundings. A very limited number of oblique incidence soundings are available through the WDC-A for Upper Atmosphere Geophysics. This same WDC-A subcenter can assist in the identification of currently operating stations which may have observational records that can be made available.

### Fixed-Frequency Soundings

Fixed-frequency bottomside sounders (also called virtual height recorders) are in operation at some ground ionospheric observatories. Recordings are not generally available except through the individual stations. These recordings normally operate continuously and are used to monitor ionospheric changes.

## Topside Soundings

### Sweep-Frequency Soundings

A sample topside sweep-frequency ionogram is shown in figure 22. Such ionograms have been obtained by equipment and techniques described in Franklin and Maclean (1969) and Franklin et al. (1969). These techniques and the equipment were used on the Alouette 1 (launched 9/62), Alouette 2 (launched 11/65), and ISIS 1 (launched 1/69) satellites. All are near-polar satellites and were operating as of January 1971. Observations have been taken in the vicinity of as many as 22 telemetry stations, and a limited number of ionograms from ISIS 1 have been tape-recorded at other locations. The availability of observations depends on many factors, including:

1. Location of telemetry station.
2. Satellite altitude and other orbit characteristics.
3. Satellite operating conditions (power supply, etc.).
4. Satellite scheduling at telemetry stations.

For telemetry reception with elevation angles $\geq 15°$, the observing range of a satellite at a height of 1000 km is within a radius of 2100 km from the station. For some stations, elevations of 0° are not uncommon, with a resulting observing range of nearly 3400 km for satellites at a height of 1000 km (Franklin et al., 1969). Of about 24 stations which have received the telemetered data, all but a few lie near the 90th geographic meridian; these stations are fairly well distributed in latitude. The satellite sounders have generated one ionogram every 20 to 30 seconds for up to 9 hours per day. For Alouette 1, in a circular orbit at about 1000 km, this means typically one ionogram (20 seconds per frame) for each degree of latitude along the orbit when in range of, and scheduled by, a telemetry station. For ISIS 1 and Alouette 2, with an orbit perigee/apogee of about 500/3000 km, it means typically one ionogram (30 seconds per frame) for each 2° of

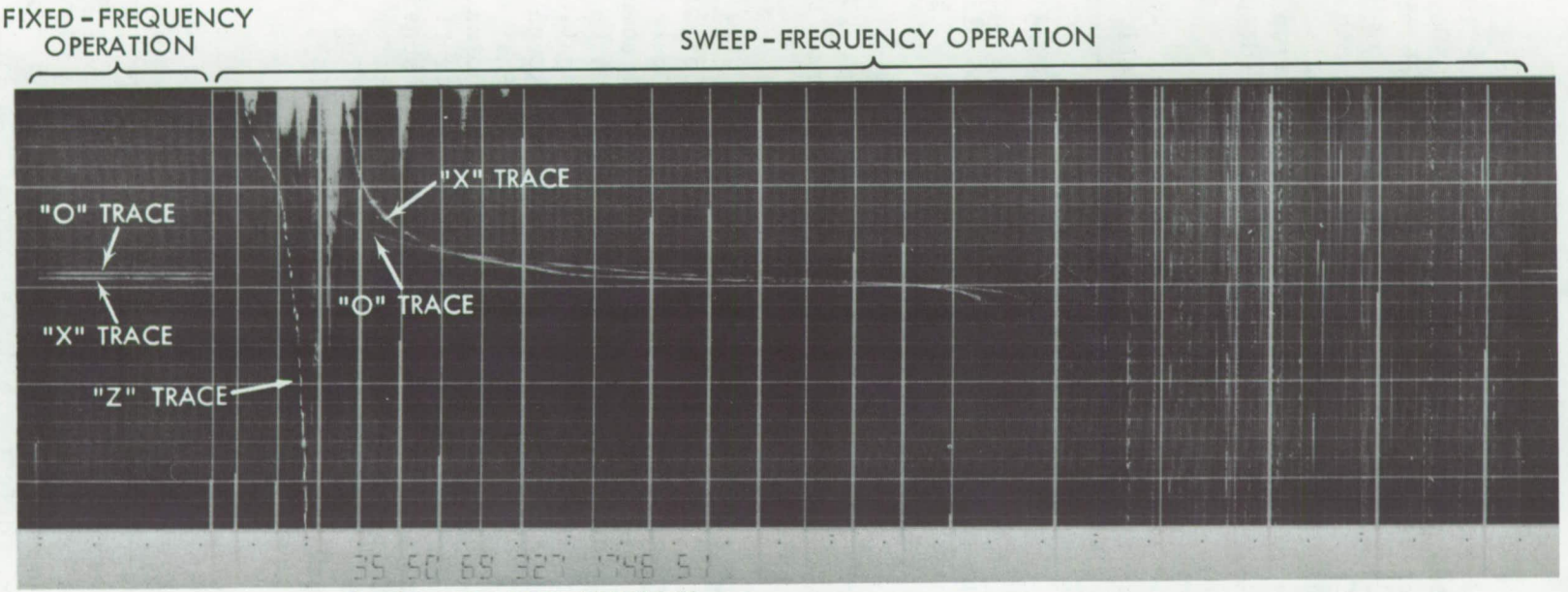


ISIS 1 ionogram: Frame identification is similar to that in fig. 23 with three additions: ISIS program satellite number (C=3=ISIS 1), fixed-frequency indicator (F=5=4.0 MHz), and seconds of UT (SS=51) are given. Range markers appear every 200 km counting downward from the top of the ionogram (satellite altitude). For frequency range, see text page 112; time ticks appear every second along the abscissa, and SS is valid for the tick appearing above C.

Figure 22. Sample Topside Sweep-Frequency Ionogram

latitude near perigee and one for each 1.1° of latitude near apogee. Microfilmed copies of these ionograms are available from NSSDC approximately 2 years after observation. These ionograms can be obtained also through the WDC-A for Rockets and Satellites or the WDC-A for Upper Atmosphere Geophysics. Current listings of specific times and places for processed observations (i.e., prepared ionograms) are also maintained at NSSDC. As with bottomside ionograms, interpretation of topside ionograms requires experience, skill, and training. (Hagg et al., 1969).

The appearance of the ionograms from each of the three sweep-frequency topside sounders is different. Sweep rates are all the same above 2 MHz (i.e., about 1 MHz/sec), but below 2 MHz, the rate for Alouette 2 is 0.13 MHz/sec and for ISIS 1 is 0.31 MHz/sec. This causes the frequency marker intervals below 2 kHz on the ionograms to be stretched out on the two later satellites, with a resulting change in appearance of the ionograms. The frequency ranges are also different for each satellite: Alouette 1, 0.5 to 12 MHz; Alouette 2, 0.12 to 14.5 MHz; and ISIS 1, 0.1 to 20 MHz. An added feature on the ISIS 1 ionograms is a short record of fixed-frequency sounding normally appearing prior to each sweep-frequency ionogram. (See figure 23.) No enhanced electron density regions, except for the F2 maximum, can be identified regularly on topside ionograms.

Electron Density Profiles - The principles used in obtaining electron density profiles from topside ionograms are the same as those used for bottomside ionograms. Reduction of topside ionograms has been done primarily by the lamination method described by Jackson (1969) or by some modification of this technique. Important differences which must be taken into account are (1) that errors due to non-vertical propagation cannot be assumed to be small when the sounder range starts to exceed 1000 km (bottomside sounder range seldom exceeds 500 km) and (2) that the X trace, in contrast to the O trace for bottomside reductions, is normally used to make reductions from topside ionograms. Use of the X trace also makes the computation more complex since its use requires consideration of the magnetic field and its variations along the propagation path. In addition to Jackson (1969), other primary references treating topside reduction are Jackson (1967), Fitzenreiter and Blumle (1964), and Thomas et al. (1965).

Of the approximately 2.5 million satellite ionograms that have been produced to date by the two Alouette satellites, it is estimated that about 5% to 7% will be reduced. At present, reductions are being made as needed to support research projects of the major ISIS project participants including the Communications Research Center (CRC), Ottawa; the Radio and Space Research Station, Slough, Bucks, England; NOAA, Boulder; NASA-Goddard Space Flight Center, Greenbelt, Maryland; and NASA-Ames Research Center, Moffett Field, California. A limited

number of these reductions prepared by the CRC and the Radio and Space Research Station are available in hard copy and on tape from NSSDC or directly from the agency (see references 2, 3, and 28). The NASA-Ames Research Center facility has reduced satellite ionograms on a mass production basis, and a quantity of Alouette 1 profiles are available in hard copy (Chan et al., 1966; Thomas et al., 1966; and Colin and Chan, 1967) or on tape from NSSDC. About 8000 Alouette 2 ionograms have also been reduced by the Ames Research Center, and it is expected that these will also be available on tape soon. Since October 1967, a Japanese telemetry station has been taking observations at Kashima, Japan. Their first reductions for October to December 1967 are now available in hard-copy form, and continuation of routine reduction of Kashima ionograms is expected (Ref. 12).

Scaled Digital Data - Alouette Synoptic (Alosyn) data have been tabulated from a large number of the Alouette 1 ionograms recorded at 11 of the primary telemetry stations. They contain satellite position information and related geophysical data such as zenith angle and electron gyrofrequency based on a model geomagnetic field. Listed with each satellite position are observed values of plasma frequency at the sounder at $F_2$ penetration and any observed sporadic E. For topside sounding, the X trace is normally used in scaling, but both ordinary (O) and extraordinary (X) trace observed values, as well as O values computed from the X values, are included in the Alosyn data. Ground echo occurrence and intensity have also been listed. Alouette 1 Alosyn data are available from launch (September 29, 1962) through January 1965 and for a few months in 1967 and 1968. It is anticipated that additional listings will be prepared by CRC. Additional information and/or copies of these data are available on tape, microfilm, or hard copy through the experimenter (CRC) or NSSDC.

## Fixed-Frequency Soundings

A typical fixed-frequency topside ionogram is shown in figure 23. These ionograms have been obtained by equipment and techniques described by Russell and Zimmer (1969). There have been two satellite-borne fixed-frequency sounders, one on Explorer 20 and the other on ISIS 1. Explorer 20 sampled each of six frequencies sequentially, and, in processing, records of each frequency were placed on separate ionograms. About 1000 hours of soundings made during 1964 and 1965 near telemetry stations are available on microfilm. ISIS 1, still operational, sounds for 3 to 5 seconds at one of six possible frequencies prior to each sweep-frequency sounding. These are recorded ahead of the sweep-frequency ionograms on microfilm and have been observed near telemetry stations since January 1969. These data have been used to study plasma resonances and small-scale ionospheric structure. No digital scaled data are available.

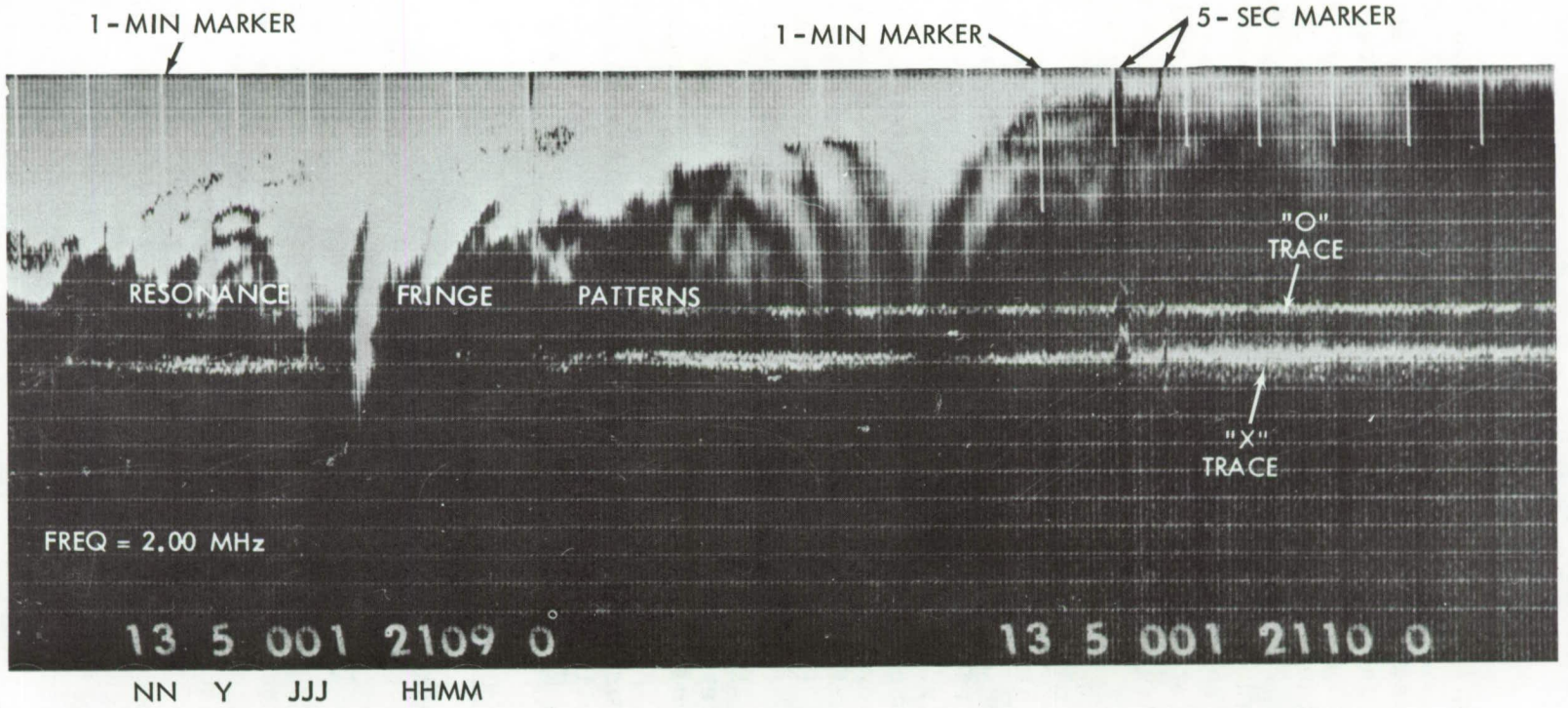


Explorer 20 ionogram: The frame identification gives station number (NN = 13, College, Alaska), year (Y = 5 = 1965), day of year (JJJ = 001, 1 Jan.), and UT (HHMM = 2109). The last counter is meaningless and always set to zero. Range (height) markers are every 100 km counting downward from the top of the ionogram (satellite altitude).

Figure 23. Typical Fixed-Frequency Topside Ionogram

## INCOHERENT BACKSCATTER RADAR OBSERVATIONS (THOMSON SCATTER)

For radio waves transmitted through the ionosphere with frequencies much larger (50 to 1300 MHz) than the plasma frequency (up to 15 MHz), very small-scale fluctuations of electron density in the plasma will scatter a portion of the signal back toward the transmitter. These fluctuations are caused by the random thermal motions of the electrons (Evans, 1969, and Davies, 1965). The height at which the scattering occurs can be determined by either a pulse technique or by the use of two intersecting cylindrical radar beams. The height resolution of a backscattered pulse or beam varies from 4 to 35 km at a height of 100 km to about 300 km at altitudes above 1000 km, depending on the equipment used and the geographical location of the station.

From analysis of the backscattered signals, electron density profiles, electron and ion temperature profiles, and ion composition and ionospheric drift can be determined. The equipment used for the observations determines the vertical extent of the backscatter profiles and the resolution, as well as influencing the procedures used to convert the scattered return to measures of meaningful ionospheric parameters.

Radar installations that can make these observations are complex and expensive to operate; consequently, these observations are not scheduled on a routine basis. Rather, they are scheduled on an "as needed" basis, and the equipment is shared for other uses. The available data can be obtained by inquiry to the observatory or to the WDC-A for Upper Atmosphere Geophysics. The seven stations taking incoherent backscatter radar observations are located in the U.S., Canada, France, and England. The stations are listed and described in detail by Evans (1969).

## IONOSPHERIC ABSORPTION OF RADIO WAVES

Absorption of radio waves occurs when electrons responding to the wave fields collide with and transfer energy to the neutral particles. A study of ionospheric absorption yields information on both the D and E regions, where both electrons and neutral particles exist in sufficient quantity to produce significant absorption. Knowledge of D region characteristics is unattainable from normal sweep-frequency

ionograms because absorption prevents the return of a detectable reflected signal. In practice, absorption characteristics are studied primarily in connection with radio communications applications.

Three techniques of observing ionospheric radio wave absorption, identified as A1, A2, and A3, have been designated by the International Council of Scientific Unions. They are (A1), radio waves transmitted vertically and received at the same station (vertical ionosondes), (A2), waves received from extraterrestrial sources by riometers, and (A3), waves transmitted obliquely and received by spatially separated stations. Discussions of ionospheric absorption theory, techniques, and results are found in Geisweid et al. (1963, 1968), Piggott et al. (1957), Allcock (1954), and Mitra (1970).

## Pulse Reflection Method (A1)

An amplitude versus time oscilloscope (A scan) display of a single-frequency vertical ionosonde pulse is used to measure the amplitude (I) of an echo pulse. Comparison of this value with the amplitude that would have been returned in the absence of collision losses (Io) provides a quantitative scale with which to measure absorption. This ratio is called the apparent reflection coefficient ($\rho$)

$$\rho = \frac{I}{Io}$$

The absorption loss (L) is measured in decibels.

$$L = -20 \log\rho$$

The reference value Io is determined by nighttime observations, usually a mean of values over night observations for several different dates. The noon observation of L is most frequently available and is generally considered representative of absorption for that day.

It is usually difficult to determine the relative contributions to L arising from the D and E regions.

Data are available from the WDC-A for Upper Atmosphere Geophysics for 37 stations, 14 of which have records that cover more than 5 years. Data for a given station and month appear on a single page. Local observing time (usually noon) and values of absorption for each day and observing frequency (usually one value near 2.2 MHz and at least one other value) are listed. Monthly median values for each frequency are also listed. For further details, see the WDC-A Catalogue of Data on Solar-Terrestrial Physics. Symbolism used in recording these A1 observations has been standardized (Piggott et al., 1957).

## Riometer Method (A2)

A riometer (Relative Ionospheric Opacity Meter) is a detector that measures the absorptivity properties of the ionosphere. This directional detector is oriented in a fixed direction relative to the earth (usually vertical) and measures the incident cosmic radio noise at a single frequency between 8 MHz and 120 MHz (usually 20, 30, or 60 MHz). During the course of each sidereal day, the riometer receives noise from all celestial longitudes ($\Phi$). On days of negligible ionospheric disturbance, the riometer signal power will be $Po(\Phi)$. Due to the general constancy of cosmic radio noise, $Po(\Phi)$ will be constant except for a large-scale, small-amplitude, daily solar effect which regresses through the observations at the rate of 1 day per year (4 minutes earlier each day). Deviations of observed riometer signal power (P) from Po are primarily attributable to ionospheric variations particularly in the D and E regions. This method is particularly useful during radio blackout (high absorption) since it involves the use of higher frequency signals that are not completely absorbed. More detailed discussions of riometers are found in Little (1959) and Little and Leinbach (1957).

Roll chart recordings of riometer output current versus time obtained at over 60 stations are available in hard-copy and microfilm forms from the WDC-A for Upper Atmosphere Geophysics. Availability information, by station and time period, is found in the WDC-A Catalogue of Data on Solar-Terrestrial Physics.

Absorption (A) in decibels is defined as $A = -10 \log (P/Po)$. Tables of the maximum absorption reading for each hour are also available in hard-copy and microfilm formats at WDC-A, Boulder. No conversions are routinely made from absorption data to total electron content or changes in content.

## Continuous Wave (CW) Field Strength Method (A3)

Method A3 consists of comparing signal strengths of radio signals obliquely reflected from the ionosphere during times when absorption is present with similarly obtained signal strengths for times when absorption is absent (Geisweid et al., 1963, 1968). Criteria for observing practices depend upon many factors. The normal operating range between the transmitter and receiver is greater than 200 km in order to avoid any contribution to the received signal from the ground wave, and the distance is normally less than 500 km so that the reflection from one level (E region) is much stronger than from any other level. Signal strength observations from night sporadic E (or adjusted values from

the F region) reflections are used for reference "no absorption" values, against which the day values are normalized. The absorption is given by

$$L = -(\cos \alpha)\ 20 \log \frac{E_d\ l_d}{E_n\ l_n}$$

where $\alpha$ is the incident angle, $E_d$ and $E_n$ are the received day and night signal strengths, and $l_d$ and $l_n$ represent the signal path lengths for day and night observations. The absorption occurs in the D and E regions; again, separation of D and E effects is very difficult. As with the A1 method, relatively small changes in electron density can be deduced from these observations, but with large enhancements of electron density, the signals may be entirely absorbed and no reflections detected. Data are available for 19 receiving stations. Unscaled data are available from 10 stations, all for periods of over 6 years. Digitized values are available from the other nine stations. These are tabulated values for day of month versus time of day on each sheet. Six of these nine stations have records available for periods of over 5 years.

"F min" as a Measure of Absorption

Another measure of absorption that is sometimes used is the f min value scaled from the ionogram (Piggott et al., 1957). Caution must be used when interpreting f min as absorption since changes in recorder gain and variation in noise level also affect this value. The f min value is the lowest frequency at which combined recorder gain, noise, and absorption permit echoes of the ionosonde transmitter to be returned and detected on the ionosonde receiver. These data are readily available from WDC-A, Boulder, for most ionosonde stations as one of the scaled parameters for which both daily values and monthly medians are available (see page 106).

## SATELLITE BEACON EXPERIMENTS

Changes in radio frequency signal characteristics in the range of 15 to 150 MHz result when a radio signal traverses the ionosphere. The signal changes can be studied to deduce ionospheric characteristics

and their variations (Mass, 1963, and Garriott et al., 1970). Several arrangements have been used to measure these signal variations, including reflection of ground transmissions from the moon or a satellite, transmission from the ground to a satellite, and the most commonly used arrangement, transmission from a satellite beacon to the ground. A synchronous altitude (approximately 35,800 km) satellite transmission is convenient for the study of time changes of ionospheric conditions at any given location. Transmissions from other satellites can be used to obtain wide geographical coverage, but numerous ground stations are required for obtaining wide coverage.

The signal characteristics affected by the ionosphere are signal strength, frequency, direction of arrival, and polarization angle. The observations of variations in these characteristics are interpreted in terms of ionospheric total electron content, scintillations, and irregularities. Determinations of the changes in time and space of these ionospheric features, as well as the processes related to these changes, are the objectives of these satellite beacon studies. The results of these studies are useful in the design and operation of radio communications and tracking equipment.

Ionospheric effects on radio signals increase rapidly with decreasing radio frequency. However, signals with frequencies lower than the F layer critical frequency will not penetrate the ionosphere but will be reflected. Since F layer critical frequencies range from 5 to 15 MHz (depending primarily on time of day, location, and solar cycle phase), optimum frequencies for beacon experiments are around 20 MHz, with a higher frequency sometimes used concurrently for comparison. Transmissions that have not been specifically designed for use in ionospheric study have often been successfully employed; one example is the Syncom tracking beacon, which transmitted at 136 MHz.

One major difficulty with all beacon observations is that the propagation path does not pass perpendicularly through the ionosphere. Even if the satellite were at zenith, tilts in the ionospheric layer, multipath propagation, refraction, etc., would make it difficult to normalize observations to some standard path. Nevertheless, some normalizations or assumptions must be made in order to make comparisons between sequential observations. It is common practice to use a simple geometric adjustment in allowing for the incident angle of the wave, to assume a horizontally stratified ionosphere, and to limit observations to zenith angles of less than 40° in order to avoid gross errors.

## Total Electron Content (TEC)

TEC is the total number of electrons in a column of unit cross section extending from the transmitter to the receiver. TEC is calculated from observations of the rotation of a polarized signal (Faraday rotations) transmitted from the satellite. TEC can also be computed from observations of the dispersive Doppler frequency shift of the beacons due to the ionosphere (Mass, 1963). There are several specific techniques for obtaining TEC by using Faraday rotation and/or Doppler shift observations. Estimates of accuracy for these data range from 2% up to 30%, depending on the technique and on the validity of assumptions for the particular observational conditions. Digitized tabulations of TEC data taken in the vicinity of several stations for various time periods between 1960 and 1970 may be obtained from the WDC-A for Upper Atmosphere Geophysics, and its catalog gives information on the availability of TEC data. Yuen and Roelofs (1970) contains a large number of diurnal TEC profiles using the synchronous altitude ATS 1 and Syncom 3 satellite located at the equator over the Pacific Ocean. The data, which cover the period 1964 through 1968, are considered valid for a sub-ionospheric point a few hundred kilometers south of Hawaii.

## Scintillation

Scintillations are rapid fluctuations in the amplitude, frequency, polarization, or direction of an observed signal. Scintillation of beacon signals is caused by small-scale variations of electron content that occur along the propagation path. These irregularities in the structure of the ionosphere are usually considered to extend less than 1 km. The scintillations are commonly observed as noise-like structures (rapid signal strength variation) on strip chart recordings of satellite tracking records or Faraday rotation recordings. Tracking records of selected equatorial and polar stations are available for a few satellites from WDC-A. The intensity and the start and stop times of scintillations occurring on records of signal polarization changes (Faraday rotation) are sometimes noted in the tables of TEC.

## Irregularities

Ionospheric irregularities are generally considered to represent middle-scale variations of total electron content, i.e., those with horizontal dimensions from 1 to 1000 km. Irregularities are sometimes identified by rapid changes in TEC which show strong horizontal electron density gradients in the ionosphere. The large areas in the ionosphere in which scintillation occurs are also referred to as irregularities.

Joint Satellite Studies Group - An informal organization of scientists who are particularly interested in using beacon equipment and data has been formed and is called the Joint Satellite Studies Group. If more detailed information about the availability of beacon data is desired, it can be obtained through the chairman of this group, Dr. Jules Aarons, AFCRL, Bedford, Massachusetts 01730.

## IONOSPHERIC DRIFTS

Ionospheric motion is a complex phenomenon. At ionospheric heights of 100 to 500 km, less than 1% of the particles are ionized. Ionospheric motions, then, may be expected to respond to neutral motions as well as to electrical fields and currents, magnetic fields, diffusive processes, etc. Ionospheric motions of various scales of magnitude have been observed. As for most ionospheric observations, remote sensing techniques are used also for observing ionospheric drift. Some identifiable ionospheric feature is tracked, and the motion of that feature is then assumed to represent the "drift" motion of the ionosphere.

Several papers in the literature compare observations from different observing techniques and attempt to give physical reasons for differences in results. There are five well-known drift observing techniques. A considerable amount of the data that are readily available have resulted primarily from the fading method described below. IGY data (1957 to 1959) from over 20 stations are available at the WDC-A for Upper Atmosphere Geophysics. In subsequent years, about 10 stations have routinely provided data to WDC-A. Detailed availability of data is given in the WDC-A for Upper Atmosphere Geophysics data catalog. Rawer (1965) contains summary data of fading method observations from 10 stations for the years 1957 to 1959. The drift tracking methods, along with comments on the procedures and availability of data, are outlined below. For a more detailed survey on ionospheric drifts, see Beynon and Brown (1957), Briggs (1957), Huxley and Greenshow (1957), Rawer (1968, 1969), Spencer (1955), and Spizzichino (1968).

### Fading Method (D1)

Radio pulses are transmitted upward, and their downcoming reflections are monitored by three receivers spaced some distance (about one wavelength) apart. Pulsed transmissions at fixed frequencies between

2 and 10 MHz are most frequently used. Signal fading that occurs along the propagation paths will appear on the amplitude records of the received signals. When similar fading features are noted on all three records of the received signal, it is assumed that that particular signal results from the same ionospheric feature. The differences in time of reception of the commonly returned signal occurrence at the three receivers can be interpreted as twice the velocity of the ionospheric motion near the reflection height. It is assumed that (1) the cause of fading is due to small-scale variations in electron density near reflection height, (2) these variations are conservative over short time periods, and (3) time changes in these small-scale variations represent general horizontal motion of the ionosphere.

The altitude of the observed drift is a function of both electron density and frequency; thus, for a given frequency, the height of drift information will show considerable diurnal variation and occasional shorter term storm variation. Data are limited to the bottomside ionosphere (80 to 350 km).

Data listings for each station consist of observation time; speed of the irregularity, v (one half the observed ground speed) (Wright, 1968); azimuth toward which the drift moves, $\phi$; and component velocities, $+V_X$ and $+V_Y$. The listed values are a composite of values obtained from many individual observations and thus represent a mean motion over a period of minutes. There are several methods for converting observations to drift motions (Briggs, 1957; Rawer, 1969, p. 123-25; and Pfister and Bibl, 1968), but all result in data listings of similar form. Most of the hard-copy data readily available in WDCs are derived from this fading method. A large amount of data from Breisach, Germany, has been summarized recently (Harnischmacher and Rawer, 1968).

## Radio Star Scintillation Method (D3)

Radio signals from radio stars are received at a selected frequency between 30 and 100 MHz. Three receivers are spaced at about 4 km or less, and signal strength fluctuations that are similar on all three receiver records are presumed to be caused by the same ionospheric feature. In a manner similar to the fading method, the time delays can be converted to drift motions given in speed, V, and azimuth, $\phi$. The altitude of drift has been associated with the F layer (Little and Maxwell, 1951), but it is possible for the altitude range affecting these observations to extend over a considerable range of both the bottom and top sides of the ionosphere. The observation itself cannot resolve the drift altitude accurately. Observations by this technique have not been extensively made, and no records are available at WDCs. Observations were made

in the early 1950's at Jodrell Bank, University of Manchester; the University of Cambridge; and Mayaguez, Puerto Rico (Chivers, 1961; Dueno, 1961; Hewish, 1952; and Maxwell and Little, 1952.)

Meteor Trail Method (D2)

The ionized trails created by collisions of meteors with neutral particles between 80 and 100 km are tracked, and the tracking data are converted to speed and direction values. Two methods have been used, one a continuous wave technique and the other a coherent-pulse technique. Both techniques involve similar principles: a radio frequency signal is directed toward a selected area of the sky, and the portion of the signal that is scattered back from the trail is "beat" with a known signal; these beat characteristics are used to determine range and radial motion of the trail.

Varying the transmitted signal characteristics and observing in two different areas of the sky at a zenith angle of about 45° provides adequate additional information to obtain horizontal drift motions at relatively accurate determined altitudes. The smaller vertical components of motion are sometimes computed. For the continuous wave technique, the trail must persist for 0.5 to 3 seconds, and the trails must occur frequently enough to allow an average of four to five observations per hour to be made. For the pulsed observations, trails persisting for less than 0.1 second can be used, and hundreds of such meteor trails per hour normally are available for making observations. No extensive files of meteor trail data are readily available, but observations have been made at the following stations (Bradley et al., 1970):

Australia, Adelaide, University of Adelaide

Australia, Newcastle, University of Newcastle

Canada, Ottawa, National Research Council

Czechoslovakia, Prague, Ondrejov Astronomical Observatory

East Germany (GDR), Kühlungborn, Institut für Ionosphären Forschung

France, Garchy, National Center for Telecommunications Studies (CNET)

Sweden, Lund, Lund Observatory

U. K., Sheffield, University of Sheffield

U. K., Malvern, Royal Radar Establishment

U. S. A., Alaska, College, University of Alaska

U. S. A., California, Stanford, Stanford University

U. S. S. R., Kazan, Kazan University

## Characteristic Reflection Method (D4)

Records of unique reflection patterns from ionospheric soundings can be recognized as the same pattern at different receiving station locations. When time differences between station passage of these patterns can be determined, an ionospheric drift velocity vector can be computed. The most useful arrangement is for a single station to receive pulsed signals that were sent at the same sounding frequency by three or more transmitting stations. Continuous records of signal transit time versus time are kept for each of the three stations. Many kinds of patterns that are returned can be recognized as originating from the identical ionospheric feature. An ionospheric drift can be calculated from the time differences between pattern occurrence and distances between transmitters and receivers. Patterns from sweep-frequency ionograms spaced at greater distances have also been used in a similar way. No long periods of such drift observations have been prepared using this technique.

## Chemical Release Methods (D5)

Both luminous and illuminated (by twilight) chemicals that are released from rocket vehicles can be used to observe drift velocities. An identifiable part of the cloud is optically tracked, or sequential photographs are taken. Chemicals may be released either as a trail or in discrete blobs. The altitudes are known from rocket trajectory information. Some of these wind data for mid latitudes have recently been summarized (Rosenberg, 1968).

# IONOSPHERIC EVENTS

There are a variety of observable effects accompanying ionospheric events that are commonly referred to by their abbreviations (Lincoln, 1968; Warwick, 1963; Hultqvist, 1963; and Solar-Geophysical Data, 1970). The events are related to enhancements of electromagnetic radiation, energetic particle flux, and plasma flow (and the resulting geomagnetic storm) associated with solar activity. The observable effects result from enhanced ionospheric electron density, mainly in the D region; these enhancements are due to photo-detachment and/or collisions.

## PCA

Polar Cap Absorption refers to D region electron enhancement over the entire polar cap and is caused by incoming solar protons and particles with energies of 1 to 100 Mev. A PCA event begins 15 minutes to several hours after a flare occurrence, and it may persist for 1 to 6 days. PCA was first identified in 1956 from VHF scatter data, vertical sounder ionograms, and riometer records. An early criterion for PCA was shortwave blackout (i.e., absorption below 3 to 4 MHz on vertical sounder records), which persisted for over 3 hours and covered a considerable polar geographic area. More recent definitions utilize a given absorption loss.

There is no standard definition for PCA; thus, any particular list of events will reflect definitions that were adopted for its preparation. Lists available from the literature are noted on page 193 of Hultqvist (1963). Routine listings by the WDC-A for Upper Atmosphere Geophysics are expected soon; they will likely include UT, time of maximum, start and stop, technique, frequencies, locations, remarks, and observations of related phenomena. An index of auroral blackout (Ip) is described below.

## AZA

Auroral Zone Absorption, also known as "auroral blackout" or "auroral absorption" (AA), is delayed 20 to 40 hours from the associated solar disturbance (not necessarily a flare) and is caused primarily by precipitating electrons with low energies between 50 and 500 kev. As with PCA, high frequencies (3 to 30 MHz) are strongly absorbed. These occurrences normally persist for periods ranging from 1 to 6 hours, and the blackout zone is generally concentric with, and a few degrees equatorward of, the auroral oval. Since identification of AZA depends upon

information other than that contained in any one particular observational record (i.e., geographical distribution of absorption, delay time from disturbance, etc.), these events are most frequently included in listings of PCA events. They are sometimes referred to as a type of PCA and are presently not identified separately in any known listings. Frequencies absorbed are the same as for PCA; only the geographical area covered, the time relations to flare occurrence, and species and energies of incident particles are different.

PCA and AZA blackout indices, Ip and Ia, have been discussed by Hakura et al. (1967). These daily blackout indices provide a measure of the temporal extent of blackout for a given day. The index values run from 0 to 9 and are related to the number of hours (H) of the day during which blackout occurred, as shown in the following table.

| Ip or Ia | Hp or Ha |
|---|---|
| 0 | 0.0-0.4 |
| 1 | 0.5-0.9 |
| 2 | 1.0-1.5 |
| 3 | 1.6-2.5 |
| 4 | 2.6-3.5 |
| 5 | 3.6-5.5 |
| 6 | 5.6-8.5 |
| 7 | 8.6-13.0 |
| 8 | 13.1-20.0 |
| 9 | 20.1-24.0 |

These indices are tabulated for the period 1957 to 1965 in Annals of the IQSY, volume 2, and in the "Abbreviated Calendar Records" from 1964 to the current issue. (See Part VII of this Handbook.)

## SID

The Sudden Ionospheric Disturbance is usually attributed to solar flare electromagnetic radiation incident on the ionosphere. SIDs are observed on the sunlit hemisphere and occur almost simultaneously with visual flare observations. SIDs and subsequent recovery of the ionosphere have a time duration somewhat longer than flare duration; generally from minutes to an hour, with rise more rapid than decay.

Several of the various SID observations are routinely identified and digitized. Samples of several types of original records as they appear before digitizing are nicely illustrated by Lincoln (1968). The types of SID are alphabetically listed below with brief descriptions of each. The SCNA, SEA, SES, SFD, and SWF listings are available from the

WDC-A for Upper Atmosphere Geophysics and have also been published in issues of Solar-Geophysical Data since 1963. Bursts and SFE are also listed in Solar-Geophysical Data. Information available in the data listings includes, in addition to that noted for PCA, the "definiteness" rated on a subjective scale.

Burst - A solar noise burst at riometer frequencies is a sudden increase of signal strength on the riometer records. This is caused by solar radio noise emissions at riometer frequencies. This noise is affected by and can mask the ionospheric absorption that is present. The bursts are of such short duration, however, that absorption changes during the burst can be estimated. In addition to riometer observations, solar noise is routinely observed at much higher frequencies than those used for riometer receivers.

Crochet - See SFE.

SCNA - Sudden Cosmic Noise Absorption, also referred to as CNA (Cosmic Noise Absorption) Type I (see below), is characterized on riometer recordings by a sudden daytime absorption increase of several db within a few minutes. Decay is somewhat slower than rise, and the riometer record is perturbed for a period of minutes to over an hour. SCNA involves absorption outside of auroral regions.

SEA - Sudden Enhancement of Atmospherics is observed as an increase in signal strength on wideband equipment operated to detect electromagnetic emissions from lightning. This equipment operates in the VLF (10 to 50 kHz) range with the most commonly used frequency near 27 kHz.

SES - Sudden Enhancement of Signal is observed on VLF frequencies (15 to 50 kHz). These observations are nearly identical to SEA except that the receivers are narrow-band receivers designed to pick up man-made VLF transmissions. As with SEA, signal strength increase is the SID indicator.

SFD - Sudden Frequency Deviation, caused by ionospheric disturbances, is observed by beating the received radio signal with a reference frequency that is near the received frequency. This technique allows small frequency changes to be observed. SFD is observed in the high-frequency range, and the reference signal is obtained locally from a stable oscillator. Occurrence times and deviations in frequency are listed in data presentations.

SFE - Solar Flare Effect, or crochet, is observed as a small hook on magnetometer records. It is caused by the magnetic field response to increased current flow in the E region due to electron enhancement induced by flare X rays.

SPA - Sudden Phase Anomaly is observed in the same manner as SFD, except that VLF frequencies are used and the reference signal is the ground wave. For observing SPA on transmitters more distant than possible for ground wave propagation (about 200 km), the ground wave reference signal is provided by telephone, or a local reference signal source is used as in SFD observations.

SWF - Short Wave Fadeout is observed from signal strength records of any shortwave (3 to 30 MHz) receiver. Signals from sweep-frequency ionosondes (vertical or oblique incidence) may be completely absorbed. SWF is categorized as gradual (G), slow (S1), or sudden (S), depending primarily on how rapidly the signal loss occurs.

## CNA

In addition to SCNA discussed under SID, there are two other types of CNA. Data on these latter types are not generally available but are mentioned here to broaden perspective. Cosmic Noise Absorption is observed on riometers that operate between 15 and 60 MHz, but most often near 25 MHz. Absorption is normalized to low nighttime absorption occurrences for that station. CNA can be divided into SCA (sudden commencement absorption), CNA Type I, also called SCNA (sudden cosmic noise absorption), and CNA Type II. CNA Type II is local nighttime absorption associated with active aurora. The absorption may persist for hours with irregular variation including individual peaks as high as 8 to 10 db persisting for several minutes. This is sometimes called auroral absorption, but is not the same as AZA, which is not a local phenomenon.

SCA (Sudden Commencement Absorption) is characterized by sudden onset, occurrence in zones centered on the auroral zone (58° to 75° geomagnetic), and persistence for less than 1 hour. The SCA is similar to SCNA in rise time and duration. Types I and II CNA are somewhat local and irregularly distributed in longitude in contrast to the zonal occurrence of SCA. SCAs have been associated with geomagnetic storm sudden commencement X-ray fluxes.

# VLF EMISSIONS, WHISTLERS

Natural VLF emissions are recognized as structured noises in the 0.2- to 40-kHz radio band (Helliwell, 1965). They are normally observed by use of a long antenna connected to an audio amplifier. The signals are usually tape-recorded and studied either by ear, using a speaker or earphones, or visually by use of a spectrogram. The aural data consist of multi-frequency or single-frequency noises, whistles, chirps, hiss, chorus, and many combinations of the structured noises which are possible. The spectrogram graphically depicts frequency on an ordinate versus time on the abscissa, with signal intensity indicated qualitatively by the relative brightness of the plotted signals. Spectrograms are normally available on 4- x 12-1/2-inch sheets of facsimile paper (Kay Electric Sonograph) or rolls of 35-mm paper or film (Raytheon Rayspan). Data summaries have been prepared from some observations which consist of counts of selected noises (e.g., whistlers) by time of day and day, based on one short observation repeated hourly.

Most frequently, the noises are studied to determine their origin and their propagation characteristics. Such study is of value in understanding the structure of the propagating medium, along with its temporal and spatial variations. It has been determined that whistlers result from frequency dispersion of lightning-generated emissions. The origin of other noises has not been so specifically identified, but these are generally attributed to origins located in ionospheric and magnetospheric regions. Propagation is strongly influenced by the magnetic field in the ionosphere and magnetosphere.

Since 1957, a VLF technique has been used to observe propagation characteristics (transmission loss and group delay) of pulsed, fixed-frequency emissions (Helliwell, 1965). With this technique, the strength of the received signal versus time is observed. A closely related technique is to transmit a frequency modulated pattern instead of a pulse and to compare the frequency spectrum of the transmitted and received wave. Both methods require a man-made transmission of known characteristics and a receiver at a considerable distance from the transmitter.

Time coverage of VLF wideband observations is irregular and very limited from 1951 to 1957. Subsequent to 1957, a limited volume of VLF data (spectrograms and digital summaries on hard copy or microfilm) are available from the WDC-A for Upper Atmosphere Geophysics and are indexed in its catalog. More complete data for both wideband and fixed-frequency observations at other times may be available at the "observing station" or at the sponsoring institution (e.g., Stanford University has sponsored Antarctic observations). A list of VLF ground transmitters has been prepared by Watt (1967).

# ATMOSPHERIC RADIO NOISE

Atmospheric radio noise is the term applied to electromagnetic disturbances at radio frequencies, which occur naturally in the atmosphere. Lightning strokes associated with thunderstorms represent the major source of this noise below the ionospheric electron density maximum.

Discussions on atmospheric radio noise can be found in Watt (1967), CCIR Report 322 (1964), and Hartz (1969).

## Ground-Based Observations

During 15-minute intervals each hour, and at each of a series of frequencies between 0.013 and 20.0 MHz, a given station measures the effective omnidirectional antenna noise in decibels above a reference value ($kT_0b$). (See the 54-member station list in the WDC-A data catalog.) Here, k is Boltzmann's constant ($1.38 \times 10^{-16}$ ergs/deg). $T_0$ is a reference temperature (288°K), and b is the bandwidth in Hz. The average over the 15-minute period of observation is recorded as the hourly value. At the end of each month, 24 monthly median values of noise power, one for each hour, are determined. Upper and lower decile values of noise power are also determined for each hour.

Hard-copy tables of monthly values determined by individual stations are available at WDC-A for Upper Atmosphere Geophysics, Boulder, Colorado. Parameters presented include the monthly median values and the ratios of the upper and lower decile values to the median noise power in decibels.

## Satellite-Based Observations

Observations of radio noise between .1 and 20 MHz have been made by the ionospheric satellites Alouette 1, Alouette 2, and ISIS 1. The noise observations consist of the AGC voltages measured by the receiver of the sounding equipment and represent noises originating in the ionosphere and above, which cannot be ordinarily observed at the ground due to the shielding effect of the ionosphere. These data are presently available only through the experimenter.

## REFERENCES


1. Allcock, G., "Ionospheric Absorption at Vertical and Oblique Incidence," Proc. of the Inst. of Elect. Engineers, 101, Pt. 3, 360-370, 1954.

2. Alouette 1 Ionospheric Data N(h), Defence Research Telecommunications Establishment, Vols. 1-5, 1965-1967.

3. Alouette 1 Ionospheric Data Interpolated N(h), Defence Research Telecommunications Establishment, Vols. 1-4, 1965-1967.

4. Beynon, W. J. G., and G. M. Brown, "Brief Summary of Other Techniques for Measuring Ionospheric Drifts," Ann. IGY, 3, 275-279, 1957.

5. Booker, H. G., and E. K. Smith, "A Comprehensive Study of Ionospheric Measurement Techniques," J. Atmospheric Terrest. Phys., 32, 467-497, 1970.

6. Bradley, P. A., D. Eccles, and J. W. King, "Ionospheric Probing Using Pulsed Radio Waves at Oblique Incidence," J. Atmospheric Terrest. Phys., 32, 499-516, 1970.

7. Briggs, B. H., "The Determination of Ionospheric Drift Velocities from Three Receiver Fading Records," Ann. IGY, 3, 235-249, 1957.

8. "CCIR Report 322," International Radio Consultative Committee, 1964.

9. Chan, K. L., L. Colin, and J. O. Thomas, "Electron Densities and Scale Heights in the Topside Ionosphere: Alouette 1 Observations over the American Continents," Vol. 1, NASA SP-3031, 1966; Vol. 2, NASA SP-3032, 1966; Vol. 3, NASA SP-3033, 1966.

10. Chivers, H. J. A., "A Statistical Study of Ionospheric Drifts Measured by the Radio Star Scintillation Technique," J. Atmospheric Terrest. Phys., 21, 221-229, 1961.

11. Colin, L., and K. L. Chan, "Electron Densities and Scale Heights in the Topside Ionosphere: Alouette 1 Observations Recorded at Hawaii," NASA SP-3038, 1967.

12. "Data on Topside Ionosphere: Electron Densities and Scale Heights from Alouette 2 Observations over Japan," 1, Radio Research Laboratories, Tokyo, 1970.

13. Davies, K., "The Uses of Oblique Ionograms in Frequency Utilization," ITU Telecommunication Journal, Oct. 1964.

14. Davies, K., B. Landmark, W. Dieminger, J. S. Belrose, and R. Bolgiano, Radio Wave Propagation, AGARD Lecture Series XXIX, July 1968.

15. Davies, S. K., "Ionospheric Radio Propagation," NBS Monogram #80, U.S. Government Printing Office, Apr. 1965.

16. Dueno, B., "Measurement of Ionospheric Drift by Radio-Star Observations," J. Geophys. Res., 66, 2355-2364, 1961.

17. Evans, I. V., "Theory and Practice of Ionospheric Study by Thomson Scatter Radar," Proc. IEEE, 57, 496-530, Apr. 1969.

18. Fitzenreiter, R. J., and L. J. Blumle, "Analysis of Topside Sounder Records," J. Geophys. Res., 69, 407-415, 1964.

19. Franklin, C. A., R. J. Bibby, and N. S. Hitchcock, "A Data Acquisition and Processing System for Mass Producing Topside Ionograms," Proc. IEEE, 929-944, June 1969.

20. Franklin, C. A., and M. A. Maclean, "The Design of Swept-Frequency Topside Sounders," Proc. IEEE, 897-929, June 1969.

21. Garriott, O. K., A. V. DaRosa, and W. J. Ross, "Electron Content Obtained from Faraday Rotation and Phase Length Variations," J. Atmospheric Terrest. Phys., 32, 705-728, Apr. 1970.

22. Geisweid, K. H., C. G. Little, K. Oberlander, H. Schwentek, and G. Umlauft, "Ionosphere-Absorption Measurements," Ann. IQSY, 1, 74-116, 1968.

23. Geisweid, K. H., K. Oberlander, G. Umlauft, H. Schwentek, and C. G. Little, "Absorption Measurements," IQSY Instruction Manual No. 4, Ionosphere, International Council of Scientific Unions, 1963.

24. Hagg, E. L., E. J. Hewens, and G. L. Nelms, "The Interpretation of Topside Sounder Ionograms," Proc. IEEE, 949-960, June 1969.

25. Hakura, U., Y. Takenoshita, and K. Matsuoka, "Influence of Solar Activity on the Ionosphere Blackout Index," J. Radio Research Laboratories of Japan, 14, No. 73, 1967.

26. Harnischmacher, E., and K. Rawer, "A Simple Description of Ionosphere Drifts in the E Region as Obtained by the Fading Method at Breisach," Winds and Turbulence in the Stratosphere, Mesosphere, and Ionosphere, ed. K. Rawer, 242-276, North-Holland Publishing Co., Amsterdam; J. Wiley, New York, 1968.

27. Hartz, J. R., "Radio Noise Levels Within and Above the Ionosphere," Proc. IEEE, 1042-1050, June 1969.

28. "Height Distributions of Electron Concentration in the Topside Ionosphere as Deduced from Topside Sounder Satellite Ionograms," Vols. 1-3, 1963-1965, Radio Research Station, Slough, Bucks, England.

29. Helliwell, R. A., Whistlers and Related Ionospheric Phenomena, Stanford University Press, Stanford, California, 1965.

30. Hewish, A., "The Diffraction of Galactic Radio Waves as a Method of Investigating the Irregular Structure of the Ionosphere," Royal Society of London Proceedings, A214, 494, 1952.

31. Hines, C. O., I. Paghis, T. R. Hartz, and J. A. Fejer, Physics of the Earth's Upper Atmosphere, Prentice Hall, 1965.

32. Hultqvist, B., "Studies of Ionospheric Absorption of Radio Waves by the Cosmic Noise Method," Radio Astronomy and Satellite Studies of the Atmosphere, ed. J. Aarons, North-Holland Publishing Co., Amsterdam, 1963.

33. Huxley, L. G. H., and J. S. Greenshow, "Investigation of Winds in the Upper Atmosphere By Means of Drifting Meteor Trails," Ann. IGY, 3, 250-274, 1957.

34. Jackson, J. E., "The Analysis of Topside Ionograms," NASA/GSFC X-615-67-452, Sept. 1967.

35. Jackson, J. E., "The Reduction of Topside Ionograms to Electron Density Profiles," Proc. IEEE, 57, 960-975, 1969.

36. Lincoln, J. V., "Reporting of Sudden Ionospheric Disturbances," Ann. IQSY, 1, 1968.

37. Little, C. G., "The Measurement of Ionospheric Absorption, IV, The Measurement of Ionospheric Absorption Using Extraterrestrial Radio Waves," Ann. IGY, 3, 207-217, 1959.

38. Little, C. G., and H. Leinbach, "The Riometer - A Device for Continuous Measurement of Ionospheric Absorption," Proc. IRE, 47, 315-319, 1957.

39. Little, C. G., and A. Maxwell, "Fluctuations in the Intensity of Radio Waves from Galactic Sources," Phil. Mag., 42, 267, 1951.

40. Mass, J., "Survey of Satellite Techniques for Studying Propagation," Radio Astronomical and Satellite Studies of the Atmosphere, ed. J. Aarons, North-Holland Publishing Company, Amsterdam, 256-288, 1963.

41. Maxwell, A., and C. G. Little, "A Radio-Astronomical Investigation of Winds in the Upper Atmosphere," Nature, 169, 746, 1952.

42. Mitra, A. P., "HF and VHF Absorption Techniques in Radio Wave Probing of the Ionosphere," J. Atmospheric Terrest. Phys., 32, 623-646, 1970.

43. Pfister, W., and K. Bibl, "Pulse Sounding with Closely Spaced Receivers as a Tool for Measuring Atmospheric Motions and Fine Structure in the Ionosphere," AFCRL-68-0662, Dec. 1968.

44. Piggott, W., and L. G. Bossy, "Vertical Incidence Soundings," IQSY Instruction Manual No. 4, Ionosphere, International Council of Scientific Unions, 1963.

45. Piggott, W. R., and K. Rawer, eds., URSI Handbook on Ionogram Interpretation and Reduction, Elsevier Publishing Co., Amsterdam, 1961.

46. Piggott, W. R., W. J. G. Beynon, G. M. Brown, and C. G. Little, "The Measurement of Ionospheric Absorption," Ann. IGY, 3, 175-226, 1957.

47. Rawer, K., "Ionosphere: Drift Measurements," Ann. IQSY, 1, 119-125, 1968.

48. Rawer, K., "Synoptic Ionospheric Observations, Including Absorption Drifts and Special Programmes," Ann. IQSY, 5, 97-130, 1969.

49. Rawer, K., ed., "Results of Ionospheric Drift Observations," Ann. IGY, 33, 1965.

50. Rishbeth, H., and O. K. Garriott, Introduction to Ionospheric Physics, Academic Press, New York, 1969.

51. Rosenberg, N. W., "Statistical Analysis of Ionospheric Winds - II," J. Atmospheric Terrest. Phys., 30, 907-917, 1968.

52. Russell, S., and F. C. Zimmer, "Development of the Fixed-Frequency Topside Sounder Satellite," Proc. IEEE, 57, 876-881, 1969.

53. Shapley, A. H., ed., "Atlas of Ionograms," ESSA Research Report UAG-10, May 1970.

54. Spencer, M., "The Shape of Irregularities in the Upper Ionosphere," Proceedings of the Physical Society, B68, 493, 1955.

55. Spizzichino, A., "Measures de Vents par Meteores," Winds and Turbulence in the Stratosphere, Mesosphere, and Ionosphere, ed. K. Rawer, 201-236, North-Holland Publishing Company, Amsterdam; J. Wiley, New York, 1968.

56. Thomas, J. O., B. R. Briggs, L. Colin, M. J. Rycroft, and M. Covert, "Ionosphere Topside Sounder Studies, I: The Reduction of Alouette 1 Ionograms to Electron Density Profiles," NASA TN D-2882, July 1965.

57. Thomas, J. O., M. J. Rycroft, and L. Colin, "Electron Densities and Scale Heights in the Topside Ionosphere: Alouette 1 Observations in Mid Latitudes," NASA SP-3026, 1966.

58. Warwick, C. S., "The Sudden Ionospheric Disturbance," Radio Astronomy and Satellite Studies of the Atmosphere, ed. J. Aarons, North-Holland Publishing Co., Amsterdam, 457-475, 1963.

59. Watt, A. D., VLF Radio Engineering, Pergamon Press, London, 1967.

60. Wright, J. W., "Ionospheric Electron-Density Profiles with Continuous Gradients and Underlying Ionization Corrections. III. Practical Procedures and Some Instructive Examples," Radio Sci., 2, 1159-1168, 1967.

61. Wright, J. W., "The Interpretation of Ionospheric Radio Drift Measurements-I. Some Results of Experimental Comparisons with Neutral Wind Profiles," J. Atmospheric Terrest. Phys., 30, 919-930, 1968.

62. Wright, J. W., and D. McKinniss, "Format of Ionospheric Electron Density Profile Tabulations," ITSA/ESSA, undated.

63. Wright, J. W., and R. W. Knecht, "Atlas of Ionograms," NBS Report 5097, June 1957.

64. Wright, J. W., R. W. Knecht, and K. Davies, "Ionospheric Vertical Soundings," Ann. IGY, 3, 1957.

65. Yuen, P. C., and T. H. Roelofs, "Atlas of Total Electron Content Plots," 1-4, Radio Science Laboratory, University of Hawaii, updated, 1970.

# PART VI

# NEUTRAL ATMOSPHERE

Prepared By

Russell A. Hankins

CONTENTS

## INTRODUCTION

This section presents a discussion of the instrumentation and techniques used for measuring upper level temperature, winds, pressure, and ozone concentrations and identifies the availability and sources of data obtained from these measurements. The availability of satellite cloud photographs is also discussed. The last section of Part VI describes some of the available global atmospheric models and the assumptions upon which they are based. Specific models and their sources are given for both the lower atmosphere and the upper atmosphere.

## UPPER LEVEL MEASUREMENTS OF TEMPERATURE, WINDS, AND PRESSURE

Observations of temperature, winds, and pressure are routinely taken in the first 250,000 feet of the atmosphere.

Temperature is a measure of the molecular kinetic energy of the air. Near the surface of the earth, it is measured by a thermometer; upper air temperatures are measured by balloon-borne instruments (radiosondes) and rocket-borne instruments (rocketsondes). The temperature measuring instrument on a radiosonde is a thermistor, which is a device having an electrical resistance that varies markedly with temperature. Rocketsonde temperature instrumentation consists of a modified 1680-MHz radiosonde transmitter unit and a bead thermistor sensor.

Wind is air in motion relative to the surface of the earth. Since the vertical component of wind is usually relatively small, the term refers to the horizontal component unless specified otherwise. Surface wind speed or force is measured by anemometers, and the direction by wind vanes. Upper level winds are measured by tracking pilot balloons, balloon-borne rawin or rawinsondes,* and rocketsondes. These upper level wind measuring devices are tracked visually with radio direction finders, or by radar.

*Rawin -- A method of determining upper level wind speeds and directions by tracking a balloon-borne radar target, responder, or radiosonde transmitter with either radar or a radio direction finder.
Rawinsonde -- A method of determining upper level temperature, pressure, relative humidity, and wind speed and direction by tracking a radiosonde with a radar or radio direction finder.

Atmospheric pressure is the pressure exerted by the atmosphere as a consequence of gravitational attraction exerted upon the column of air lying directly above the point in question. It is measured by many varieties of barometers and is expressed in several unit systems. The most common unit used is the millibar (1 millibar equals 1000 dynes per $cm^2$).

Balloon-borne instruments are capable of making observations only in the lower 100,000 feet (30 km) of the atmosphere. Meteorological rockets routinely take observations in the lower 250,000 feet (76 km), especially in that portion inaccessible to balloons. See reference 16 for a complete description of meteorological rocket instrumentation.

## Meteorological Rocket Network Data

The Meteorological Rocket Network (MRN) was formed in October 1959 to combine the efforts of a number of organizations engaged in upper atmospheric studies. The data are presented in the series: "Data Report of the Meteorological Rocket Network Firings," Document 109-62, of the Inter-Range Instrumentation Group (IRIG) of the Range Commands Council and later the Meteorological Working Group (MWG) of the IRIG. The Meteorological Rocket Network data reports were first published in the fall of 1959. These data reports began on a quarterly basis but were changed to a monthly publication with the September 1962 data. Each report contains the wind and temperature measurements from all available network firings for that particular month, along with computed values for pressure, density, and speed of sound. It also includes the rawinsonde observations nearest the time (within 6 hours) of rocket firing. All stations attempt to launch rockets concurrently and at regular intervals. In 1959, data from only five stations were included in the data reports, but by 1966, data from a greater number of stations were included (see table 11). These data are available from October 1959 through February 1966. Copies of any of the 54 volumes of the "Data Report of the Meteorological Rocket Network Firings" can be obtained by writing to the Defense Documentation Center, Cameron Station, Alexandria, Virginia 22314.

Since 1966, the "Data Report of Meteorological Rocket Network Firings" has been issued monthly by the World Data Center A (WDC-A) for Meteorology at the National Climatic Center (formerly National Weather Records Center), Asheville, North Carolina 28801. These reports are basically the same as the previously issued IRIG data reports, but they also include data from other countries. The first issue of the WDC-A data report began with January 1964 data. Thus the 1964 to 1966 issues of the Meteorological Rocket Network data reports are essentially a reprint of the data

TABLE 11

METEOROLOGICAL ROCKET NETWORK STATIONS

| Station | Lat | Long. | Start Date | Stop Date |
|---|---|---|---|---|
| Antigua AAFB, BWI | 17°09'N | 61°47'W | May 1963 | |
| Ascension Island AFB | 07°59'S | 14°25'W | Aug. 1962 | |
| Barking Sands (Kauai), Hawaii | 22°03'N | 159°47'W | Oct. 1960 | |
| Cape Kennedy, Florida | 28°27'N | 80°32'W | Mar. 1960 | |
| Eglin AFB, Florida | 30°23'N | 86°42'W | Sept. 1960 | |
| Eniwetok, Marshall Islands | 11°26'N | 162°20'E | Mar. 1961 | June 1969 |
| Fort Churchill, Canada | 58°44'N | 93°49'W | Oct. 1959 | |
| Fort Greely, Alaska | 64°00'N | 145°44'W | Dec. 1959 | |
| Fort Sherman, Canal Zone | 09°20'N | 79°59'W | Jan. 1964 | |
| Grand Turk Island AAFB, BWI | 21°27'N | 71°09'W | Sept. 1963 | Dec. 1966 |
| Green River, Utah | 38°56'N | 110°04'W | Jan. 1964 | |
| Harp, Seawell, West Indies | 13°06'N | 59°37'W | Jan. 1964 | |
| Holloman AFB, New Mexico | 32°51'N | 106°06'W | Nov. 1959 | June 1961 |
| Kindley AFB, Bermuda | 32°21'N | 64°39'W | Dec. 1961 | |
| Kwajalein, Marshall Islands | 08°44'N | 167°44'E | Oct. 1963 | |
| McMurdo Sound, Antarctica | 77°51'N | 166°39'E | Mar. 1962 | Oct. 1963 |
| Point Barrow, Alaska | 71°21'N | 156°59'W | July 1961 | Aug. 1961 |
| Point Mugu, California | 34°07'N | 119°07'W | Oct. 1959 | |
| Primrose Lake, Alberta, Canada | 54°45'N | 110°03'W | Jan. 1964 | |
| San Salvador Island AFB | 24°04'N | 74°31'W | Sept. 1963 | Dec. 1964 |
| Thule AFB, Greenland | 76°33'N | 68°49'W | Jan. 1964 | |
| Tonopah Range, Nevada | 38°00'N | 116°30'W | Mar. 1960 | |
| Wallops Island, Virginia | 37°50'N | 75°29'W | Nov. 1959 | |
| West Geirinish, Scotland | 57°21'N | 07°22'W | | |
| White Sands Missile Range, New Mexico | 32°23'N | 106°29'W | Oct. 1959 | |
| Yuma Proving Ground, Arizona | 32°52'N | 114°19'W | Jan. 1964 | |

report of the IRIG Document 109-62, with a few more rocket stations reporting. Meteorological rocket data from January 1964 to the present time are available at the WDC-A for Meteorology. These data are on magnetic tape and hard copy. Subscriptions to the WDC-A "Data Report of the Meteorological Rocket Network Firings" should be requested from the Superintendent of Documents, Government Printing Office, Washington, D.C. 20402.

Beginning with 1969 data, the data publication entitled "Meteorological Rocketsonde Network" has been changed to "High Altitude Meteorological Data."

## EXAMETNET Data

Upper level wind data from rocketsondes are also available for the period 1966 to 1968 from the Experimental InterAmerican Meteorological Rocket Network (EXAMETNET). This is a cooperative program among the national space organizations of Argentina, Brazil, and the U.S. The EXAMETNET meteorological rocket launchings and data dissemination are conducted synoptically from launch sites at Chamical, Argentina (Lat 30°22' S, Long. 66°17' W), Natal, Brazil (Lat 05°55' S, Long. 35°10' W), and Wallops Island, Virginia (Lat 37°51' N, Long. 75°29' W). These data are available in the EXAMETNET Data Report Series, Annual Report for 1966 (NASA SP-175), 1967 (NASA SP-176), and 1968 (NASA SP-231), respectively. The reports can be obtained from the National Technical Information Service, Springfield, Virginia 22151. The 1969 EXAMETNET data are to be included in the new World Data Center A "High Altitude Meteorological Data" publication.

## NOAA Stratosphere Data

A series of weekly constant-pressure charts for the upper stratosphere, based on rocketsonde and very high level rawinsonde data obtained over North America and adjacent ocean areas, is prepared. These high level data consist of a series of charts for 5, 2, and 0.4 mb (corresponding to approximately 36, 42, and 55 km, respectively). Wind, temperature, and pressure values are included. These charts are available for the years 1964 through 1967 as Environmental Science Services Administration (ESSA) Technical Reports WB-2, 3, 9, and 12 (see references 19, 20, 21, and 22). Copies of these documents can be obtained by writing to the Superintendent of Documents, U.S. Government Printing Office.

## Upper Air Network Data

Wind, temperature, relative humidity, and pressure data measured by rawinsondes (or rocketsondes from which wind data are not available) are obtained from the Upper Air Network Stations, which are reasonably well distributed over the land masses of the Eastern and Western Hemispheres. The soundings are usually taken twice each day at 0000 GMT and 1200 GMT. These data are available at National Climatic Center, Asheville. Data listed daily by station are available on microfiche. The data are tabulated by average monthly values year by year. Synoptic charts of plotted data are available for sea level and the 850-, 700-, 500-, 300-, 200-, 100-, 50-, and 30-mb levels.

Wind data are also obtained from pibals (pilot balloons). A pibal is a small balloon whose ascent is followed by a theodolite in order to obtain data for the computation of the speed and direction of winds in the upper air. The pibals are released as many as four times each day but usually at 0600 GMT and 1800 GMT, which are off-times for the soundings. Most of the Upper Air Network Stations release pibals as do many of the principal surface weather observing stations. These data are also available at the National Climatic Center.

# SATELLITE CLOUD PHOTOGRAPHS

All usable cloud photographs taken by meteorological satellites are available from the National Climatic Center, Asheville.

A complete listing of the TIROS and ESSA cloud photographs are contained in the Key to Meteorological Records Documentation (KMRD) series, which is made up of catalogs of meteorological satellite television cloud photography. This series has been established to provide guidance to personnel making use of the cloud photographs. It also describes how copies of these photographs may be obtained from the National Climatic Center. The catalogs are published by the National Oceanic and Atmospheric Administration and are available from the Superintendent of Documents, U.S. Government Printing Office. The first of these catalogs is the "Catalog of Meteorological Satellite Data - Tiros 1 Television Cloud Photography," KMRD Series No. 5.31. (See table 12.)

TABLE 12

CATALOGS OF METEOROLOGICAL SATELLITE DATA

TELEVISION CLOUD PHOTOGRAPHY

| | | | | |
|---|---|---|---|---|
| 5.31 | TIROS 1 | 1961 | Apr. 1, 1960 - | June 15, 1960 |
| 5.32 | TIROS 2 | 1963 | Nov. 23, 1960 - | Sept. 27, 1961 |
| 5.33 | TIROS 3 | 1962 | July 12, 1961 - | Jan. 23, 1962 |
| 5.34 | TIROS 4 | 1963 | Feb. 8, 1962 - | June 18, 1962 |
| 5.35 | TIROS 5 | 1964 | June 19, 1962 - | May 14, 1963 |
| 5.36 | TIROS 6 | 1964 | Sept. 18, 1962 - | Oct. 21, 1963 |
| 5.37 | TIROS 7 | 1965 | June 19, 1963 - | Dec. 31, 1963 |
| 5.37 | TIROS 7 | 1965 | Jan. 1, 1964 - | June 30, 1964 |
| 5.37 | TIROS 7 | 1965 | July 1, 1964 - | Dec. 30, 1964 |
| 5.37 | TIROS 7 | 1966 | Jan. 1, 1965 - | Dec. 31, 1965 |
| 5.38 | TIROS 8 | 1965 | Dec. 21, 1963 - | June 30, 1964 |
| 5.38 | TIROS 8 | 1965 | July 1, 1964 - | Dec. 31, 1964 |
| 5.38 | TIROS 8 | 1966 | Jan. 1, 1965 - | Aug. 31, 1965 |
| 5.39 | TIROS 9 | 1966 | Jan. 22, 1965 - | Apr. 30, 1965 |
| 5.39 | TIROS 9 | 1967 | May 1, 1965 - | July 26, 1965 |
| 5.310 | TIROS 10 | 1967 | July 2, 1965 - | Sept. 30, 1965 |
| 5.311 | ESSA 1 | 1966 | Feb. 3, 1966 - | Mar. 31, 1966 |
| 5.311 | ESSA 1 | 1968 | Apr. 1, 1966 - | Oct. 6, 1966 |
| 5.313 | ESSA 3 | 1968 | Oct. 4, 1966 - | Jan. 1, 1967 |
| 5.313 | ESSA 3 | 1967 | Jan. 1, 1967 - | Mar. 31, 1967 |
| 5.314 | ESSA 3 & 5 | 1968 | Apr. 1, 1967 - | June 30, 1967 |
| 5.315 | ESSA 3 & 5 | 1968 | July 1, 1967 - | Sept. 30, 1967 |
| 5.316 | ESSA 3 & 5 | 1969 | Oct. 1, 1967 - | Dec. 31, 1967 |
| 5.317 | ESSA 3 & 5 | 1969 | Jan. 1, 1968 - | Mar. 31, 1968 |
| 5.318 | ESSA 3 & 5 | 1970 | Apr. 1, 1968 - | June 30, 1968 |
| 5.319 | ESSA 3, 5, & 7 | 1970 | July 1, 1968 - | Sept. 30, 1968 |

The Nimbus television cloud photographs are listed and described in the following NASA/GSFC documents:

"Nimbus I Users' Catalog: AVCS and APT, August 28 through September 22, 1964"

"The Nimbus II Data Catalog, Vol. 1, 15 May through 30 June, 1966"

"The Nimbus II Data Catalog, Vol. 2, 1 July through 31 July, 1966"

"The Nimbus II Data Catalog, Vol. 3, 1 August through 31 August, 1966 (Orbits 1035 - 1447)"

"The Nimbus II Data Catalog, Vol. 4, 1 September through 30 September, 1966 (Orbits 1448 - 1846)"

"The Nimbus II Data Catalog, Vol. 5, 1 October through 15 November, 1966 (Orbits 1847 - 2458)"

"The Nimbus III Data Catalog, Vol. 1, Part 1, 14 April through 31 May, 1969 (Orbits 109 - 639)"

"The Nimbus III Data Catalog, Vol. 2, June 1969 (Orbits 640 - 1041)"

"The Nimbus III Data Catalog, Vol. 3, July 1969 (Orbits 1042 - 1457)"

"The Nimbus III Data Catalog, Vol. 4, August 1969 (Orbits 1458 - 1872)"

"The Nimbus III Data Catalog, Vol. 5, 1 September to 31 December, 1969 (Orbits 1873 - 3508)"

Copies of these catalogs can be obtained from NSSDC. Additional Nimbus III and Nimbus IV data catalogs are currently being compiled and, when printed, will also be available from NSSDC.

Cloud photographs are also available from the Applications Technology Satellites (ATS) spin scan camera system. These data are listed and described in the following volumes of the "Meteorological Data Catalog for the Applications Technology Satellites":

Vol. I - "Users' Guide, ATS I, January 1 through June 30, 1967"

Vol. II - "ATS I Data Catalog, ATS II Summary, and ATS III Users' Guide and Data Catalog, November 7, 1967 through January 31, 1968"

Vol. III - "ATS I Data Catalog and ATS III Data Catalog, February 1 through December 31, 1968"

Vol. IV - "ATS I Data Catalog and ATS III Data Catalog, January 1 through July 31, 1969"

Vol. V - "ATS I Data Catalog, August 1, 1969 through May 25, 1970"

Copies of these catalogs can be obtained from the Nimbus-ATS Data Utilization Center, Code 450, GSFC, Greenbelt, Maryland 20771.

When the desired cloud photographs have been identified from these catalogs, they may be obtained from the National Climatic Center, Asheville, North Carolina 28801.

## OZONE DATA

Ozone, $O_3$, a nearly colorless gaseous form of oxygen, is found in trace quantities in the earth's atmosphere with a maximum concentration occurring between 20 and 30 km above the surface. Ozone's absorption of solar ultraviolet light makes possible the presence of life as we know it on earth. Extensive discussions of ozone and ozone measurement techniques can be found in Vasay (1965).

Parameters measured include total ozone content and vertical distribution versus location and time. Total ozone content is the thickness, reduced to standard pressure and temperature conditions, of the ozone contained in a vertical cylindrical column of unit cross section above a specific location. It has been recently expressed in units of millicentimeters. Ozone concentration for a given pressure level can be expressed as the ozone partial pressure and is in units of micromillibars.

Most ozone observations are taken by balloon-borne ozonesondes. The data are commonly presented in a plotted form called ozonagrams on which ozone content is given versus altitude (figure 24). Isopleths of ozone mixing ratios (micrograms of ozone per gram of air) can also be drawn on the diagram.

Ozonagrams can be obtained from a number of sources. Data from a network of six stations using chemiluminescent-type ozonesondes taken from January 1963 to January 1966 have been published in "Ozonesonde

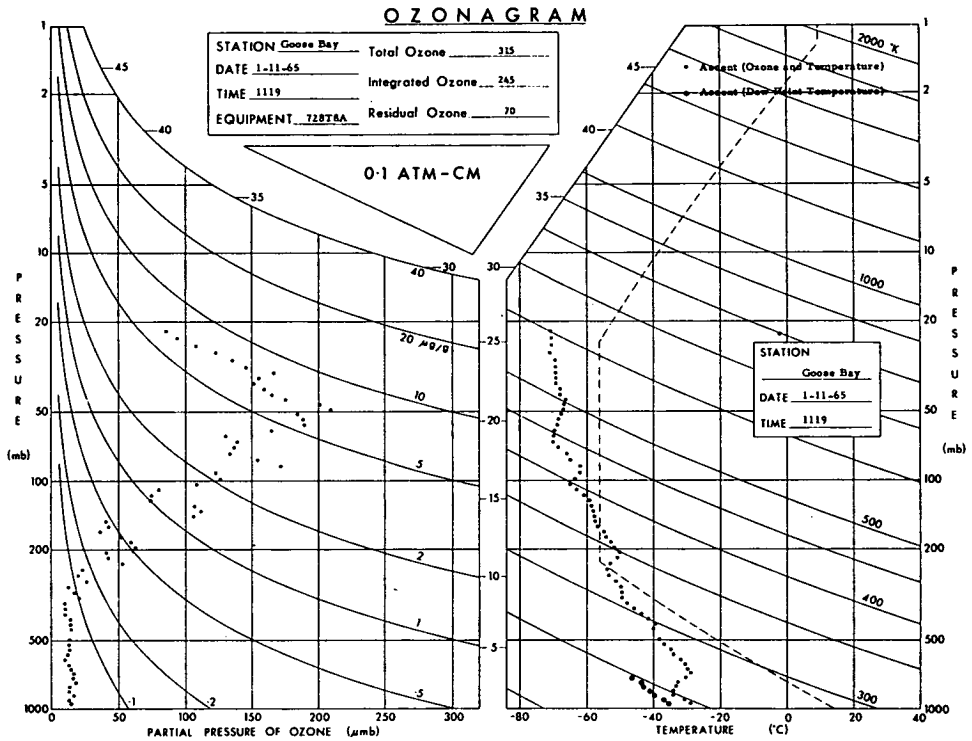


Figure 24. Sample Ozonagram

TABLE 13

OZONE NETWORK

| Station | Lat (°N) | Long. (°W) |
|---|---|---|
| Albrook Field, Canal Zone | 9.0 | 79.6 |
| Cape Kennedy, Florida | 28.2 | 80.6 |
| Goose Bay, Labrador (Canadian Meteorological Branch) | 53.3 | 60.4 |
| Grand Turk AAFB, BWI | 21.5 | 71.1 |
| L. G. Hanscom Field, Bedford, Massachusetts | 42.5 | 71.3 |
| Wallops Island, Virginia | 37.9 | 75.5 |

Observations over North America," AFCRL 64-30, Volumes I to IV. (See Hering, 1964, and Hering and Borden, 1964, 1965, and 1967.) The participating stations are listed in table 13. At the beginning of each volume, a listing is given of the days that ozonesondes were flown at the various stations.

Ozonagrams from 1962 to 1966 are available for a number of stations operated or supported by NOAA in Boulder, Colorado, in the Western Hemisphere and in Antarctica. (See Komhyr and Sticksel, 1967, and Dutsch, 1966.) During this period a major effort was made to gather ozone data during the time of the International Years of the Quiet Sun, 1964 to 1965. These Western Hemisphere ozonagrams are published in Komhyr and Sticksel (1967). Antarctic data appear in Komhyr and Grass (1968). The stations are listed in table 14. Three different types of ozonesondes were used during this period: Regener chemiluminescent, Brewer-Möst electrochemical, and carbon-iodine instruments. Ozonagrams after 1966 are not available from NOAA at this time.

The data from the Regener chemiluminescent soundings for the IQSY were extracted at 1-minute intervals and reduced by computer. These data include ozone partial pressure at specified levels and total ozone content, and can be obtained from the National Climatic Center, Asheville.

TABLE 14

NOAA OZONESONDE NETWORK

| Station | Lat. (°N) | Long. (°W) |
|---|---|---|
| Albrook Field, Canal Zone (AWS) | 9.0 | 79.6 |
| Colorado State University, Fort Collins | 40.6 | 105.1 |
| Fairbanks, Alaska (USWB) | 64.3 | 147.9 |
| Florida State University, Tallahassee | 30.4 | 84.3 |
| Fort Churchill, Manitoba (Canad. Met. Br.) | 58.8 | 94.1 |
| Goose Bay, Labrador (Canad. Met. Br.) | 53.3 | 60.4 |
| Grand Turk AFB, BWI | 21.5 | 71.1 |
| Green Bay, Wisconsin (USWB) | 44.5 | 88.1 |
| L. G. Hanscom Field, Bedford, Massachusetts | 42.5 | 71.3 |
| Point Mugu, California | 34.1 | 119.1 |
| Thule AFB, Greenland (AWS) | 76.5 | 68.8 |
| University of New Mexico, Albuquerque | 35.0 | 106.6 |
| University of Washington, Seattle | 47.4 | 122.3 |
| University of Wisconsin | 43.1 | 89.4 |

Two years of ozonagrams taken over Boulder, Colorado, are available in Dutsch (1966). Data coverage is from August 1963 to August 1965. Ozone measurements are presented in several forms other than ozonagrams: tables of ozone concentration at standard levels for single flights in monthly compilation, tables of monthly mean values of ozone concentration at standard levels for each year, and monthly mean values of ozone concentration at standard levels compiled from the 2-year period. These measurements are taken over Boulder, and all are available in Dutsch (1966).

Other statistical summaries of ozone data are available. The 3-year 1963 to 1966 average vertical ozone distribution for each season for each station listed in table 15 is given in Hering and Borden (1967). Average values of ozone density, partial pressure, and mixing ratio are

tabulated for 2-km intervals. The number of observations and average temperature and pressure values are shown for each season and altitude. Supplementary ozone data (coded values of total amount of ozone, temperature, and winds applicable to standard and significant pressure levels for all soundings) appear in Ozone Data for the World, published bimonthly by the Meteorological Branch, Canadian Department of Transport, Toronto, Ontario. These data are available from 1965 through 1968 from the National Climatic Center, Asheville. Similar Japanese ozone data are found in Aerological Data of Japan, published monthly by the Japan Meteorological Agency, Tokyo. Data are from 1947, 1948, portions of 1949, and from 1950 to June 1969. These are also available from the National Climatic Center in Asheville.

TABLE 15

LOCATION OF STATIONS
PRESENTING SEASONAL AVERAGES

| Station | Lat (°) | Long. (°) | WMO* Region |
|---|---|---|---|
| Amundsen-Scott, Antarctica | 90.0 S | 24.8 S | |
| Byrd, Antarctica | 80.0 S | 119.5 W | |
| Canton Island, South Pacific | 2.8 S | 171.7 W | V |
| USNS Eltanin, South Pacific and South Atlantic Oceans | Variable | Variable | III and IV |
| Fairbanks, Alaska | 64.8 N | 147.9 W | IV |
| Hallett, Antarctica | 72.3 S | 170.2 E | |
| Hilo, Hawaii | 19.7 N | 155.1 W | V |
| La Paz, Bolivia | 16.5 S | 68.2 W | III |
| Puerto Montt, Chile | 41.5 S | 73.0 W | III |
| Sterling, Virginia | 39.0 S | 77.5 W | IV |
| Wilkes, Antarctica | 66.3 S | 110.6 E | |

*WMO: World Meteorological Organization

# MODELS OF THE EARTH'S NEUTRAL ATMOSPHERE

Two distinct regimes can be identified in the neutral atmosphere. The lower atmosphere, or the homosphere, is that region characterized by mixing of the components; chemical composition is nearly constant. The heterosphere overlaps the upper portion of the homosphere and is characterized by diffusive equilibrium in which chemical composition depends on height. The transition altitude is between 90 and 120 km. Above about 90 km, dissociation of molecular oxygen due to extreme ultraviolet (EUV) radiation is significant.

Construction of model atmospheres is complicated by the temporal variability of the atmosphere. The homosphere exhibits diurnal and seasonal variations. The characteristics of the upper atmosphere (the heterosphere) change with the solar cycle, daily solar activity, geomagnetic activity, local time, and geographic latitude. Seasonal and semiannual variations are also exhibited.

It has proven convenient in the past to generate separate atmospheric models for the regions below and above the homosphere-heterosphere transition layer. They are likewise considered separately here.

## The Lower Atmosphere

One of the earlier models for the lower atmosphere was the "U.S. Standard Atmosphere, 1962," adopted by the United States Committee on Extension to the Standard Atmosphere (COESA). This model contains the International Civil Aviation Organization (ICAO) standard atmosphere up to 20 km, the proposed extension up to 32 km, and tables and data up to 700 km. The tables depict an idealized, moisture-free, middle-latitude atmosphere. Seasonal and solar activity variations are neglected.

"U.S. Standard Atmosphere Supplements, 1966" was prepared by COESA depicting variations of the models listed above. The document provides tabulations of atmospheric parameters from the surface up to 1000 km, based upon latitude and seasonal variations for the lower atmosphere. Both publications were sponsored jointly by the Environmental Science Services Administration (now called National Oceanic and Atmospheric Administration), the National Aeronautics and Space Administration, and the U. S. Air Force. They can be obtained from the Superintendent of Documents, U.S. Government Printing Office. The Handbook of Geophysics and Space Environments (Valley, 1965) discusses these publications and contains tables reprinted from them.

Another early model was represented in the COSPAR International Reference Atmosphere 1961 (CIRA 1961) (see Kallmann-Bijl et al., 1961). The tables appearing in CIRA 1961 depict average conditions represented by single profiles of temperature, pressure, and density for the 20- to 100-km region. These tables were revised in CIRA 1965 to account for latitude and seasonal variations.

One of the latest models of the lower atmosphere appears in a publication by Groves (1970), which was prepared as part of a COSPAR panel project. The publication contains tables that present atmospheric temperature, pressure, and density from 25 to 110 km and their seasonal and latitudinal variations. Some of the problems of atmospheric models are discussed, and many comparisons of the model with actual data are presented.

## The Upper Atmosphere

Two excellent review papers, those of Moe (1969) and of Blum et al. (1970), discuss the physics of the upper atmosphere. They also review the various atmospheric models that have been developed in the past and discuss the limitations or shortcomings of each. An extensive bibliography is included with each paper.

Some of the most significant early references are Nicolet (1961), "U.S. Standard Atmosphere, 1962," Harris and Priester (1962a), Jacchia (1965), CIRA 1965, and the "U.S. Standard Atmosphere Supplement, 1966," which incorporated the Jacchia (1965) model atmosphere.

Weidner et al. (1969) present a brief review paper that discusses the models of Harris and Priester (1962b) and of Jacchia (1965) and some of the limitations of each. Weidner also presents a static diffusion model that is a computerized version of Jacchia's model developed at the NASA Marshall Space Flight Center. The model varies with solar condition and location and can be predicted for particular times and locations. The model provides atmospheric density, chemical composition, temperature, molecular mass, and density scale height between 120 and 1000 km.

Jacchia (1970) has submitted to COSPAR (Leningrad, May 1970) a provisional model atmosphere for altitude range 90 to 2500 km. This model, with modifications in some numerical values and for altitudes above 110 km, will appear as the (CIRA 1971) model. In constructing this model, Jacchia assumes constant temperature and density values

at 90 km. He also chooses a temperature profile $T = T(h; T_\infty)$, which yields results compatible with the density data of satellite drag analysis. In the equation, h is height and $T_\infty$ is the temperature of the isothermal exosphere.*

To obtain total mass density values, Jacchia integrates the equation of hydrostatic equilibrium up to 105 km, the assumed upper limit of the mixing regime. The mean molecular mass variation, which is non-zero due to oxygen dissociation, is described by a sixth degree polynomial. To obtain densities as functions of height in the region of assumed diffusive equilibrium above 105 km, Jacchia integrates the diffusion equation, which is the equation of hydrostatic equilibrium for each species, with an additional thermal diffusion term used for helium. Special treatment is given to the hydrogen component.

The resultant tables of atmospheric parameters are presented for exospheric temperatures ($T_\infty$) between 600°K and 2000°K, at 100°K intervals. Temperature, mass density, mean molecular weight, pressure scale height, and number densities of molecular nitrogen and oxygen and of atomic hydrogen (above 500 km), helium, argon, and oxygen are given at 95 discrete altitudes between 90 km and 2500 km. Separate tables present total mass densities only as functions of altitude for exospheric temperatures between 600°K and 2000°K, in 50°K steps. Since good observational data do not exist for altitudes above 1100 km, tabular data above this height must be considered as unconfirmed extrapolation.

Jacchia (1970) includes equations and tables that permit the user of the model to choose the appropriate value of the exospheric temperature for given values of the solar activity level (as characterized by the 10.7-cm flux level), the geographic latitude and local time, the geomagnetic activity level (characterized by Kp or Ap), and the phase of the year. Seasonal and latitudinal variations of the mass density in the lower thermosphere and of helium are treated separately.

*The alternative to choosing a temperature profile empirically is to assume the presence of heat input and transport mechanisms and to solve an energy conservation equation. This approach has been followed by others. See, for example, Harris and Priester (1962a).

## REFERENCES


1. Blum, P., I. Harris, and W. Priester, "On the Physics of the Neutral Upper Atmosphere," progress report prepared for CIRA 1970, NASA Goddard Institute for Space Studies, March 16, 1970 (to appear in CIRA 1971).

2. CIRA 1965, North-Holland Publishing Company, Amsterdam, 1965.

3. Dutsch, H. U., "Two Years of Regular Ozone Soundings Over Boulder, Colorado," NCAR-TN-10, National Center of Atmospheric Research, Boulder, Colorado, 1966.

4. Groves, G. V., "Seasonal and Latitudinal Models of Atmospheric Temperature, Pressure, and Density, 25 to 110 km," Air Force Surveys in Geophysics, No. 218, AFCRL-70-0261, May 1970.

5. Harris, I., and W. Priester, "Time-Dependent Structure of the Upper Atmosphere," NASA Tech. Note D-1443, July 1962a. (Also in Journal of Atmospheric Science, 19, 286-301, 1962.)

6. Harris, I., and W. Priester, "Theoretical Models for the Solar-Cycle Variation of the Upper Atmosphere," NASA Tech. Note D-1444, Aug. 1962b.

7. Hering, W. S., "Ozonesonde Observations over North America," 1, AFCRL Research Report, Air Force Cambridge Research Laboratories, 1964.

8. Hering, W. S., and T. R. Borden, Jr., "Ozonesonde Observations over North America," 2, Environmental Research Papers, No. 38, Air Force Cambridge Research Laboratories, 1964.

9. Hering, W. S., and T. R. Borden, Jr., "Ozonesonde Observations over North America," 3, Environmental Research Papers, No. 133, Air Force Cambridge Research Laboratories, 1965.

10. Hering, W. S., and T. R. Borden, Jr., "Ozonesonde Observations over North America," 4, Environmental Research Papers, No. 279, Air Force Cambridge Research Laboratories, 1967.

11. Jacchia, L. G., "Static Diffusion Models of the Upper Atmosphere with Empirical Temperature Profiles," Smithsonian Astrophysical Observatory Special Report No. 170, 1964. (Also in Smithsonian Contributions to Astrophys., 8, 1965.)

12. Jacchia, L. G., "New Static Models of the Thermosphere and Exosphere with Empirical Temperature Profiles," Smithsonian Astrophysical Observatory Special Report No. 313, May 1970.

13. Kallmann-Bijl, H., R. L. F. Boyd, H. Lagow, S. M. Poloskov, and W. Priester, CIRA 1961, North-Holland Publishing Company, Amsterdam, 1961.

14. Komhyr, W. D., and R. D. Grass, eds., "Ozonesonde Observations 1962-1966," (Vol. 2) ESSA Technical Report, Environmental Research Laboratories, ERL 80-APCL 3, Aug. 1968.

15. Komhyr, W. D., and P. R. Sticksel, eds., "Ozonesonde Observations 1962-1966," (Vol. I) ESSA Technical Report, Institutes for Environmental Research IER 51-IAS I, 1967.

16. Meteorological Working Group of the Range Commands Council, "The Meteorological Rocket Network," Meteorological Rocket Network Committee, IRIG Document No. 111-64, Feb. 1965.

17. Moe, K., "A Review of Atmospheric Models in the Altitude Range 100 to 1000 km," AIAA Paper No. 69-50, American Institute of Aeronautics and Astronautics, 7th Aerospace Science Meeting, New York City, Jan. 20-22, 1969.

18. Nicolet, M., "Density of the Heterosphere Related to Temperature," Smithsonian Astrophysical Observatory Special Report No. 75, 1961.

19. Upper Air Branch, National Meteorological Center, "Weekly Synoptic Analyses, 5-, 2-, and 0.4-mb Surfaces for 1964," ESSA Technical Report WB-2, Apr. 1967.

20. Upper Air Branch, National Meteorological Center, "Weekly Synoptic Analyses, 5-, 2-, and 0.4-mb Surfaces for 1965," ESSA Technical Report WB-3, Aug. 1967.

21. Upper Air Branch, National Meteorological Center, "Weekly Synoptic Analyses, 5-, 2-, and 0.4-mb Surfaces for 1966," ESSA Technical Report WB-9, Jan. 1969.

22. Upper Air Branch, National Meteorological Center, "Weekly Synoptic Analyses, 5-, 2-, and 0.4-mb Surfaces for 1967," ESSA Technical Report WB-12, Jan. 1970.

23. "U.S. Standard Atmosphere, 1962," U.S. Government Printing Office, Washington, D.C.

24. "U.S. Standard Atmosphere Supplements, 1966," U.S. Government Printing Office, Washington, D.C.

25. Valley, S. L., ed., Handbook of Geophysics and Space Environments, Air Force Cambridge Research Laboratories, Office of Aerospace Research, U.S. Air Force, 1965.

26. Vasay, Arlette, "Atmospheric Ozone," Advances in Geophysics, Vol. II, eds. H. E. Landsberg and J. Van Mieghem, Academic Press, New York, 115-173, 1965.

27. Weidner, D. K., C. L. Hasseltine, and R. E. Smith, "Models of Earth's Atmosphere (120-1000 km)," NASA SP-8021, May 1969.

# PART VII

# MISCELLANEOUS DATA

Prepared By

Joseph H. King, Francis J. Hagan,
and Charles D. Wende

CONTENTS

# MODELS OF MAGNETOSPHERICALLY TRAPPED PARTICLES

Due to the large-scale geometry of the geomagnetic field, energetic charged particles may be constrained for long periods of time with a combined motion consisting of gyration about field lines, latitudinal bounce along field lines, and azimuthal drift around the earth. The trapped particle populations, often referred to as the Van Allen belts, have been studied using data from numerous spacecraft since 1958. Recent discussions of these particles include those by Hess (1968) and by Williams (1970).

Trapped particle data gathered by various spacecraft have been analyzed, synthesized and presented in a format useful to space systems analysts and space scientists. The resultant model environments are distinguished from each other by particle species, spatial and temporal coverage, and energy range.

Within a given model, the integral omnidirectional flux, $J(>E, B, L)$, is given as a product of the flux, $F(B, L)$, above a certain energy, $E_1$, times a spectral function, $N(>E, E_1; B, L)$. For proton models, the spectral function is represented over a limited energy interval by an exponential function, $N = N_0 \exp[(E-E_1)/E_0(B, L)]$, or by a power law, $N = N_0(E/E_1)^{-P(B, L)}$. Thus, a proton model includes specification of the functions $F(B, L)$ and $E_0(B, L)$ or $P(B, L)$. On the other hand, for electron models, the spectral function N is given as a tabular function of E and L, with no B dependence. For each environment, the daily accumulated fluxes above certain energy levels and within certain energy intervals are also given for an assumed spacecraft in various orbits.

The exception to this discussion is the synchronous-altitude electron environment, AE3, in which the mean differential and integral fluxes (for solar minimum) are explicitly presented for given values of $B/B_0$, local time, and energy. Probability distributions for deviations from mean values are also given.

The following model electron environments are currently available:

| Env. Name | $E_1$ (Mev) | Energy (Mev) Range | Spatial Range | Temporal Range | EPOCH |
|---|---|---|---|---|---|
| AE1 | 0.5 | >0.3 | 1.2<L<3.0 | 1962-1963 | 7/63 |
| AE2 | 0.5 | 0-∞ | 1.2<L<6.2 | 1962-1964 | 8/64 |
| E68 | 0.5 | 0-∞ | 1.2<L<6.2 | 1962-1964 | 1968 |
| AE3 | --- | 0.01-5 | L=6.6 | 1959-1965 | 1964 |

The following model proton environments are currently available:

| Env. Name | $E_1$ (Mev) | Energy Range (Mev) | Spatial Range | Temporal Range | Remarks |
|---|---|---|---|---|---|
| AP1 | 34 | 30-50 | 1.2<L<2.8 | 1958-1963 | |
| AP2 | 15 | 15-30 | 1.2<L<3.0 | 1958-1963 | |
| AP3 | 50 | >50 | 1.2<L<2.8 | 1958-1963 | |
| AP4 | 4 | 4-15 | 1.2<L<4.2 | 1962-1963 | |
| AP5 | 0.4 | 0.1-4* | 1.2<L<6.6 | 1961-1965 | |
| AP6 | 4 | 4-30 | 1.2<L<4.0 | 1962-1965 | Supersedes AP2 & 4 |
| AP7 | 50 | >50 | 1.15<L<3.0 | 1961-1966 | Supersedes AP3 |

New inner and outer zone electron environments are currently being prepared. Updating of model environments will proceed as warranted by new data as they become available.

Except for E68, the model environments have been published in the NASA SP-3024 series, Models of the Trapped Radiation Environment. The following volumes are currently available from NSSDC:

Volume 1: Inner Zone Protons and Electrons (Vette, 1967)
(Includes model environments AE1, AP1, AP2, AP3, AP4)

Volume 2: Inner and Outer Zone Electrons (Vette, Lucero, and Wright, 1967)
(Includes model environment AE2)

Volume 3: Electrons at Synchronous Altitudes (Vette and Lucero, 1968)
(Includes model environment AE3)

Volume 4: Low Energy Protons (King, 1967)
(Includes model environment AP5)

Volume 5: Inner Belt Protons (Lavine and Vette, 1969)
(Includes model environment AP6)

Volume 6: High Energy Protons (Lavine and Vette, 1970)
(Includes model environment AP7)

Using AP1, AP2, AP3, AP4, and AE2, Stassinopoulos (1970) has generated isoflux contours for integral electron and proton fluxes. These contours in geographic latitude and longitude are given at discrete altitudes in 100-km increments between 200 and 1000 km.

*The lower energy limit is L dependent, being 0.1 at L>3.5 and 1.0 at L<1.8.

Except for AE3, NSSDC can supply a BCD tape or card decks containing distribution functions F(B, L) and spectral functions N(E, L) for electrons and $E_0$(B, L) or P(B, L) for protons. NSSDC can also supply punched-card copies of the TRECO program, with which a user can generate the orbital integrated fluxes mentioned earlier.

## SOLAR WIND

The solar wind is the interplanetary extension of the solar corona in its state of dynamical expansion. Parker (1969) and the references contained therein provide detailed information on the solar wind.

Using multichannel observations (in energy and in angle) of positive ion fluxes, macroscopic bulk flow parameters such as flow velocity and particle density are derived. A secondary derived parameter is the time required for a steady-state solar corotating plasma beam to rotate from the spacecraft to the earth; this time is referred to as the corotation delay time.

In Solar-Geophysical Data, the bulk velocity and corotation delay times as provided by both the NASA/AMES and MIT plasma groups from their Pioneer 6 and 7 data are given for the month prior to the publication date. Proton densities are also provided by the MIT group from Pioneer 6 data. In addition, bulk velocity and proton density values are provided by the Los Alamos plasma group from its Vela 3 and 4 data.

## AIRGLOW

Airglow is a faint luminescence of the earth's upper atmosphere. The emitted electromagnetic radiation results mainly from chemical reactions of upper atmospheric constituents, although ionic recombination and bombardment by energetic particles are other mechanisms that can cause airglow. The main emissions include the atomic oxygen forbidden green line (5577 A) and forbidden red line (6300 A), the sodium doublet (5890 A and 5896 A), and the hydroxyl (OH) band system. For a more complete discussion of airglow, see Chamberlain (1961). More information on photometric observations of airglow can be found in Roach (1957).

A photometer is used to measure the intensity of the various lines and bands in the airglow spectrum. Photometric data have been obtained at several stations on a regular basis. The World Data Center A Catalogue of Data on Solar-Terrestrial Physics lists 41 stations active during at least part of the time since 1959, according to the wavelength at which measurements were made. The data from some stations are held at the WDC-A for Upper Atmosphere Geophysics, and the catalog indicates the completeness of these data. Zenith intensities in rayleighs and ratios of intensities at equal angular distances (usually 75°, although 70° and 67° are common) north and south from the zenith are the two types of data held at WDC-A. Observations are made for each hour on the hour (UT). The ratio data have advantages in that they are independent of the absolute calibration of the photometer, and they give the relative intensities at widely separated geographic locations. Most of these data are available in printed tabular form. However, some data obtained during the IGY and IQSY are available on punched cards.

Photometric data, zenith and ratio, from 19 stations for the IQSY are contained in WDC-A report UAG-1, July 1968. The report, entitled "IQSY Night Airglow Data," was prepared by L. L. Smith, F. E. Roach, and J. M. McKennan.

In some instances, the data from a particular station exist or are presumed to exist but are not held at WDC-A. The catalog indicates this, and, in these cases, WDC-A will assist in obtaining information concerning the completeness and availability of data from these stations.

## AURORA

An aurora involves emitted electromagnetic radiation that results primarily from the interaction of energetic, extra-atmospheric particles with the neutral gases of the upper atmosphere. These emissions extend from the ultraviolet to the infrared. The portion of the emitted electromagnetic radiation that is visible to the human eye is referred to as the visual aurora. For an in-depth treatment of the aurora, see Chamberlain (1961).

The World Data Center A for Upper Atmosphere Geophysics in Boulder is a repository for visual auroral data. Photographs obtained from all-sky cameras constitute the principal type of available data. These photographs are taken throughout all clear nights, and at least 12

exposures per hour are made. The photographs show the whole sky as reflected in a convex mirror, and all but the faintest aurora are recorded. The data are then put on 16- or 35-mm film in rolls 100 feet long.

All-sky camera photographs have been taken on a regular basis. Camera stations are located mainly in the northern and southern auroral regions (60°N to 90°N, 60°S to 90°S), but a few are in the subauroral regions (45°N to 60°N, 45°S to 60°S). (All references are to geomagnetic latitude.) Locations of stations that have been involved in this type of observation for any substantial length of time during the period since 1957 are listed in the WDC-A Catalogue of Data on Solar-Terrestrial Physics. In instances where data from a particular station are held at WDC-A, the time period and completeness of the data are indicated. The catalog also lists cases for which data exist or are presumed to exist but are not held at WDC-A. In these cases, WDC-A will assist both in determining the availability of data and in obtaining it.

In addition to microfilm, all-sky camera data can be obtained in the form of the ascaplot. The ascaplot contains information such as the part of the sky where the display is located, the auroral intensity (weak, medium, strong), and the presence of cloudiness. Information is recorded on the plot every half hour. Only a limited amount of data, essentially the IGY and IQSY data, is held at WDC-A in this form.

Visual observations form the basis of another type of data. Information is collected from a network of observers. This information is then summarized and can be put into several different forms.

One form, which indicates the occurrence or nonoccurrence of auroras without any reference to form or brightness, is known as a visoplot. With geomagnetic latitude as ordinate and universal time as abscissa, various symbols are used to indicate whether, at a certain location, an aurora is observed or is estimated to be overhead, to the north, or to the south. This is done for each of eight 45° geomagnetic longitude sectors. Magnetic activity index values, Kp, are given for 3-hour periods. Northern and Southern Hemisphere visoplots for the IGY period are contained in volume 29 of the Annals of the International Geophysical Year.

Another form that shows the auroral geometry and the geomagnetic latitude and longitude of a display at each hour of universal time is the synoptic auroral map on polar projection. By the use of various symbols, these maps show the location of veils, patches, arcs, rays, and bands. Also given is the value of Kp for that particular time. These maps are available on microfilm from WDC-A for certain time periods. Northern Hemisphere maps are available for 1964, 1965, 1967, and 1968. Southern Hemisphere maps can be obtained for the years

1964 and 1965. A similar form for displaying auroral data from the U.S. and Canada is the North American map. This type of map is not on polar projection, but it does indicate the locations and forms of observed aurora. A large number of these maps are held at WDC-A, and the available time periods can be obtained upon inquiry. Still another form in which some visual data are recorded is punched cards. Since 1957, various modifications have been made in the system that is used to convert data from observers' reports to cards, and, consequently, a wide variety of basic data cards are at WDC-A. Information recorded on punched cards may include time, point of observation, location of the display in the sky, duration, motion, forms, form sequence, and color.

These three types of data, i.e., visoplots, synoptic maps, and punched cards, can be obtained from WDC-A for certain periods. The available time periods are listed in the WDC-A catalog.

The all-sky camera and visual observation data are supplemented by several other groups of data. A limited amount of radar echo and patrol spectrograph data is available. Radio aurora is a term used for the ionization associated with the aurora and is responsible for certain types of radio reflections. Some radar echo data are available for the period 1957 to 1962. The data are on 16-mm film and consist of pictures of radar range echoes taken from the face of a cathode-ray tube. A patrol spectrograph is a low-resolution measurement that can be used for verifying the presence or absence of spectral lines and bands. Some patrol spectrograph data are available for the period 1957 to 1960. Spectrograms have been recorded on 16-mm film. The WDC-A catalog lists the stations that recorded these two types of data and the amount of data available. Most of these same patrol spectrograph data can be found in tabular form in volumes 25 and 40 of the Annals of the International Geophysical Year. The information from the spectrograms was punched on cards, and the card data were used to compile the tables in these volumes. In addition, both volumes contain a description of the instrumentation and of the data reduction procedures.

## SOLAR GEOPHYSICAL CALENDAR RECORDS, ABBREVIATED CALENDAR RECORDS, AND CONDENSED CALENDAR RECORDS

Solar Geophysical Calendar Records contain the daily highlights of solar geophysical activity for the period 1957 to 1964. They consist of a collection, on a daily basis, of data related to geomagnetism, solar activity, ionosphere, aurora, and cosmic rays. Charts, mainly

containing indices, and brief textual discussions comprise the Calendar Records. The Calendar Records are useful in that they may readily suggest correlations between various phenomena; however, it is recommended that original data be used for more detailed studies.

Calendar Records for the IGY and for the IGC (International Geophysical Cooperation - 1959) are found in the Annals of the International Geophysical Year, volume 16 (pp. 1-159 and 201-300, respectively). Calendar Records for the 1960 to 1965 period are found in the Annals of the IQSY, volume 2.

Since 1964, Abbreviated Calendar Records have been generated. These Records contain a somewhat smaller quantity of tabulated data than the earlier Calendar Records, but, at least through June 30, 1967, they contain expanded textual discussion of daily highlights. Since July 1, 1967, most data have been presented in chart form, with very limited textual discussion.

Data currently included in Abbreviated Calendar Records are as follows. For each month, a calcium plage map is given; for each day, the times (start and duration), importance, and associated calcium plage region of flares greater than 1f, start times of solar noise bursts in four frequency ranges, occurrence of spectral types II or III radio events, start times of SID, start times of solar X-ray bursts (2 to 12A), geomagnetic indices Ap and Kp, ionospheric indices I, Ip, and Ia, 10-cm solar flux value, sunspot number Rz, and central meridian passage information related to calcium plages are given. When appropriate, textual information relates to the geomagnetic character of the day (quiet or disturbed), auroral displays, general ionospheric conditions, Forbush decreases, polar cap absorption, noctilucent clouds, coronal emission, and solar proton flux increases.

Some data contained in Abbreviated Calendar Records are based on provisional data reports available at WDC-A for Upper Atmosphere Geophysics. Thus, it is recommended that the Records be used as a guide to more definitive data that can be obtained from WDC-A or found in standard data publications.

For the period January 1964 to December 1966, Abbreviated Calendar Records can be found in selected issues of the IQSY Notes. For the period January 1966 to December 1967, these Records are found in WDC-A for Upper Atmosphere Geophysics Report UAG-4. (See Data Sources, Part IX, for a description of the document and procedures for acquiring it.) For the periods January 1967 to April 1967, May 1967 to September 1967, November 1967 to April 1968, May 1968 to June 1968, and July 1968 to November 1968, Abbreviated Calendar Records are found in STP Notes, No. 1, 2, 3, 5, and 7, respectively. (See Data Sources, Part IX, for

discussion of STP Notes.) For the period December 1968 to the present, these Records are found in the Solar-Geophysical Data (Comprehensive Reports), with a 7-month lag.

An even more succinct presentation of solar-terrestrial data is the Condensed Calendar Record, the first of which appeared for the period December 1968 through September 1969 in STP Notes, No. 7 (May 1970). One line gives the following data for one day: the sunspot number Rz, the 10-cm solar flux value; the geomagnetic Ap index; the ionospheric I, Ip, and Ia indices; the number of flares of importance one or above; the number of X-ray and SID events; occurrence of type IV radio emission; a proton event index; and comments. A monthly summary of two to five lines is also given. Future Condensed Calendar Records will also be published in the STP Notes.

## SOLAR-TERRESTRIAL ACTIVITY CHARTS

As an outgrowth of the First General Assembly of the Inter-Union Commission on Solar Terrestrial Physics (London, January 1969), T. Obayashi and others at the National Committee on Solar-Terrestrial Physics, Science Council of Japan (Tokyo), are generating solar-terrestrial activity charts on three time scales: yearly charts, 27-day charts, and special event charts. Each chart displays individual time plots related to: solar radio and X-ray emission, solar flare occurrence, solar proton flux, solar wind velocity and density, interplanetary magnetic field intensity and direction, neutron monitor data, and geomagnetism (Dst and Ap). On the yearly charts, most parameters are presented as daily averages. On the 27-day charts and special event charts, greater time resolution is presented. A sample yearly chart for the year 1968 appears in STP Notes, No. 7. Information specifying the publication in which these charts will routinely appear will be given in a subsequent issue of the STP Notes.

## JOVIAN RADIO EMISSIONS

Except for the sun, the planet Jupiter is the only source of intense sporadic radio emissions that can be observed from the earth. These Jovian emissions occur at wavelengths greater than 7.5 meters (a frequency

of 40 MHz). These emissions are observed with either fixed-frequency or sweep-frequency receivers such as those described by Kraus (1966). A comprehensive review of Jovian radio astronomy is given by Warwick (1967). Jovian radio emission data include relative intensity, burstiness, and frequency range of the emissions.

Data from the University of Colorado 7.6- to 41-MHz sweep-frequency receiver, covering the period January 1960 to September 8, 1968, are available in hard-copy form from WDC-A at Boulder. Florida State University data from single-frequency or multichannel receivers operating between 18 and 38 MHz and covering the 1961 to 1964 period are available in tabular form on microfilm and as oscillograph tracings on microfilm at NSSDC. Similar data from the University of Florida and from a cooperative station in Santiago, Chile, for the period 1957 to 1962, are also available at NSSDC. Goddard Space Flight Center (GSFC) data taken at 16.7 and 22.2 MHz between November 11, 1965, and February 28, 1966, are available in hard-copy tabular form at NSSDC.

Data are still being taken by the University of Florida and the GSFC groups and are published on an irregular basis.

## REFERENCES


1. Chamberlain, J. W., Physics of Aurora and Airglow, Academic Press, New York, 1961.

2. Hess, W. N., The Radiation Belt and the Magnetosphere, Blaisdell Publishing Company, Waltham, Mass., 1968.

3. King, J. H., Models of the Trapped Radiation Environment, Volume 4: Low Energy Protons, NASA SP-3024, 1967.

4. Kraus, J. D., Radio Astronomy, McGraw-Hill, New York, 1966.

5. Lavine, J. P., and J. I. Vette, Models of the Trapped Radiation Environment, Volume 5: Inner Belt Protons, NASA SP-3024, 1969.

6. Lavine, J. P., and J. I. Vette, Models of the Trapped Radiation Environment, Volume 6: High Energy Protons, NASA SP-3024, 1970.

7. Parker, E. N., "Theoretical Studies of the Solar Wind Phenomena," Space Science Reviews, 9, 325-360, 1969.

8. Roach, F. E., "Photometric Observation of the Airglow," Ann. IGY, 4, 115-138, 1957.

9. Smith, L. L., F. E. Roach, and J. M. McKennan, "IQSY Night Airglow Data," WDC-A Report UAG-1, July 1968.

10. Stassinopoulos, E. G., World Maps of Constant B, L and Flux Contours, NASA SP-3054, 1970.

11. Vette, J. I., Models of the Trapped Radiation Environment, Volume I: Inner Zone Protons and Electrons, NASA SP-3024, 1967.

12. Vette, J. I., and A. B. Lucero, Models of the Trapped Radiation Environment, Volume 3: Electrons at Synchronous Altitudes, NASA SP-3024, 1968.

13. Vette, J. I., A. B. Lucero, and J. Wright, Models of the Trapped Radiation Environment, Volume 2: Inner and Outer Zone Electrons, NASA SP-3024, 1967.

14. Warwick, J. W., "Radiophysics of Jupiter," Space Science Reviews, 6, 841-891, 1967.

15. Williams, D. J., "Sources, Losses, and Transport of Magnetospherically Trapped Particles," ESSA Technical Report ERL 180-SDL 16, 1970.

# PART VIII

# MISCELLANEOUS INFORMATION

Prepared By

Joseph H. King and Leland L. Dubach

CONTENTS

# COORDINATE SYSTEMS

A number of coordinate systems that have proven useful in the analysis of space science data are discussed in this part. Some coordinate systems are better suited for certain studies than are others. The various systems are distinguished by the orientation of their axes. Except for the B, L and $\alpha$, $\beta$ coordinate systems, all systems are right handed and orthogonal; as such, the directions of the Y axes are not explicitly given. Coordinate systems used principally in spacecraft trajectory analyses or similar studies are not included in this discussion.

## Geographic Coordinate System

In the geographic coordinate system, the positive Z axis is aligned northward along the earth's spin axis. The positive X axis lies in the Greenwich meridian and intersects the earth's surface in the Atlantic Ocean, south of Ghana, Africa.

The geocentric latitude of a point, P, is the angle measured at the earth's center between the equatorial plane and a radius to P. The geodetic latitude of P (sometimes called the geographic latitude) is the angle between the equatorial plane and the line which passes through P and which is normal to the oblate ellipsoid whose surface most nearly approximates the mean sea-level surface of the earth (i.e., the geoid). The maximum difference between geodetic and geocentric latitudes at the earth's surface is 11.6 minutes of arc and occurs near 45° latitude. The astronomical latitude of P is the angle between the equatorial plane and the plumb-bob vertical direction at P. The difference between geodetic and astronomical latitudes is almost everywhere less than 1 minute of arc.

## Equatorial Coordinate System

In the equatorial coordinate system, the positive Z axis is perpendicular to the earth's equatorial plane (positive north), while the X axis points from the earth to the sun at the moment of the vernal equinox (or, equivalently, to the point of Aries). This is an inertial system and is sometimes referred to as the geocentric celestial inertial coordinate system. Due to the slow precession of the earth's equatorial plane, an epoch date should be defined for the sake of completeness.

Right ascension is defined as the angular distance east of the vernal equinox as measured along the earth's equator; declination is the angular distance north (positive) or south of the earth's equatorial plane. Right ascension and declination are often used in specifying vector directions (as of magnetic fields) in an inertial coordinate system.

## Geomagnetic Dipole Coordinate System

In the geomagnetic dipole coordinate system, the positive Z axis is aligned northward along the geocentric geomagnetic dipole axis. When the field model defined by the $g_1^0$, $g_1^1$, and $h_1^1$ terms of the IGRF 1965.0 model is used (a common choice), this positive Z axis intersects the earth's surface at 11.44° geocentric colatitude and 290.24° geographic east longitude (extreme western Greenland). The positive X axis lies in the plane formed by the geographic and geomagnetic Z axes and intersects the earth in southeastern Peru. Analogous to the conventional local time system, geomagnetic local time is defined by replacing the geographic axis with the geomagnetic axis and defining geomagnetic noon for a location P as the time when the subsolar point lies on the geomagnetic meridian of P (Sugiura and Heppner, 1968).

The transformation between the geocentric and geomagnetic coordinate systems is given in a spherical representation as follows. If $\Theta$ and $\Phi$ are geomagnetic colatitude and east longitude, respectively, while $\theta$ and $\phi$ are geocentric colatitude and east longitude, respectively, then

$$\cos\Theta = \cos\theta\cos(11.44°) + \sin\theta\sin(11.44°)\cos(\phi-290.24°)$$
$$\sin\Phi = \sin\theta\sin(\phi-290.44°)/\sin\Theta$$
$$\cos\Phi = \cos\theta\cos 11.44° - \cos\phi/(\sin\Theta\sin 11.44°)$$

A Fortran program to transform positions and field components from geocentric to geomagnetic dipole coordinates and vice versa has been generated by G. D. Mead (1970). Program decks are available at NSSDC.

## Solar Magnetic Coordinate System

In the solar magnetic coordinate system, the positive Z axis is aligned northward along the geocentric geomagnetic dipole axis while the X axis lies in the plane formed by the Z axis and the earth-sun line; X is positive in the sunward hemisphere. Solar magnetic coordinates are recommended for those magnetospheric studies in which the main geomagnetic field is a dominant factor.

## Solar Magnetospheric Coordinate System

In the solar magnetospheric coordinate system, the positive X axis points toward the sun while the Z axis lies in the plane formed by the X axis and the geomagnetic dipole axis; Z is positive in the Northern Hemisphere. This coordinate system is recommended for those magnetospheric studies involving the geomagnetic tail and for others in which the overall magnetosphere configuration is a dominant factor.

## Solar Ecliptic Coordinate System

In the solar ecliptic coordinate system, the Z axis is perpendicular to the ecliptic plane (positive north) and the X axis is directed toward the sun. In terms of the equatorial coordinate system previously discussed, the Z axis of the solar ecliptic coordinate system has a right ascension of -90° and a declination of 66.56°

The solar ecliptic coordinate system is recommended for studies of solar-wind-related interplanetary phenomena. The solar ecliptic coordinate system should not be confused with the heliocentric ecliptic coordinate system used in some spacecraft trajectory analyses. In the latter system, the Z axis is also normal to the ecliptic plane, but the X axis lies along the earth-sun line defined at the time of the vernal equinox.

## B, L Coordinates, Invariant Geomagnetic Coordinates

To properly organize magnetospheric trapped particle data, McIlwain (1961, 1966) introduced the B, L coordinate system. B is the magnetic field strength at the point of interest, and L is explained as follows. In a dipole field, the equatorial crossing distance, $R_0$, of a field line passing through a spatial point of interest is functionally related to the values, at that point, of B and I. Here, I is the integral (or longitudinal) invariant. Thus, in a dipole field, $R_0 = F(B,I)$. For a nondipolar field, L is defined by $L = F(B,I)$. B and I are evaluated at the point of interest using the nondipolar field, and the function F is taken to be the same as for the dipole field.

The advantage in the use of the B, L coordinates is that a particle conserving its first two adiabatic invariants mirrors at the same B, L values as it drifts around the earth. Thus, in the absence of significant azimuthal gradients in particle populations such as those resulting from the South Atlantic magnetic anomaly, B, L coordinates

organize perpendicular flux data very well. To the extent that the geomagnetic field approximates a dipole field, the B, L coordinates are useful in organizing omnidirectional fluxes. This is the case for L values out to about 5. At L values greater than about 5, the geomagnetic field is sufficiently nondipolar that each field line is characterized by a range of L values, and the B, L coordinates are somewhat deficient in organizing omnidirectional fluxes.

The INVAR program deck, generated by McIlwain, used for calculating B, L values at a given point in the earth's vicinity for any given geomagnetic field model is available from NSSDC. A second Fortran program, generated by Kluge (1970) computes B and L values faster and more accurately than does INVAR. This deck will become available at NSSDC shortly. A coefficient deck for a field model, such as those discussed in the geomagnetic field models section in Part IV of this Handbook, are used with these B, L programs.

Using the Hendricks and Cain 1960.0 geomagnetic field model, as projected to 1965.0, Stassinopoulos (1970) has generated contours of constant B and L. These contours in geographic latitude and longitude are given at discrete altitudes in 100-km increments between 0 km and 3000 km. Similar plots, based on the GSFC (12/66) geomagnetic field as updated to 1970.0, are found in Wiley and Barish (1970) for 21 altitudes between 0 km and 10,000 km. (This reference also contains contours of constant conjugate altitude difference, conjugate latitude and longitude, field dip angle and declination, and horizontal field intensity.)

Useful auxiliary quantities have been defined to complement B, L coordinates. Variables R and $\lambda$ (a radius and a latitude) have been defined in terms of B and L by assuming dipolar relations (Roberts, 1964). The quantity x [$x=(1-B_0/B)^{1/2}$], where $B_0$ is the equatorial value of B, is the cosine of the equatorial pitch angle of a particle mirroring at the point of interest (Roberts, 1965). Of the five variables, B, L, R, $\lambda$, and x, only two are independent. Vette and Porjes (1966) have generated 17 tables showing the relation of one of the five variables to two others; the Jensen and Cain (epoch 1960) model magnetic field was used. Copies of this document are available at NSSDC.

Another pair of useful variables is the invariant geomagnetic latitude and longitude, $\Lambda$ and $\Phi$, respectively. $\Lambda$ is defined simply by $\cos^2\Lambda = 1/L$ (see Sugiura and Heppner, 1968); $\Lambda$ is a field line earth-intersection latitude derived from the actual L value using a dipolar relation. The invariant geomagnetic longitude $\Phi$ cannot be defined as simply as the invariant geomagnetic latitude $\Lambda$ because the choices of a polar axis, of an equatorial plane, and of a prime meridian involve a series of arbitrary decisions.

Evans et al. (1969) present a system of invariant geomagnetic coordinates (not to be confused with the geomagnetic coordinate systems discussed previously) based on the International Geomagnetic Reference Field [IGRF 1965.0 discussed previously] as updated to 1969.75. This document, which can be obtained from the authors (see page 196), describes the difficulties encountered in constructing such a system and presents reasons for the decisions that lead to their definition of the invariant geomagnetic longitude $\Phi$.

They present, at each of six altitudes (0, 100, 300, 600, 1000, and 3000 km) and in each hemisphere, a polar azimuthal equidistant projection plot containing concentric constant-geographic-latitude ($\lambda$) circles ($40° \leq \lambda \leq 90°$; $\Delta\lambda = 5°$) and radial constant-geographic-longitude ($\phi$) lines ($0° \leq \phi \leq 360°$; $\Delta\phi = 30°$). Superposed on these are lines of constant invariant geomagnetic latitude ($\Delta\Lambda = 5°$) and lines of constant invariant geomagnetic longitude ($\Delta\Phi = 10°$). They also present, at each of the six altitudes identified above, a cylindrical equidistant projection plot containing a Cartesian grid of constant geographic latitude ($-90° \leq \lambda \leq 90°$; $\Delta\lambda = 30°$) and longitude ($0° \leq \phi \leq 360°$; $\Delta\phi = 30°$) lines. Superposed on these lines are lines of constant invariant geomagnetic latitude ($\Delta\Lambda = 10°$) and longitude ($\Delta\Phi = 10°$) lines. Finally, they present for each of the same six altitudes numerical listings of calculated values of geographic latitude and longitude for specified values of invariant geomagnetic latitude ($-90° \leq \Lambda \leq 90°$; $\Delta\Lambda = 5°$) and longitude ($0° \leq \Phi \leq 360°$; $\Delta\Phi = 10°$).

NSSDC has available for full scale reproduction the master copies of the graphs found in Evans et al. (1969).

## $\alpha$, $\beta$ Coordinate System

The $\alpha$, $\beta$ coordinates, also called Euler Potentials, are constant on a given field line and satisfy $\underline{B}(\underline{r}, t) = \underline{\nabla}\,\alpha(\underline{r}, t) \times \underline{\nabla}\,\beta(\underline{r}, t)$. A third coordinate, usually designated by s, provides a measure of distance along a field line from some reference point. The $\alpha$, $\beta$ coordinates are not unique in that two $\alpha$, $\beta$ pairs related by a Jacobian of unity are equally valid. Some of the advantages of this system are indicated in Stern (1968); the relation of $\alpha$, $\beta$ to B, L is also given in this reference.

## Heliocentric Corotating Coordinate System

For studies involving the evolution of solar surface features, a coordinate system in which these features are stationary is advantageous. An approximation to such a system was developed by Carrington and is discussed in The American Ephemeris and Nautical Almanac (1968, p. 494). In this system, the positive Z axis points northward along the solar spin axis. Heliographic longitudes on the solar surface are measured from the solar meridian which passed through the ascending node of the solar equator on the ecliptic on January 1, 1854, Greenwich mean noon; the longitudinal angle increases in the direction of solar rotation. A sidereal period of rotation of 25.38 mean solar days is assumed for this coordinate system. Note that the differential character of solar rotation is neglected.

# INTERNATIONAL URSIGRAM AND WORLD DAYS SERVICE

## Data Exchange and Forecasts

A system for the real-time collection, interchange, and distribution of solar and geophysical data, alerts, and forecasts has been established under the direction of the International Ursigram and World Days Service (IUWDS). A thorough description of this system, along with a list of contributing observatories and the operating procedures of each of 11 Regional Warning Centers (RWCs), is given in the "International Ursigram and World Days Service Synoptic Codes for Solar and Geophysical Data."

Briefly, individual observatories report data to the most convenient RWC. These data may involve sunspots, calcium plages, solar flares, solar X rays, solar radio emission, coronal line emission, solar particle events, solar wind parameters (Pioneer satellite data), ionospheric critical frequencies, sudden ionospheric disturbances, ionospheric absorption, geomagnetic activity, auroral observations, or cosmic rays. These data are exchanged among RWCs on a scheduled basis once or twice daily; each RWC then forwards the data to users in its region.

When an observatory records a major event (optical or radio flare, cosmic-ray event, geomagnetic storm), the pertinent information is transmitted to the most convenient RWC, which immediately issues an ADALERT (ADvance ALERT) to all other RWCs.

The Regional Warning Center for the Western Hemisphere, located at the National Oceanic and Atmospheric Administration (NOAA), Boulder, Colorado, serves as the World Warning Agency (WWA). Once each day, this RWC issues to all other RWCs a GEOALERT (GEOphysical ALERT) containing information on the commencement, continuation, or termination of geomagnetic storms, cosmic-ray events, and stratospheric warnings, as well as forecasts of flares, solar proton events, and geomagnetic storms. The contents of the GEOALERTs are based on the data provided by the worldwide network of RWCs.

The data handled in the IUWDS-sponsored activity also go to the World Data Centers (WDCs). The data catalogs from the various WDCs are referenced in the discipline-oriented parts of this Handbook and are discussed further in Part IX. This system will probably be of interest primarily to those data users who require essentially real-time data.

### International Geophysical Calendar

Each year, a set of "world days" is selected by IUWDS and is presented on the International Geophysical Calendar. The selections provide various kinds of samples (3 days per month, 14 contiguous days about every third month, etc.) for intensified measurement of the time variation of geophysical phenomena. The calendar also indicates predictable events such as meteor showers and eclipses and any special intervals selected for intensified cooperative observations such as for the Proton Flare Project.

The International Geophysical Calendars for the period 1957 to 1969 are contained in Shapley and Lincoln (1969). This is a useful document in that for some disciplines the data held by World Data Centers is increased for some of the world days marked on the calendar. Current calendars appear annually in the WDC-A Catalogue of Data on Solar-Terrestrial Physics and in the January 1 issue of the Journal of Geophysical Research.

## ROCKET DATA

Rocket data may be conveniently categorized into three types as follows.

## Synoptic Observations

Synoptic observations are rocket observations that involve repeated time-scheduled observations of the parameters by very similar sensors from a relatively unchanging set of launch sites. At present, this category consists primarily of relatively small meteorological rockets with apogees of 60 to 100 km. Profiles of wind, pressure, temperature, and/or density are obtained. Synoptic observations are routinely reduced (usually at the observing site) and then collected by the National Climatic Center, Asheville, North Carolina.

## Research Rockets

Research rockets are launched with a scientific payload aboard and obtain data that are used for the study of some aspect of the natural environment. The discipline areas include astronomy, solar physics, aeronomy, and energetic and thermal particles. By international agreement, research rocket launches are routinely reported to World Data Centers. A machine-sensible file, which contains selected information on these launches, is maintained at NSSDC. The information in this file is taken from the launch reports and from open literature. From this listing, launches can be selected by location, by time of day or date, by type of experiment, etc. The data must be obtained directly from the experimenter, but NSSDC can provide the experimenter's name and current address in most cases. A current copy of this listing or a uniquely sorted version of this listing can be obtained from NSSDC. Also available is a library file that lists publications that contain or have used rocket data. A very small number of engineering and development rockets are included in this file when the rocket type under development or testing is being prepared especially for subsequent use as a research rocket.

## Engineering and Development Rockets

Engineering and development rockets are instrumented to obtain rocket performance data. These data are intended to improve or evaluate rocket design. Occasionally, research payloads are included on this type of rocket. In such a case, a WDC attempts to include information about the flight in this file along with the research rockets.

## REFERENCES


1. Evans, J. E., L. L. Newkirk, and B. M. McCormac, "North Polar, South Polar World Maps and Tables of Invariant Magnetic Coordinates for Six Altitudes: 0, 100, 300, 600, 1000, and 3000 km," DASA 2347, Oct. 1969.

2. "International Ursigram and World Days Service Synoptic Codes for Solar and Geophysical Data, Second Revised Edition," IUWDS Secretariat, Boulder, Colorado, 1969.

3. Kluge, G., "Computer Program SHELL for the Calculation of B and L from Models of the Geomagnetic Field," ESOC Internal Note No. 67, European Space Operations Center of ESRO, Darmstadt, Germany, 1970.

4. McIlwain, C. E., "Coordinates for Mapping the Distribution of Magnetically Trapped Particles," J. Geophys. Res., 66, 3681-3691, 1961.

5. McIlwain, C. E., "Magnetic Coordinates," Radiation Trapped in the Earth's Magnetic Field, ed. B. M. McCormac, D. Reidel Publishing Company, Dordrecht, Holland; 45-61, 1966.

6. Mead, G. D., "International Geomagnetic Reference Field 1965.0 in Dipole Coordinates," NASA-GSFC X-641-70-198, May 1970, and J. Geophys. Res., 45, 4372-4374, 1970.

7. Roberts, C. S., "Coordinates for the Study of Particles Trapped in the Earth's Magnetic Field: A Method of Converting from B, L to R, $\lambda$ Coordinates," J. Geophys. Res., 69, 5089-5090, 1964.

8. Roberts, C. S., "On the Relationship Between the Unidirectional and Omnidirectional Flux of Trapped Particles on a Magnetic Line of Force," J. Geophys. Res., 70, 2517-2527, 1965.

9. Shapley, A. H., and J. V. Lincoln, "International Geophysical Calendars 1957-1969," World Data Center A for Upper Atmosphere Geophysics Report UAG-6, 1969.

10. Stassinopoulos, E. G., "World Maps of Constant B, L and Flux Contours," NASA SP-3054, 1970.

11. Stern, D., "Euler Potentials and Geomagnetic Drift Shells," J. Geophys. Res., 73, 4373-4378, 1968.

12. Sugiura, M., and J. P. Heppner, "Electric and Magnetic Fields in the Earth's Environment," prepared for the American Institute of Physics Handbook, Dec. 1968.

13. The American Ephemeris and Nautical Almanac for 1968, U.S. Naval Observatory, Washington, D. C., 1966.

14. Vette, J. I., and H. S. Porjes, "Geomagnetic Geometry Tables," NASA CR-390, Mar. 1966.

15. Wiley, R. E., and F. D. Barish, "Plots of Geomagnetic Field Geometry," AFWL-TR-69-144, Air Force Weapons Laboratory, 1970.

# PART IX

# SOURCES

CONTENTS



## PART IX - SOURCES

This part contains brief descriptions of the principal sources of correlative data. Both data centers and publications are discussed. A single alphabetically ordered list of documents containing correlative data or information on the availability of such data is also given. Sufficient detail is given to enable the reader to obtain the document. In general, no attempt has been made to include the publications of individual observatories either in this part or in the discipline-oriented parts of this Handbook. More extensive lists of data sources

can be found in: Report UAG-4 of the World Data Center A (WDC-A) for Upper Atmosphere Geophysics, 1969 ("Abbreviated Calendar Record 1966-1967"); Annals of the IQSY, volume 1, 1968; and the AFCRL Geophysics and Space Data Bulletin, volume IV, No. 2, 1967.

## IUCSTP, STP NOTES

The Inter-Union Commission on Solar Terrestrial Physics (IUCSTP) was established in 1966 to provide a single international organization with a comprehensive interest in solar-terrestrial physics. IUCSTP is composed of five preexisting ICSU (International Council of Scientific Unions) organizations, each interested in certain aspects of solar-terrestrial physics. These organizations are the International Union of Astronomy (IAU), the International Union of Geodesy and Geophysics (IUGG), the International Union of Radio Science (URSI), the International Union of Pure and Applied Physics (IUPAP), and the Committee on Space Research (COSPAR).

Since April 1968, IUCSTP has published the STP Notes to provide solar-terrestrial physicists at the working level with information on relevant research that is being performed or proposed throughout the world. Recommendations of IUCSTP and its individual working groups are published, as are data synopses in the form of "Abbreviated Calendar Records." (See Part VII.) STP Notes are published three to four times a year and are available through the IUCSTP Secretariat, c/o National Academy of Sciences, 2101 Constitution Avenue, N.W., Washington, D. C. 20418.

## WORLD DATA CENTERS

World Data Centers (WDC) conduct international exchange of geophysical observations in accordance with the principles set forth by the International Council of Scientific Unions. First established for the International Geophysical Year (IGY), 1957 to 1958, they provide the means by which data gathered at individual observatories are made available to the international scientific community.

Three major centers exist: WDC-A in the U.S.A., WDC-B in the U.S.S.R., and WDC-C in Western Europe, Australia, and Japan. Each WDC is made up of a number of subcenters, each of which is devoted to one or more specific geophysical disciplines. The geographical location of each subcenter is usually different than that of the other subcenters. Certain of the subcenters have recently been designated as Solar Terrestrial Physics World Data Centers (STP-WDC) by the Inter-Union Commission on Solar Terrestrial Physics.

Overall responsibility for WDC-A (coordination office and nine subcenters) resides with the U.S. National Academy of Sciences through the Geophysics Research Board (GRB) and its Committee on Data Exchange and Data Centers. The WDC-A subcenters related to the phenomena discussed in this Handbook are:

WDC-A for Upper Atmosphere Geophysics
National Oceanic and Atmospheric Administration
Boulder, Colorado, U.S.A. 80302
Telephone: (303) 447-1000, Ext. 3181

WDC-A for Geomagnetism, Seismology, and Gravity
Environmental Data Service, NOAA
Rockville, Maryland, U.S.A. 20852
Telephone: (301) 496-8160

WDC-A for Meteorology
National Climatic Center, NOAA
Asheville, North Carolina, U.S.A. 28801
Telephone: (704) 254-0236

WDC-A for Rockets and Satellites
Goddard Space Flight Center, Code 601
Greenbelt, Maryland, U.S.A. 20771
Telephone: (301) 982-6695

More extensive discussions of the WDC system can be found in IQSY Instruction Manual No. 6 or in the IQSY Annals, volume 1, "Geophysical Measurements, Techniques, Observational Schedules, and Treatment of Data." These references contain the "Guide to International Data Exchange through the World Data Centers." Likewise STP Notes No. 6, "Guide for International Exchange of Data in Solar-Terrestrial Physics," contains a full discussion of the STP-WDCs.

Individual WDC subcenters periodically issue catalogs listing their data holdings; any special publications involving data syntheses or special data compilations are also listed in the catalogs. Detailed information on the method of ordering data and the associated costs is presented. The catalogs are available upon request to the appropriate WDC subcenter.

Of principal interest to most users of this Handbook will be the WDC-A Catalogue of Data on Solar-Terrestrial Physics, which has been issued annually during recent years. This data catalog lists the holdings of the WDC-A for Upper Atmosphere Geophysics, the WDC-A for Geomagnetism, and the WDC-A for Rockets and Satellites. The June 1970 issue of the catalog is Report UAG-11 of the WDC-A for Upper Atmosphere Geophysics. The annual series of UAG documents can be obtained by subscription (see Data Compilations, p. 194), or a single copy of the catalog can be obtained from the Superintendent of Documents or from WDC-A at a cost of $1.50.

For the convenience of the reader, the contents of the data catalog (1970) are given here in table 16. The numbering scheme shown not only reflects the organization of the catalog but also shows the discipline classification system as proposed by IUCSTP.

In addition to the data listed, this WDC-A catalog contains an alphabetically ordered, cross-discipline station list that gives observing program, station latitude and longitude (geographic and geomagnetic), magnetic dip angle, L value, open and close dates, and, in appropriate cases, cosmic ray cutoff rigidity and altitude.

Volume 7 of the Annals of the IQSY, "Sources and Availability of IQSY Data," contains lists of observing stations, rockets, satellites, and space probes active during part or all of the 1964 to 1965 period. This source also lists data available at the World Data Centers for the period 1957 to 1965.

## SOLAR-GEOPHYSICAL DATA

The Institutes for Environmental Research (IER/NOAA) publish Solar-Geophysical Data (SGD) monthly in two parts. The first part is Solar-Geophysical Data (Prompt Reports), which contains data for the first and second months prior to publication; the second part is Solar-Geophysical Data (Comprehensive Reports), which contains data for the sixth and seventh months prior to publication along with other miscellaneous information. A descriptive text is published annually. Prior to July 1969, data for the first, second, and sixth months prior to publication appeared in the single monthly issue of Solar-Geophysical Data. Between November 1955 and November 1965, this series was the CRPL-FB-Solar Geophysical Data, issued by the Central Radio Propagation Laboratory of the National Bureau of Standards.

TABLE 16

CONTENTS OF THE WORLD DATA CENTER A
CATALOGUE OF DATA ON SOLAR-TERRESTRIAL PHYSICS

MASTER STATION LIST

SOLAR AND INTERPLANETARY PHENOMENA



IONOSPHERIC PHENOMENA

TABLE 16 (continued)

FLARE-ASSOCIATED EVENTS

| | |
|---|---|
| C.1 | H-α Flares |
| C.2 | Solar Magnetic Field in Active Regions and Their Short-Term Changes |
| C.3 | Solar Radio Events, Fixed Frequency |
| C.4 | Solar Radio Spectrograms of Events |
| C.5 | Solar X-Ray Observations |
| C.6 | Sudden Ionospheric Disturbances - Ground-Based Observations |
| C.7 | Solar Protons - Direct Measurement |
| C.8 | Solar Protons - Riometer |
| C.9 | Solar Protons - Ionospheric Vertical Incidence Soundings |
| C.10 | Solar Protons and Electrons - VHF Forward Scatter |
| C.11 | Solar Protons - Other Types of Measurements |
| C.12 | Solar, Ionospheric, or Aeronomical Rockets Launched During an Event |
| C.13 | Cosmic-Ray Ground Level Increases |

GEOMAGNETIC PHENOMENA

| | |
|---|---|
| D.1 | Standard and Rapid Run Measurements |
| D.2 | Magnetospheric Micropulsation Phenomena |
| D.3 | Space Magnetism |

AURORA

| | |
|---|---|
| E.1 | All-Sky Cameras and Others |
| E.2 | Satellite Measurements (particle precipitation and photometers) |

COSMIC RAYS

| | |
|---|---|
| F.1 | Neutron Monitors and Supermonitors |
| F.2 | Ionization Chambers |
| F.3 | Meson Telescope (cubical, crossed, narrow angle, and wide angle) |
| F.4 | Balloon Measurements |
| F.5 | Aircraft and Ship Measurements |
| F.6 | Satellite Measurements |

AIRGLOW

| | |
|---|---|
| G.1 | Ground-Based Photometers |
| G.2 | Satellite Measurements (photometers) |

MISCELLANY

| | |
|---|---|
| H.1 | Noctilucent Clouds |
| H.2 | Meteorological Rockets |
| H.3 | Ozone |

The Solar-Geophysical Data series is presently edited by Miss Hope J. Leighton under the supervision of Miss J. Virginia Lincoln of the Aeronomy and Space Data Center, NOAA, Boulder. Copies can be obtained on a data exchange basis from the World Data Center A for Upper Atmosphere Geophysics. Copies can be purchased from the Superintendent of Documents, Government Printing Office, Washington, D.C. 20402. The annual subscription cost is $30.50 for both parts or $15.50 for one part. (Add $4.00 per part for foreign mailing.) The single issue price is $1.25 per part.

Table 17, based on the index of Issue No. 304, December 1969, indicates the volume in which data of a certain type and for a given month can be found. Issue No. 303, for example, which was published in November 1969, contains $R_A$ data for October 1969.

## GEOPHYSICS AND SPACE DATA BULLETIN

The Air Force Cambridge Research Laboratories (AFCRL), Bedford, Massachusetts, issues the Geophysics and Space Data Bulletin on a quarterly basis. The bulletin contains AFCRL-sponsored data which are collected from sites throughout the world.

The first four issues, encompassing 1964 data, constitute Volume I, No. 1-4. Volume II, with few exceptions, contains quarterly data for 1965; Volume III, 1966; Volume IV, 1967; and Volume V, 1968. Each of four appendices have been published in various issues as follows:

Auxiliary Data Sources: Volume I, No. 1, 2; II, No. 1; III, No. 2; IV, No. 2.

Trapped Radiation Model Environments: Volume II, No. 4; IV, No. 1.

Annual Summary of Activity Cycle No. 20 Solar Flares: Volume IV, No. 3.

Cumulative Index: Volume IV, No. 1, No. 4.

Program descriptions for all data sections are updated annually or as required and are presented in Issue No. 1 of each volume. Each new section is described the first time it appears.

TABLE 17

DATA PUBLISHED IN SOLAR-GEOPHYSICAL DATA

| | 1969 | | | | | | | |
|---|---|---|---|---|---|---|---|---|
| | Apr. | May | June | July | Aug. | Sep. | Oct. | Nov. |
| American Relative Sunspot Numbers $R_A$ | 297 | 298 | 299 | 300 | 301 | 302 | 303 | 304 |
| Zürich Provisional Relative Sunspot Numbers $R_Z$ | 297 | 298 | 299 | 300 | 301 | 302 | 303 | 304 |
| Zürich Final Sunspot Numbers $R_Z$ | --- | --- | --- | --- | --- | --- | --- | --- |
| 2800 MHz - Daily Values of Solar Flux (ARO-Ottawa) | 297 | 298 | 299 | 300 | 301 | 302 | 303 | 304 |
| 2800 MHz - Daily Values of Adjusted Solar Flux (ARO-Ottawa) | 297 | 298 | 299 | 300 | 301 | 302 | 303 | 304 |
| 8800, 4995, 2695, 1415, 606 MHz Adjusted Solar Flux (AFCRL) | 297 | 298 | 299 | 300 | 301 | 302 | 303 | 304 |
| Mt. Wilson Magnetic Characteristics of Sunspots | 298 | 299 | 300 | 301 | 302 | 303 | 304 | --- |
| Mt. Wilson Magnetograms | 298 | 299 | 300 | 301 | 302 | 303 | 304 | --- |
| Hα (Sacramento-Peak or Boulder) | 298 | 299 | 300 | 301 | 302 | 303 | 304 | --- |
| Sunspots (Boulder or Sacramento Peak) | 298 | 299 | 300 | 301 | 302 | 303 | 304 | --- |
| Calcium Plage Maps (McMath-Hulbert or Catania) | 298 | 299 | 300 | 301 | 302 | 303 | 304 | --- |
| Calcium Plage and Sunspot Region | 298 | 299 | 300 | 301 | 302 | 303 | 304 | --- |
| Coronal Line Emission | 298 | 299 | 300 | 301 | 302 | 303 | 304 | --- |
| Optical Observations Flares | 297 | 298 | 299 | 300 | 301 | 302 | 303 | 304 |
| Optical Observations Flares (Including Standardized Data) | 302 | 303 | 304 | --- | --- | --- | --- | --- |
| Flare Patrol Observations | 297 | 298 | 299 | 300 | 301 | 302 | 303 | 304 |
| Flare Patrol Observations | 302 | 303 | 304 | --- | --- | --- | --- | --- |
| Solar X-Ray Spectroheliograms (OSO 5) | --- | --- | --- | 301 | 302 | 303 | 304 | --- |
| Solar X-Ray Radiation (Explorer 37) (Graphs) | 302 | 303 | 304 | --- | --- | --- | --- | --- |
| Solar X-Ray Radiation (Explorer 37) | 298 | 299 | 300 | 301 | 302 | 303 | 304 | --- |
| Solar X-Ray Radiation (Explorers 33 & 35) | 303 | 304 | 304 | --- | --- | --- | --- | --- |
| Solar Protons (Explorer 34) | 303 | 303 | 304 | --- | --- | --- | --- | --- |

TABLE 17 (Continued)

| | 1969 | | | | | | | |
|---|---|---|---|---|---|---|---|---|
| | Apr. | May | June | July | Aug. | Sep. | Oct. | Nov. |
| Solar Proton Events (Riometer) | --- | --- | --- | --- | --- | --- | --- | --- |
| Cosmic-Ray Protons (Pioneers 6 & 7) | 297 | 298 | 299 | 300 | 301 | 302 | 303 | 304 |
| Cosmic-Ray Protons (Pioneers 8 & 9) | --- | --- | --- | --- | --- | --- | --- | --- |
| Solar Wind (Pioneers 6 & 7) | 297 | 298 | 299 | 300 | 301 | 302 | 303 | 304 |
| Solar Wind (Vela 2, 3, & 4) | 297 | 298 | 299 | 300 | 301 | 302 | 303 | 304 |
| Magnetic Field (Pioneer 9) | --- | --- | --- | --- | --- | --- | --- | --- |
| Solar Radio Waves - Outstanding Occurrences - Worldwide | 302 | 303 | 304 | --- | --- | --- | --- | --- |
| Sudden Ionospheric Disturbance (SWF-SCNA-SEA-SPA-SES-SFD) | 297 | 298 | 299 | 300 | 301 | 302 | 303 | 304 |
| Sudden Ionospheric Disturbance (Addenda) | 302 | 303 | 304 | --- | --- | --- | --- | --- |
| 10700, 2700, 960, 328 MHz - Outstanding Occurrences (Pennsylvania State University) | 297 | 298 | 304 | --- | --- | --- | --- | --- |
| 15400, 8800, 4995, 2695, 1415, and 606 MHz Outstanding Occurrences (AFCRL, Sagamore Hill) | 297 | 298 | 304 | --- | --- | --- | --- | --- |
| 7000 MHz - Outstanding Occurrences (Sao Paulo) | 297 | 298 | 304 | --- | --- | --- | --- | --- |
| 2800 MHz - Outstanding Occurrences (ARO-Ottawa) | 297 | 298 | 304 | --- | --- | --- | --- | --- |
| 486 MHz - Outstanding Occurrences (Washington State University) | 297 | --- | --- | --- | --- | --- | --- | --- |
| 408 MHz - Outstanding Occurrences (San Miguel) | 297 | 298 | 304 | --- | --- | --- | --- | --- |
| 408 MHz - Interferometric Observation (Nançay) | 297 | 298 | 299 | 300 | 301 | 302 | 303 | 304 |
| 169 MHz - Interferometric Observation (Nançay) | 297 | 298 | 299 | 300 | 301 | 302 | 303 | 304 |
| 184 MHz- Outstanding Occurrences (Boulder) | 297 | 298 | 304 | --- | --- | --- | --- | --- |
| 18 MHz - Bursts (Boulder) | 297 | 298 | 304 | --- | --- | --- | --- | --- |
| 18 MHz - Bursts (McMath) | 297 | 298 | 304 | --- | --- | --- | --- | --- |
| 30-1000 MHz - (Weissenau, G.F.R.) | 298 | 299 | 300 | 301 | 302 | 303 | 304 | --- |

TABLE 17 (Continued)

| | 1969 | | | | | | | |
|---|---|---|---|---|---|---|---|---|
| | Apr. | May | June | July | Aug. | Sep. | Oct. | Nov |
| 10-580 MHz - (Fort Davis) | 298 | 299 | 300 | 301 | 302 | 303 | 304 | --- |
| 10-210 MHz - (Culgoora)* | 298 | 299 | 300 | 301 | 302 | 303 | 304 | --- |
| 7.6-80 MHz - (University of Colorado)** | 298 | 299 | 300 | 301 | 302 | 303 | 304 | --- |
| 19-41 MHz - (AFCRL, Sagamore Hill) | 298 | 299 | 300 | 301 | 302 | 303 | 304 | --- |
| 9.1-cm Spectroheliograms (Stanford) | 298 | 299 | 300 | 301 | 302 | 303 | 304 | --- |
| 21-cm Spectroheliograms (Fleurs) | 298 | 299 | 300 | 301 | 302 | 303 | 304 | --- |
| 10.7-cm Solar Scans (Ottawa-ARO) | 297 | 298 | 299 | 300 | 301 | 302 | 303 | 304 |
| 21-cm Solar Scans (Fleurs) | 297 | 298 | 299 | 300 | 301 | 302 | 303 | 304 |
| 43-cm Solar Scans (Fleurs) | 297 | 298 | 299 | 300 | 301 | 302 | 303 | 304 |
| Cosmic-Ray Neutron Counts (Deep River) | 298 | 299 | 300 | 301 | 302 | 303 | 304 | --- |
| Cosmic-Ray Neutron Counts (Alert) | 298 | 299 | 300 | 301 | 302 | 303 | 304 | --- |
| Cosmic-Ray Neutron Counts (Churchill) | 298 | 299 | 300 | 301 | 302 | 303 | 304 | --- |
| Cosmic-Ray Neutron Counts (Climax) | 298 | 299 | 300 | 301 | 302 | 303 | 304 | --- |
| Cosmic-Ray Neutron Counts (Dallas) | 298 | 299 | 300 | 301 | 302 | 303 | 304 | --- |
| Geomagnetic Indices Ci, Cp, Kp, Ap - Selected Days | 298 | 299 | 300 | 301 | 302 | 303 | 304 | --- |
| Principal Magnetic Storms | 298 | 299 | 300 | 301 | 302 | 303 | 304 | --- |
| Reduced Magnetograms | 302 | 303 | 304 | --- | --- | --- | --- | --- |
| Sudden Commencement and Solar Flare Effects | 303 | 303 | 303 | 304 | 304 | 304 | --- | --- |
| 27-Day Chart of Kp Indices for Year | --- | --- | --- | --- | --- | --- | --- | --- |
| 27-Day Chart of $C_9$ for Year | --- | --- | --- | --- | --- | --- | --- | --- |
| High Latitude Quality Figures and Forecasts | 298 | 299 | 300 | 301 | 302 | 303 | 304 | --- |
| High Latitude Comparison Graphs | 298 | 299 | 300 | 301 | 302 | 303 | 304 | --- |
| Graphs of Transmission Frequency Range | 298 | 299 | 300 | 301 | 302 | 303 | 304 | --- |
| IUWDS Alert Decisions | 297 | 298 | 299 | 300 | 301 | 302 | 303 | 304 |
| Abbreviated Calendar Record | 303 | 304 | --- | --- | --- | --- | --- | --- |

*8-2000 MHz beginning August 1969.
**7.6-41 MHz beginning September 1968.

The bulletin lists the data by category and by station name and date. The following categories of data are included:

- Total Field Intensity Magnetometer
- Cosmic-Ray Neutron Intensity Monitor
- Extremely Low Frequency Noise
- Riometer
  Hourly Absorption Values
- Solar Optical Patrol Observations
  Sunspot
  Chromospheric Flares
  Flare Film Record
  Chromospheric Activity Other Than Flares
  White-Light Visual Sunspot Drawing
  Spectrographic Coronal Observations
  Sunspot Group Analysis (White-Light Photographic Patrol)
  Solar Event Atlas
- Solar Radio Emission
  Spectral Observations
  Radio Noise Measurements
  Radio Map
- Vertical Incidence Ionospheric Soundings
  Absorption Loss
  Median Values
  Median Curves and Hourly Values

Copies of the Geophysics and Space Data Bulletin may be requested from:

Miss Anne L. Carrigan (editor)
Space Physics Laboratory
Air Force Cambridge Research Laboratories
L. G. Hanscom Field
Bedford, Massachusetts 01730

## IAGA BULLETINS NO. 12 AND NO. 18

The International Association of Geomagnetism and Aeronomy (IAGA) of the International Union of Geodesy and Geophysics (IUGG) publishes bulletins that contain, in some cases, transactions of meetings and, in other cases, listings of geomagnetic data. Copies of the bulletins can be purchased from the IUGG Publication Office, 39ter, Rue Gay-Lussac, Paris (V), France.

In 1948, Bulletin No. 12 was issued to present compilations of the geomagnetic indices, C and K, that were received from participating observatories from 1940 to 1946. Since the publication of Bulletin No. 12, annual supplementary bulletins (No. 12a to 12ℓ) have been published to present data that were collected between 1947 and 1957. (Bulletin No. 12d is an exception.) In each of subsequent years, two bulletins have been published, e.g., 12m1 and 12m2. Typically, data for the third year prior to publication are presented.

An example of the contents of the IAGA Bulletin No. 12 series, supplements 12o1 and 12o2, is given below:

(12o1)

List of observatories
Observatories reporting K-indices
Three-hour-range indices K, 1960
Magnetic character-figures C, 1960
International character-figures Ci, 1960
Magnetically selected days
International character-figures Ci, 1900-1960
Planetary indices Kp, equivalent ranges ap, daily average ranges Ap, daily character-figures Cp, 1960
Frequencies of Kp-indices, 1960
Monthly averages of Ap and Cp, 1960
Very quiet intervals
27-day recurrence for Kp, 1960
References to tables and diagrams for Kp, ap, and Cp

(12o2)

List of observatories
Storm sudden commencement, ssc, 1960
Bays and pulsational disturbances, b, bs, bp, bps, pt, pg, 1960
Pulsational disturbances, 1960 (pt and pg) not associated with bays

Sudden impulses, s.i., 1960
Minor disturbances, 1960
Solar-flare effects
Doubtful solar-flare effects, 1960
Rejected solar-flare effects, 1960

IAGA Bulletin No. 18, "Geomagnetic Planetary Indices Kp, Ap, and Cp, 1932 to 1961" contains, in addition to the data indicated by its title, values of ap for the periods 1932 to 1936 and 1952 to 1958, and 27-day recurrence diagrams for Kp for the period 1932 to 1961. These diagrams are also referred to as Bartel's musical diagrams.

## QUARTERLY BULLETIN ON SOLAR ACTIVITY

The Quarterly Bulletin on Solar Activity (QBSA) is published for the International Astronomical Union by the Eidgen, Sternwarte in Zurich, Switzerland, with financial assistance from UNESCO. Since only a limited number of the bulletins are printed, only one copy is sent to a single institution. The data contained in an issue nominally were taken 1-1/2 years prior to publication. The QBSA is divided into four parts: Part 1, "Sunspots," written in English, contains sunspot numbers and areas; Part 2, "Eruptions Chromospheriques Brillantes" (solar flares), in French, contains flare listings, observing hours, and a table of active regions; Part 3, "Intensities de la Couronne Solaire" (coronal emissions), in French, contains listings of coronal line emission intensities; and Part 4, "Solar Radio Emissions," in English, contains tables of flux values, a list of distinctive events, maps showing the location of active regions, and a list of the spectral class of activity. These data have been more complete than those published in Solar-Geophysical Data. For instance, QBSA has contained worldwide radio data, whereas, prior to mid-1969, SGD contained only Western Hemisphere radio data. The Quarterly Bulletins for January 1917 to June 1968 are available on four rolls of microfilm from WDC-A, Boulder.

## DATA COMPILATIONS FOR INDIVIDUAL EVENTS

A number of data compilations related to individual, outstanding solar-terrestrial events are available in published form.

- Solar Event of May 23, 1967
  "Data on Solar Event of May 23, 1967, and its Geophysical Effects," WDC-A for Upper Atmosphere Geophysics Report UAG-5.

- October 24-November 6, 1968, Solar Activity
  "Data on Solar Geophysical Activity October 24-November 6, 1968," WDC-A for Upper Atmosphere Geophysics Report UAG-8, two parts.

- Cosmic-Ray Event, November 18, 1968
  "Data on Cosmic-Ray Event of November 18, 1968, and Associated Phenomena," WDC-A for Upper Atmosphere Geophysics Report UAG-9.

These reports were compiled by Miss J. Virginia Lincoln and contain discussions by principal investigators in addition to the actual data. Published by the Environmental Data Service of NOAA at Asheville, North Carolina, the documents can be purchased from the Superintendent of Documents, Government Printing Office, Washington, D.C. 20402. The single issue price varies: for UAG-5 the price is $0.65; for UAG-8, $1.75; and for UAG-9, $0.55. The annual subscription rate for the Upper Atmosphere Geophysics series is $9.00 in the U.S. and $11.50 for subscribers outside the U.S. The number of issues varies from year to year.

- Solar Flare of July 7, 1966
  The solar flare of July 7, 1966, and its geophysical effects is the subject of Volume 3 of the Annals of the IQSY. Both the solar flare data and discussions by the principal investigators are presented.

- Solar Event of February 25, 1969
  Another potentially useful document is "Ground Based Observations for the Solar Event of February 25, 1969," compiled by K. G. Lenhart, European Space Operations Center, Darmstadt, Federal Republic of Germany. Solar, ionospheric, geomagnetic, and neutron monitor data from several observatories are presented.

## MISCELLANEOUS DOCUMENTS

Infrequent references are made in this Handbook to publications that may not be readily available to most readers. This section lists these publications along with the publisher and/or center of distribution. The publications are listed here alphabetically by title.

Aerological Data of Japan, published by the Japan Meteorological Agency, Tokyo, available from the National Climatic Center, Asheville, North Carolina 28801.

"Data Report of the Meteorological Rocket Network Firings," published by IRIG. Copies issued prior to 1966 are available from the Defense Documentation Center, Cameron Station, Alexandria, Virginia 22314. Subscriptions for current editions are available from the Superintendent of Documents, Government Printing Office, Washington, D.C. 20402.

Environmental Science Services Administration Technical Reports WB-2, 3, 9, 12 (1964-1967), available from the Superintendent of Documents, U.S. Government Printing Office, Washington, D.C. 20402.

EXAMETNET Data Report Series, Annual Report for 1966 (NASA SP-175), Annual Report for 1967 (NASA SP-176), and Annual Report for 1968 (NASA SP-231), available from the National Technical Information Service, Springfield, Virginia 22151.

"Format of Electron Density Profile Tabulations," prepared by J. W. Wright and D. McKinnis, available from Institute for Telecommunication Sciences and Aeronomy, NOAA, Boulder, Colorado 80302.

"Handbook of Geophysics and Space Environments," edited by Shea L. Valley, available from Air Force Cambridge Research Laboratories, L. G. Hanscom Field, Bedford, Massachusetts 01730.

"International Geophysical Calendars 1957-1969," published by WDC-A for Upper Atmosphere Geophysics, available from the Superintendent of Documents, Government Printing Office, Washington, D.C. 20402 ($.30).

International Ursigram and World Days Service Synoptic Codes for Solar and Geophysical Data, available from Miss J. V. Lincoln, Deputy Secretary, IUWDS Steering Committee, NOAA, Boulder, Colorado 80302.

Key to Meteorological Records (KMRD) Series, published by the National Oceanic and Atmospheric Administration, available from the Superintendent of Documents, Government Printing Office, Washington, D.C. 20402.

"North Polar, South Polar, World Maps and Tables of Invariant Magnetic Coordinates for Six Altitudes: 0, 100, 200, 600, 1000, and 3000 km," published by DASA, available from the authors, J. E. Evans, L. L. Newkirk, and B. M. McCormac, Lockheed Palo-Alto Research Laboratory, 3251 Hanover Street, Palo Alto, California 94304.

Ozone Data for the World, published bimonthly by the Meteorological Branch, Canadian Department of Transport, Toronto, Ontario, available from the National Climatic Center, Asheville, North Carolina 28801.

Photographic Journal of the Sun, M. Cimino, editor, published by Osservatorio Astronomico di Roma, Italia.

"Preliminary Report and Forecast of Solar-Geophysical Activity," published by the National Oceanic and Atmospheric Administration, Boulder, Colorado 80302.

"Royal Observatory Bulletins," published in Photoheliographic Results, available from WDC-A for Upper Atmosphere Geophysics, Boulder, Colorado 80302.

"The American Ephemeris and Nautical Almanac" published by U.S. Naval Observatory, available from the Superintendent of Documents, Government Printing Office, Washington, D.C. 20402. ($4.25).

"Three-monthly Bulletin on Geomagnetic Indices and Rapid Variations," International Service of Geomagnetic Indices, c/o Royal Netherlands Meteorological Institute, DeBilt, The Netherlands.

USSR Academy of Sciences Solar Data, available from Astronomical Observatory of the U.S.S.R. Academy of Sciences, Leningrad M-140, U.S.S.R.

"U.S. Standard Atmosphere, 1962" and "U.S. Atmosphere Supplements," published jointly by the Environmental Science Services Administration, the National Aeronautics and Space Administration, and the U.S. Air Force, available from the Superintendent of Documents, Government Printing Office, Washington, D.C. 20402.

# LIST OF ABBREVIATIONS

| | |
|---|---|
| A | angstrom |
| AAFB | Auxiliary Air Force Base |
| ADALERT | Advance Alert |
| AFB | Air Force Base |
| AFCRL | Air Force Cambridge Research Laboratories |
| ATS | Applications Technology Satellite |
| BCD | binary coded decimal |
| Bev | billion electron volts |
| C&GS | Coast and Geodetic Survey |
| CIRA | COSPAR International Reference Atmosphere |
| cm | centimeter |
| COESA | Commission on Extension to the Standard Atmosphere |
| COSPAR | Committee on Space Research |
| Dst | axisymmetric component of geomagnetic disturbance field |
| ELF | extremely low frequency |
| env | environment |
| ESRO | European Space Research Organization |
| ESSA | See NOAA |
| ETAC | Environmental Technical Applications Center |
| euv | extreme ultraviolet radiation |
| EXAMETNET | Experimental InterAmerican Meteorological Rocket Network |
| GEOALERT | Geomagnetic Alert |
| GMT | Greenwich mean time |
| GRB | Geophysics Research Board |
| GSFC | Goddard Space Flight Center |
| HAO | High Altitude Observatory |
| hr | hour |
| IAGA | International Association of Geomagnetism and Aeronomy |
| IAU | International Astronomical Union |
| IBM | International Business Machines |
| ICAO | International Civil Aviation Organization |
| ICSU | International Council of Scientific Unions |
| IGRF | International Geomagnetic Reference Field |
| IGY | International Geophysical Year |
| IQSY | International Years of the Quiet Sun |
| IRIG | Inter-Range Instrumentation Group |
| IUCSTP | Inter-Union Commission on Solar-Terrestrial Physics |
| IUGG | International Union of Geodesy and Geophysics |
| IUPAP | International Union of Pure and Applied Physics |
| IUWDS | International Ursigram and World Days Service |
| K | Kelvin |
| kHz | kilohertz |
| km | kilometer |
| KMRD | Key to Meteorological Records Documentation |
| mb | millibar |
| Mev | million electron volts |

| | |
|---|---|
| MHz | megahertz |
| min | minute |
| MIT | Massachusetts Institute of Technology |
| mm | millimeter |
| MRN | Meteorological Rocket Network |
| MSC | Manned Spacecraft Center |
| MSFC | Marshall Space Flight Center |
| MWG | Meteorological Working Group |
| NASA | National Aeronautics and Space Administration |
| NOAA | National Oceanic and Atmospheric Administration, formerly Environmental Science Services Administration |
| Np | North Pole |
| NSSDC | National Space Science Data Center |
| OGO | Orbiting Geophysical Observatory |
| Pc | continuous pulsation |
| Pg | giant pulsation |
| Pi | irregular pulsation |
| pibal | pilot balloon |
| POGO | Polar Orbiting Geophysical Observatory |
| Pt | trains of pulsation |
| QBSA | Quarterly Bulletin on Solar Activity |
| rms | root mean square |
| RWC | Regional Warning Center |
| sc, ssc | sudden storm commencement |
| SGD | Solar-Geophysical Data |
| s.i. | sudden impulse |
| SID | sudden ionospheric disturbance |
| Sp | South Pole |
| SP | special publication |
| SPME | Solar Proton Monitoring Experiment |
| STP-WDC | Solar Terrestrial Physics World Data Center |
| UNESCO | United Nations Economic, Scientific and Cultural Organization |
| URSI | International Union of Radio Science |
| USAF | United States Air Force |
| USCGS | United States Coast and Geodetic Survey |
| UT | universal time |
| VHF | very high frequency |
| VLF | very low frequency |
| vs | versus |
| WDC-A | World Data Center A |
| W.M.S. | World Magnetic Survey |
| WWA | World Warning Agency |

# INDEX